

Supporting Information

for

Molecular engineering to enhance reactivity and selectivity in an ultrafast photoclick reaction

Youxin Fu,^[a] Nadja A. Simeth,^{*[b,c]} Ryojun Toyoda,^[a,d] Robert Brilmayer,^[a] Wiktor Szymanski,^{*[a,e]} and Ben L. Feringa^{*[a]}

^[a]Youxin Fu, Dr. Ryojun Toyoda, Dr. Robert Brilmayer, Prof. Dr. Wiktor Szymanski, Prof. Dr. Ben L. Feringa, Centre for Systems Chemistry, Stratingh Institute for Chemistry, Faculty for Science and Engineering, University of Groningen, Nijenborgh 4, 9747 AG Groningen, The Netherlands.
E-mail: w.szymanski@umcg.nl, b.l.feringa@rug.nl

^[b]Jun.-Prof. Dr. Nadja A. Simeth, Institute for Organic and Biomolecular Chemistry, Department of Chemistry, University of Göttingen, Tammannstr. 2, 37077 Göttingen, Germany.
E-mail: nadja.simeth@uni-goettingen.de

^[c]Jun.-Prof. Dr. Nadja A. Simeth, Cluster of Excellence "Multiscale Bioimaging: from Molecular Machines to Networks of Excitable Cells" (MBExC), University of Göttingen, Germany.

^[d]current address: Department of Chemistry, Graduate School of Science, Tohoku University, 6-3 Aramaki-Aza-Aoba, Aoba-ku, Sendai, 980-8578, Japan.

^[e]Prof. Dr. Wiktor Szymanski, Department of Radiology, Medical Imaging Center, University of Groningen, University Medical Centre Groningen, Hanzeplein 1, 9713 GZ Groningen, The Netherlands.

Table of Contents

1. General Information	4
2. Synthesis of PQ compounds, BZPY compounds, and photoclick products.....	7
2.1. Synthesis of PQ-Ph-CF ₃	7
2.2. Synthesis of compound PQ-Ph-AC	8
2.3. Synthesis of compound PQ-Ph-CN.....	8
2.4. Synthesis of compound PQ-Ph-COOCH ₃	9
2.5. Synthesis of PQ-Ph-F	9
2.6. Synthesis of PQ-Ph-Br	10
2.7. Synthesis of PQ-Ph.....	10
2.8. Synthesis of PQ-Ph-CH ₃	10
2.9. Synthesis of PQ-Ph-OCH ₃	11
2.10. Synthesis of PQ-Ph-Amide	11
2.11. Synthesis of OMe-BZPY	12
2.12. Synthesis of BZPY	13
2.13. Synthesis of Br-BZPY.....	13
2.14. Synthesis of PQ-Ph-CF ₃ -PY.....	15
2.15. Synthesis of PQ-Ph-AC-PY	15
2.16. Synthesis of PQ-Ph-CN-PY	16
2.17. Synthesis of PQ-Ph-COOCH ₃ -PY	16
2.18. Synthesis of PQ-Ph-F-PY.....	16
2.19. Synthesis of PQ-Ph-Br-PY.....	17
2.20. Synthesis of PQ-Ph-PY	17
2.21. Synthesis of PQ-Ph-CH ₃ -PY	18
2.22. Synthesis of PQ-Ph-OCH ₃ -PY	18
2.23. Synthesis of PQ-Ph-Amide-PY	19
2.24. Synthesis of PQ-Ph-CF ₃ -NVP.....	19
2.25. Synthesis of PQ-Ph-Br-OCH ₃	20
2.26. Synthesis of PQ-Ph-OCH ₃ -COOH.....	21
2.27. Synthesis of PQ-Ph-OCH ₃ -Ph-Amide.....	21
2.28. Synthesis of PQ-Cyclo(-RGDfK).....	23
2.29. Synthesis of NP-PQ and NP-Control	24
3. NMR Spectra.....	26
4. Photophysical and Photochemical Studies by UV-Vis, Fluorescence, IR Spectroscopy, HPLC, and UPLC-MS.....	57
4.1. UV-Vis and Fluorescence Spectra	57
4.2. Analysis of reactions rates.....	58
4.3. Photoclick reaction quantum yields	73

4.4. HPLC Traces for the following of the orthogonal photoclick reaction in solution.....	80
4.5. Fluorescence Quantum Yields and Solvatofluorochromism.....	86
4.6. HPLC traces and additional measurements of photoclick reaction on surface	89
5. Author Contributions.....	96
6. References	96

1. General Information

Synthesis and isolation. Solvents used were of analytical grade. All other chemicals were used as received unless otherwise indicated. Deionized distilled water was used throughout. All oxygen or moisture-sensitive reactions were performed in dried glassware and under N₂ atmosphere using standard Schlenk techniques. Dry solvents were obtained from an MRBAUN solvent purification system (SPS). Column chromatography was performed on silica gel (Silica 60 M, 0.04-0.063 mm) or using a Büchi® Pure C-810 purification system with Büchi® FlashPureEcoFlex Amino cartridges. Purification by preparative reversed-phase HPLC was conducted using a Shimadzu system with a Nexera prep pump, model LC-20AP, a SIL-10AP autosampler, and an SPD-20A UV-Vis detector, using Kinetex®5µm C18 100Å LC column (250 × 30 mm)). To achieve separation a gradient of 5→95% MeCN (with 0.1% formic acid) in water (with 0.1% formic acid) was applied using 220 nm and 254 nm as monitoring wavelengths. Commercial available silica mesoporous SBA-15 (Sigma-Aldrich, <150 µm particle size, pore size 10 nm, Hexagonal pore morphology) were used to synthesize **NP-PQ**.

Reaction monitoring. Reactions were monitored using thin-layer chromatography (TLC) on aluminum sheets coated with silica gel 60 F254 (MERCK). Components were visualized by UV-light (254 nm, 365 nm) and potassium permanganate or Seebach staining. Alternatively, the progress of the reaction and conversion were determined by GC-MS (GC, HP6890: MS HP5973) with an HP1 or HP5 column (Agilent Technologies, Palo Alto, CA).

Analysis. Mass spectra were recorded on an AEI-MS-902 mass spectrometer (EI+) or a LTQ Orbitrap XL (ESI+, ESI-, APCI+). ¹H- and ¹³C- and ¹⁹F-NMR were recorded on Bruker 600 MHz (600 MHz and 151 MHz, respectively), Bruker AM-400 Spectrometer (400 MHz and 100.59 MHz, respectively), or a Varian AMX400 (400 MHz and 100.59 MHz, respectively), a 300 MHz (300 MHz and 75 MHz, respectively for ¹H- and ¹³C-NMR) using CDCl₃, DMSO-*d*₆, CD₃OD, or CD₃CN as solvent. Data are reported as follows: chemical shifts, multiplicity (s = singlet, d = doublet, t = triplet, q = quartet, m = multiplet), coupling constants (Hz), and

integration. UV-Vis spectra were recorded on a Hewlett-Packard HP 8543 Diode Array, an Agilent 8453 UV-Visible, or a JASCO V-630 spectrophotometer in a quartz cuvette with 1 cm pathlength at 25 °C. Fluorescence measurements were performed on a JASCO FP-6200 spectrophotometer in a quartz cuvette with 1 cm pathlength. Fluorescence quantum yield measurements were performed on a Edinburgh instruments FS5 spectrofluorometer. Solid-state DR UV-vis spectra were collected on a JASCO V-570 UV-vis near-infrared spectrophotometer equipped with a JASCO ISN-470 integrating sphere. The Agilent 8453 UV-Visible spectrometer was equipped with a custom-built (Prizmatix/Mountain Photonics) multi-wavelength fiber coupled LED-system (FC6-LED-WL) including the following LEDs: 365A, 390B, 420Z, 445B, 535R, 630CA. A detailed description of the setup was published earlier by our group (see Figure S1).^[1] A Quantum Northwest TC1 temperature controller was used to maintain the temperature at 20 °C during photochemical studies.

Photocycloaddition of PQs with ERAs in solution. Stock solutions of PQs (10 mM) and ERAs (100 mM) in DMSO were prepared. From them, a solution of PQs/ERAs (50/500 μ M) was prepared in MeCN (2.5 mL) in a quartz cuvette and degassed and saturated with N₂ for 3 min. A LED light (390 nm, 390B) was used as a light source for all photoclick reactions and positioned at a fixed distance to the cuvette. Changes in the absorption were monitored every 1 s.

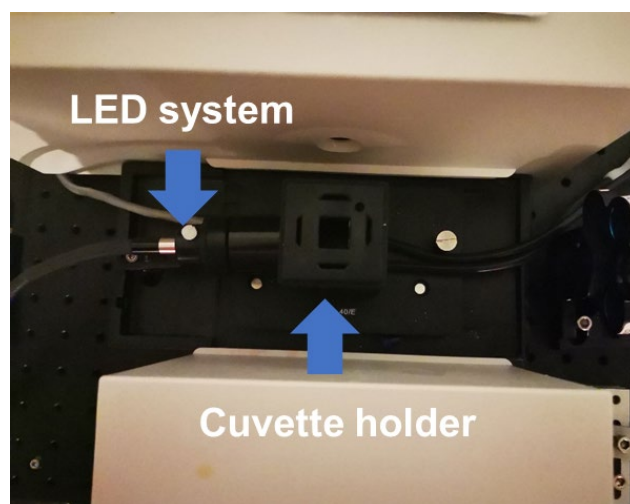
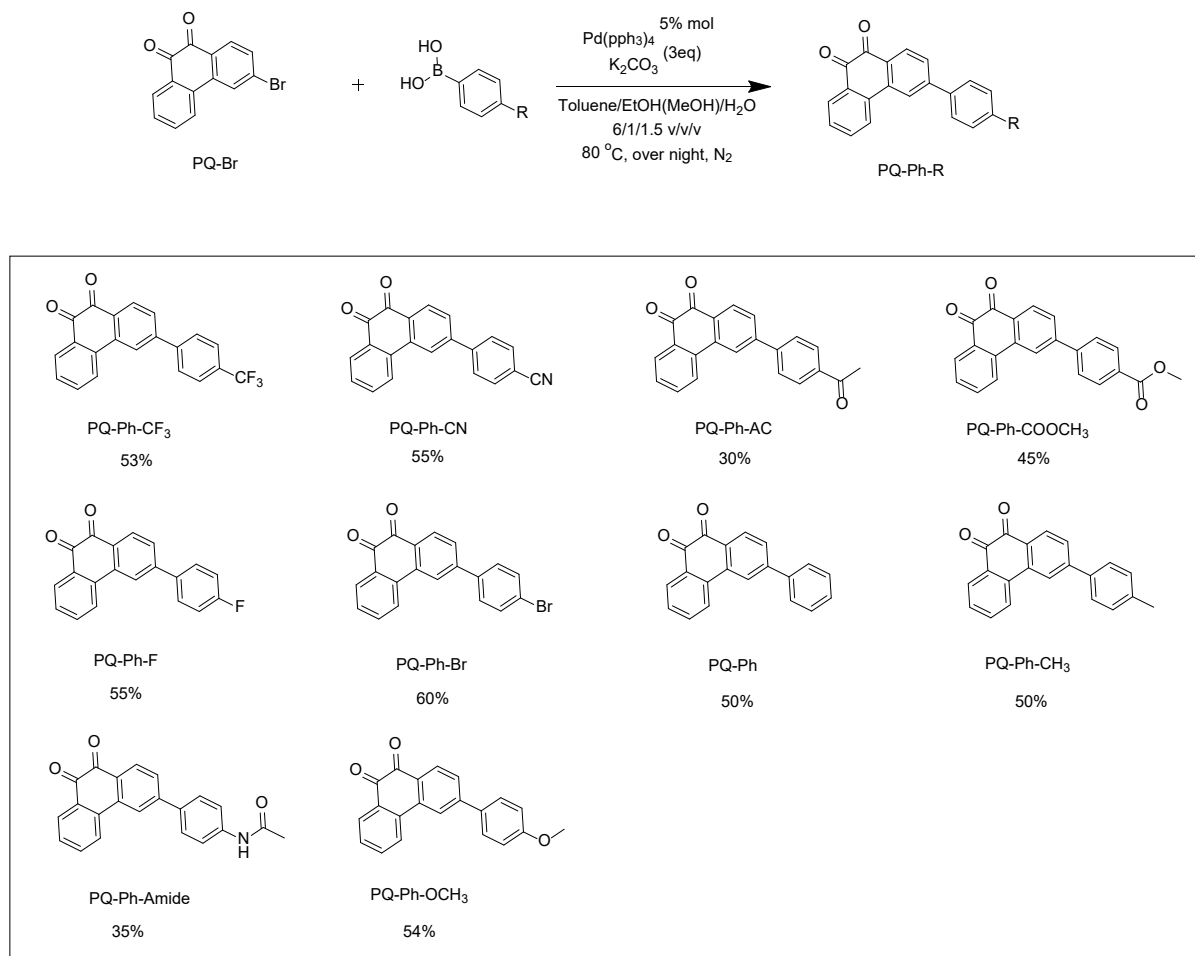


Fig. S1. Photograph of LED-system (FC6-LED-WL).

Photoclick reaction on nanoparticle. NP-PQ and ERAs were added in MeCN in a Schlenk tube and degassed by N₂. A hand-held LED lamp (395 nm, 88 mW/cm²) was used as a light source for all photoclick reactions on nanoparticle and positioned at a fixed distance to the tube.

2. Synthesis of PQ compounds, BZPY compounds, and photoclick products



Scheme S1. Synthesis and structures of **PQ** derivatives.

2.1. Synthesis of PQ-Ph-CF₃

A Schlenk tube containing **PQ-Br** (50 mg, 0.17 mmol), (4-(trifluoromethyl)phenyl)boronic acid (40 mg, 0.21 mmol) and Pd(PPh₃)₄ (10 mg, 0.008 mmol) was subjected to three vacuum-nitrogen cycles. Following the addition of degassed K₂CO₃ solution (72 mg in 1.5 mL H₂O), ethanol (1 ml), and toluene (6 mL), the tube was sealed under N₂ atmosphere and heated at 80 °C for 12 h. After being cooled to room temperature, the reaction mixture was diluted with dichloromethane, the phases were separated and the organic layer was washed with water and dried over anhydrous Na₂SO₄. Upon removal of solvents in vacuo, the residual was purified by column chromatography over silica gel eluted with ethyl acetate/dichloromethane (1/5, v/v) to

afford **PQ-Ph-CF₃** as a yellow solid, (42 mg, 0.119 mmol, yield 70%). ¹H NMR (600 MHz, DMSO-*d*₆) δ 8.61 (d, *J* = 1.6 Hz, 1H), 8.57 (d, *J* = 8.0 Hz, 1H), 8.17 – 8.13 (m, 3H), 8.07 (dd, *J* = 7.7, 1.4 Hz, 1H), 7.91 (dt, *J* = 8.1, 1.6 Hz, 3H), 7.84 – 7.80 (m, 1H), 7.60 – 7.56 (m, 1H). ¹³C NMR (151 MHz, DMSO-*d*₆) δ 179.4, 179.1, 145.5, 143.1, 136.6, 135.8, 135.5, 131.9, 131.3, 130.5, 130.1, 129.6, 128.7, 128.3, 126.3, 125.5, 123.6. ¹⁹F NMR (376 MHz, DMSO-*d*₆) δ -60.64. HR-MS (ESI) *m/z*, calculated for [M+H]⁺: 353.0784; found: 353.0776.

2.2. Synthesis of compound PQ-Ph-AC

The title compound was synthesized using the same method as for **PQ-Ph-CF₃** employing (4-acetylphenyl)boronic acid (0.29 mmol, 47 mg) to obtain **PQ-Ph-AC** as a yellow solid (30 mg, 0.092 mmol, yield 35%). ¹H NMR (400 MHz, DMSO-*d*₆) δ 8.58 (s, 1H), 8.55 (d, *J* = 8.0 Hz, 1H), 8.13 – 8.02 (m, 6H), 7.91 – 7.86 (m, 1H), 7.79 (t, *J* = 8.0 Hz, 1H), 7.55 (t, *J* = 7.4 Hz, 1H), 2.63 (s, 3H). ¹³C NMR (101 MHz, DMSO-*d*₆) δ 198.4, 179.8, 179.5, 146.2, 137.5, 136.9, 136.2, 135.9, 132.3, 131.6, 130.8, 130.4, 129.9, 129.7, 128.6, 128.5, 128.1, 125.9, 123.7, 27.7. HR-MS (ESI) *m/z*, calculated for [M+H]⁺: 327.1016; found: 327.1017.

2.3. Synthesis of compound PQ-Ph-CN

The title compound was synthesized using the same method as for **PQ-Ph-CF₃** employing (4-cyanophenyl)boronic acid (0.32 mmol, 47 mg) to obtain **PQ-Ph-CN** as a yellow solid (40 mg, 0.16 mmol, yield 55%). ¹H NMR (400 MHz, DMSO-*d*₆) δ 8.62 – 8.51 (m, 2H), 8.11 (t, *J* = 8.2 Hz, 3H), 8.01 (t, *J* = 10.0 Hz, 3H), 7.89 (d, *J* = 7.7 Hz, 1H), 7.79 (t, *J* = 7.1 Hz, 1H), 7.55 (t, *J* = 7.3 Hz, 1H). ¹³C NMR (101 MHz, DMSO-*d*₆) δ 179.3, 179.0, 145.0, 143.4, 136.5, 135.8, 135.4, 133.3, 131.9, 131.4, 130.4, 130.0, 129.5, 128.7, 128.3, 125.5, 123.5, 119.1, 111.8. HR-MS (ESI) *m/z*, calculated for [M+H]⁺: 310.0863; found: 310.0862.

2.4. Synthesis of compound PQ-Ph-COOCH₃

A Schlenk tube containing **PQ-Br** (50 mg, 0.17 mmol), (4-(methoxycarbonyl)phenyl)boronic acid (37.8 mg, 0.21 mmol), and Pd(PPh₃)₄ (10 mg, 0.008 mmol) was evacuated and backfilled with N₂ for three times. Following the addition of degassed K₂CO₃ (72 mg in 1.5 mL H₂O), methanol (1 ml) and toluene (6 mL), the tube was sealed under N₂ atmosphere and heated at 80 °C for 12 h. After being cooled to room temperature, the reaction mixture was diluted with dichloromethane, washed with water, and dried over anhydrous Na₂SO₄. Upon removal of solvents in vacuo, the residual was purified with column chromatography over silica gel eluted with ethyl acetate/dichloromethane (1/5, v/v) to obtain **PQ-Ph-COOCH₃** as a yellow solid (40 mg, 0.117 mmol, yield 50%). ¹H NMR (400 MHz, DMSO-*d*₆) δ 8.60 (d, *J* = 1.3 Hz, 1H), 8.56 (d, *J* = 7.8 Hz, 1H), 8.14 – 8.03 (m, 6H), 7.90 (dd, *J* = 8.2, 1.6 Hz, 1H), 7.83 – 7.78 (m, 1H), 7.56 (t, *J* = 7.4 Hz, 1H), 3.89 (s, 3H). ¹³C NMR (101 MHz, DMSO-*d*₆) δ 144.0, 136.4, 135.9, 135.0, 131.8, 130.5, 129.9, 129.5, 128.9, 127.7, 127.5, 125.4, 122.7, 63.0, 25.1. HR-MS (ESI) *m/z*, calculated for [M+H]⁺: 343.0965 ; found: 343.0961.

2.5. Synthesis of PQ-Ph-F

The title compound was synthesized using the same method as for **PQ-Ph-CF₃** employing (4-fluorophenyl)boronic acid (0.36 mmol, 51 mg) to providing **PQ-Ph-F** as a yellow solid (80 mg, 0.18 mmol, yield 55%). ¹H NMR (600 MHz, DMSO-*d*₆) δ 8.57 (d, *J* = 8.0 Hz, 1H), 8.53 (d, *J* = 1.6 Hz, 1H), 8.10 (d, *J* = 8.1 Hz, 1H), 8.06 (dd, *J* = 7.7, 1.4 Hz, 1H), 8.00 (dd, *J* = 8.8, 5.4 Hz, 2H), 7.82 (ddd, *J* = 17.8, 8.1, 1.6 Hz, 2H), 7.57 (t, *J* = 7.9 Hz, 1H), 7.40 (t, *J* = 8.8 Hz, 2H). ¹³C NMR (151 MHz, DMSO-*d*₆) δ 179.6, 179.1, 164.0, 162.4, 146.1, 136.5, 135.9, 135.6, 135.5, 131.9, 130.5, 130.5, 130.1, 130.0, 130.0, 129.6, 127.9, 125.5, 122.9, 116.5, 116.4. ¹⁹F NMR (376 MHz, DMSO-*d*₆) δ -113.2. HR-MS (ESI) *m/z*, calculated for [M+H]⁺: 303.0816; found: 303.0812.

2.6. Synthesis of PQ-Ph-Br

The title compound was synthesized using the same method as for **PQ-Ph-CF₃** employing (4-bromophenyl)boronic acid (0.27 mmol, 53 mg) to obtain **PQ-Ph-Br** as a yellow solid (44 mg, 0.12 mmol, yield 50%). ¹H NMR (600 MHz, DMSO-*d*₆) δ 8.57 (d, *J* = 8.0 Hz, 1H), 8.55 (d, *J* = 1.6 Hz, 1H), 8.11 (d, *J* = 8.1 Hz, 1H), 8.07 (dd, *J* = 7.7, 1.3 Hz, 1H), 7.91 (d, *J* = 8.6 Hz, 2H), 7.86 (dd, *J* = 8.1, 1.7 Hz, 1H), 7.84 – 7.80 (m, 1H), 7.76 (d, *J* = 8.6 Hz, 2H), 7.58 (t, *J* = 7.5 Hz, 1H). ¹³C NMR (101 MHz, DMSO-*d*₆) δ 179.5, 179.1, 145.8, 138.2, 136.5, 135.8, 135.6, 132.4, 131.9, 130.8, 130.5, 130.0, 129.9, 129.5, 129.3, 127.8, 127.7, 125.5, 123.1, 122.9. HR-MS (ESI) *m/z*, calculated for [M+H]⁺: 364.9994; found: 364.9988.

2.7. Synthesis of PQ-Ph

The title compound was synthesized using the same method as for **PQ-Ph-CF₃** employing phenylboronic acid (0.39 mmol, 48 mg) to obtain **PQ-Ph** as a yellow solid (50 mg, 0.18 mmol, yield 50%). ¹H NMR (400 MHz, CDCl₃) δ 8.26 (d, *J* = 8.1 Hz, 1H), 8.21 (dd, *J* = 9.4, 1.4 Hz, 2H), 8.11 (d, *J* = 8.0 Hz, 1H), 7.75 – 7.71 (m, 1H), 7.68 (td, *J* = 8.1, 7.4, 1.6 Hz, 3H), 7.55 – 7.44 (m, 4H). ¹³C NMR (101 MHz, CDCl₃) δ 180.4, 179.9, 148.9, 139.5, 136.2, 135.9, 135.8, 131.2, 130.5, 129.7, 129.2, 129.1, 128.3, 127.3, 123.9, 122.7. HR-MS (ESI) *m/z*, calculated for [M+H]⁺: 285.0910; found: 285.0911.

2.8. Synthesis of PQ-Ph-CH₃

The title compound was synthesized using the same method as for **PQ-Ph-CF₃** employing *p*-tollylboronic acid (0.39 mmol, 53 mg) to obtain **PQ-Ph-CH₃** as a yellow solid (53 mg, 0.18 mmol, yield 50%). ¹H NMR (400 MHz, CDCl₃) δ 8.23 (d, *J* = 8.1 Hz, 1H), 8.20 (dd, *J* = 7.8, 1.3 Hz, 1H), 8.18 (d, *J* = 1.4 Hz, 1H), 8.10 (d, *J* = 8.0 Hz, 1H), 7.76 – 7.70 (m, 1H), 7.65 (dd, *J* = 8.1, 1.6 Hz, 1H), 7.60 (d, *J* = 8.1 Hz, 2H), 7.51 – 7.46 (m, 1H), 7.33 (d, *J* = 7.9 Hz, 2H), 2.44 (s, 3H). ¹³C NMR (101 MHz, CDCl₃) δ 180.5, 179.9, 148.7, 139.3, 136.5, 136.2, 135.9,

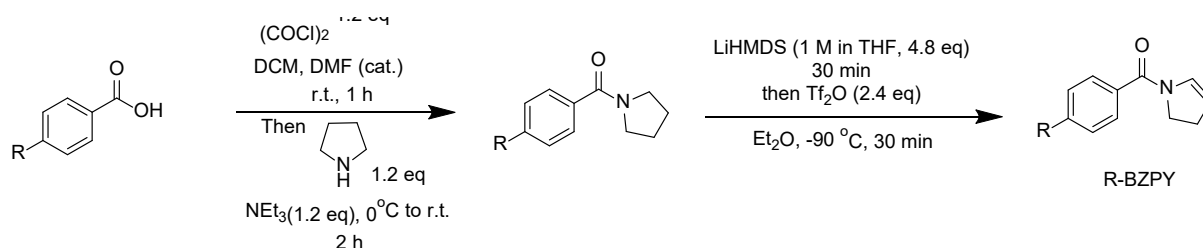
135.8, 131.2, 130.5, 129.9, 129.6, 128.0, 127.1, 123.9, 122.4, 21.3. HR-MS (ESI) m/z , calculated for $[M+H]^+$: 299.1067; found: 299.1068.

2.9. Synthesis of PQ-Ph-OCH₃

The title compound was synthesized using the same method as for **PQ-Ph-CF₃** employing (4-methoxyphenyl)boronic acid (0.34 mmol, 51 mg) to obtain **PQ-Ph-OCH₃** as a yellow solid (52 mg, 0.17 mmol, yield 54%). ¹H NMR (600 MHz, DMSO-*d*₆) δ 8.56 (d, $J = 7.9$ Hz, 1H), 8.49 (d, $J = 1.6$ Hz, 1H), 8.08 (d, $J = 8.1$ Hz, 1H), 8.05 (dd, $J = 7.8, 1.4$ Hz, 1H), 7.95 – 7.89 (m, 2H), 7.85 – 7.78 (m, 2H), 7.59 – 7.53 (m, 1H), 7.14 – 7.08 (m, 2H), 3.85 (s, 3H). ¹³C NMR (151 MHz, DMSO-*d*₆) δ 179.8, 179.1, 160.6, 147.0, 136.4, 135.9, 135.8, 131.8, 131.2, 130.6, 129.9, 129.6, 129.2, 127.3, 125.4, 122.2, 115.0, 55.8. HR-MS (ESI) m/z , calculated for $[M+H]^+$: 315.1016; found: 315.1020.

2.10. Synthesis of PQ-Ph-Amide

The title compound was synthesized using the same method as for **PQ-Ph-CF₃** employing (4-acetamidophenyl)boronic acid (0.2 mmol, 36 mg) to obtain **PQ-Ph-Amide** as a yellow solid (22 mg, 0.065 mmol, yield 35%). ¹H NMR (600 MHz, DMSO-*d*₆) δ 10.16 (s, 1H), 8.56 (d, $J = 8.0$ Hz, 1H), 8.52 (s, 1H), 8.09 (d, $J = 8.1$ Hz, 1H), 8.06 (d, $J = 7.7$ Hz, 1H), 7.92 (d, $J = 8.7$ Hz, 2H), 7.85 – 7.80 (m, 2H), 7.77 (d, $J = 8.7$ Hz, 2H), 7.57 (t, $J = 7.5$ Hz, 1H), 2.10 (s, 3H). ¹³C NMR (151 MHz, DMSO-*d*₆) δ 179.8, 179.1, 169.1, 146.8, 140.7, 136.4, 135.9, 135.8, 133.2, 131.9, 130.6, 130.1, 130.0, 129.6, 128.2, 127.3, 125.4, 122.3, 119.7, 24.6. HR-MS (ESI) m/z , calculated for $[M+H]^+$: 342.1125; found: 342.1129.



Scheme S2. Synthetic procedure of **R-BZPY** compounds adapted from Maulide and co-workers.^[2]

2.11. Synthesis of OMe-BZPY

4-Methoxybenzoic acid (2.0 g, 13 mmol, 1.0 eq.) was dissolved in dry CH_2Cl_2 (0.6 M) and a few drops of dry dimethylformamide were added. Oxalyl chloride (2.00 g, 15.6 mmol, 1.2 eq.) was added dropwise, whereby a strong gas evolution was observed. After 1 h, the pyrrolidine (1.1 g, 15.6 mmol, 1.2 eq.) was slowly added, followed by the addition of triethylamine (1.6 g, 15.6 mmol, 1.2 eq.). The reaction mixture was stirred at room temperature for 16 h and monitored by TLC. Then, the reaction mixture was transferred into a separatory funnel and sequentially washed with H_2O , 1 M NaOH (aq), 1 M HCl (aq), and brine. The organic phase was dried over anhydrous Na_2SO_4 and the filtrate was concentrated under reduced pressure, the residual was purified with column chromatography over silica gel eluted with ethyl acetate/dichloromethane (1/5, v/v) to giving the (4-methoxyphenyl)(pyrrolidin-1-yl)methanone (2.2 g, 10.7 mmol, yield 85%). ^1H NMR (400 MHz, CDCl_3) δ 7.50 (d, $J = 8.6$ Hz, 2H), 6.88 (d, $J = 8.6$ Hz, 2H), 3.81 (s, 3H), 3.61 (t, $J = 6.5$ Hz, 2H), 3.46 (t, $J = 6.1$ Hz, 2H), 1.89 (dt, $J = 33.6, 6.2$ Hz, 4H). ^{13}C NMR (101 MHz, CDCl_3) δ 169.4, 160.7, 129.4, 129.1, 113.4, 55.3, 49.8, 46.3, 26.5, 24.4. The obtained data is in accordance with the literature.^[3]

The synthesis of enamide compounds was carried out following a previously reported procedure.^[2] A flame-dried Schlenk flask was loaded with the (4-methoxyphenyl)(pyrrolidin-1-yl)methanone (1.0 g, 4.9 mmol, 1.00 eq.), which was dissolved in anhydrous Et_2O (15 mL). The solution was cooled down to -80 °C and LiHMDS (1 M in THF, 23.5 mL, 23.5 mmol, 4.80 eq.) was added slowly (ca. 5 min). After the addition, the resulting mixture was stirred for 30

min. Next, Tf₂O (2 mL, 11.8 mmol, 2.40 eq.) was added dropwise over 5 min with vigorous stirring. The reaction mixture was stirred for 30 min before remaining reagents were quenched by the addition of a saturated aqueous solution of NH₄Cl (10 mL). The solution was transferred into a separatory funnel and extracted with EtOAc (3 x 15 mL). The combined organic phase was dried over anhydrous Na₂SO₄ and the solvent was removed under reduced pressure. The crude material was purified using a Büchi® Reveleris® X2 purification system with Büchi® FlashPureEcoFlex Amino cartridges eluted with heptane/EtOAc (1/2) to afford **OMe-BZPY** as a yellow oil (162 mg, 0.8 mmol, yield 26 %). ¹H NMR (400 MHz, DMSO-*d*₆) δ 7.43 (d, *J* = 4.1 Hz, 2H), 6.97 (d, *J* = 8.8 Hz, 2H), 6.52 (s, 1H), 5.22 (s, 1H), 3.86 – 3.80 (m, 2H), 3.78 (s, 3H), 2.61 (t, *J* = 7.8 Hz, 2H). ¹³C NMR (101 MHz, DMSO-*d*₆) δ 165.8, 161.1, 130.9, 129.9, 114.1, 111.8, 55.7, 46.0, 28.2. The obtained data are in accordance with the literature.^[4]

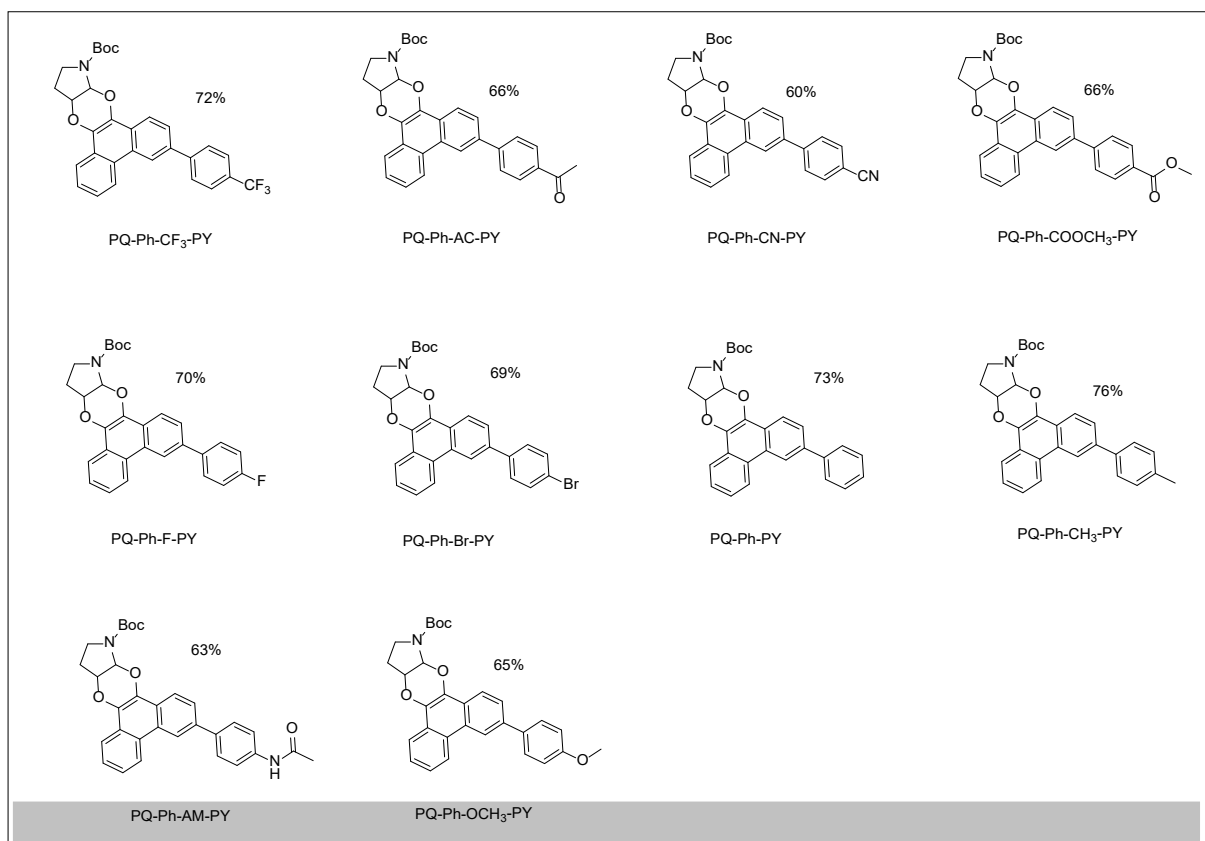
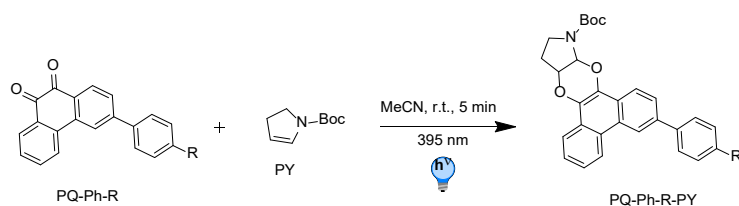
2.12. Synthesis of **BZPY**

The title compound was synthesized using the same method as for **OMe-BZPY** using phenyl(pyrrolidin-1-yl)methanone (525 mg, 3 mmol) to obtain **BZPY** as a yellow oil (120 mg, 0.69 mmol, yield 23%). ¹H NMR (400 MHz, DMSO-*d*₆) δ 7.45 (d, *J* = 3.1 Hz, 4H), 6.44 (s, 1H), 5.24 (s, 1H), 3.86 (t, *J* = 8.9 Hz, 2H), 2.66 – 2.60 (m, 2H), ¹³C NMR (101 MHz, DMSO-*d*₆) δ 166.1, 136.1, 130.8, 130.7, 129.0, 128.5, 128.0, 127.9, 112.2, 45.8, 28.3. The obtained data are in accordance with the literature.^[2]

2.13. Synthesis of **Br-BZPY**

The title compound was synthesized using the same method as for **OMe-BZPY** using (4-bromophenyl)(pyrrolidin-1-yl)methanone (372 mg, 1.5 mmol) to obtain **Br-BZPY** as a white solid (125 mg, 0.5 mmol, yield 34%). ¹H NMR (400 MHz, DMSO-*d*₆) δ 7.65 (d, *J* = 8.4 Hz, 2H), 7.40 (d, *J* = 8.2 Hz, 2H), 6.51 – 6.41 (m, 1H), 5.29 – 5.21 (m, 1H), 3.85 (t, *J* = 8.8 Hz, 2H), 2.62 (t, *J* = 8.8 Hz, 3H), ¹³C NMR (101 MHz, DMSO-*d*₆) δ 165.0, 135.2, 132.0, 130.7, 130.1,

129.9, 124.1, 112.6, 45.9, 28.3. HR-MS (ESI) m/z , calculated for $[M+H]^+$: 253.9998; found: 253.9994.



Scheme S3. Synthesis of PQ-Ph-R-PY (as a mixture of two regioisomers) derivatives and photographs of the experimental set-up (using PQ-Ph-OCH₃ + PY reaction as an example).

2.14. Synthesis of PQ-Ph-CF₃-PY

PQ-Ph-CF₃ (0.067 mmol, 24 mg) and **PY** (0.67 mmol, 113 mg) were dissolved in 20 mL MeCN. Then, the mixture was stirred and irradiated using a hand-held UV light lamp (395 nm, 88 mW cm⁻²) at a fixed distance for 5 min under N₂ atmosphere. The progress of the reaction was monitored by TLC. After completion, the volatiles were evaporated and the resulting residue was purified by column chromatography on silica gel (dichloromethane/ethyl acetate = 1:4, v/v) to afford **PQ-Ph-CF₃-PY** as a colorless powder (25 mg, 0.048 mmol, yield 72 %). ¹H NMR (400 MHz, DMSO-*d*₆) δ 9.09 (s, 1H), 8.98 (d, J = 8.1 Hz, 1H), 8.16 (dd, J = 10.5, 8.4 Hz, 3H), 8.11 – 8.06 (m, 1H), 8.05 – 7.99 (m, 1H), 7.85 (d, J = 8.3 Hz, 2H), 7.72 – 7.67 (m, 1H), 7.64 (ddd, J = 8.4, 4.8, 1.5 Hz, 1H), 5.71 (d, J = 12.7 Hz, 1H), 5.18 (ddd, J = 10.5, 6.8, 3.9 Hz, 1H), 3.53 (t, J = 9.6 Hz, 1H), 3.43 (s, 1H), 2.42 – 2.33 (m, 1H), 1.97 (dd, J = 19.7, 9.8 Hz, 1H), 1.50 (s, 9H), ¹³C NMR (101 MHz, DMSO-*d*₆) δ 153.6, 144.5, 135.6, 128.3, 127.8, 127.2, 127.1, 126.8, 126.2, 126.1, 125.8, 123.9, 121.9, 121.7, 120.8, 120.2, 112.6, 80.5, 28.5, 27.9. ¹⁹F NMR (376 MHz, DMSO-*d*₆) δ -60.8, HR-MS (ESI) *m/z*, calculated for [M+H]⁺: 522.1842; found: 522.1875.

2.15. Synthesis of PQ-Ph-AC-PY

The title compound was synthesized using the same method as for **PQ-Ph-CF₃-PY** using **PQ-Ph-AC** (30 mg, 0.092 mmol) to obtain **PQ-Ph-AC-PY** as a colourless powder (30 mg, 0.061 mmol, yield 66%). ¹H NMR (400 MHz, DMSO-*d*₆) δ 9.10 (s, 1H), 9.04 – 8.97 (m, 1H), 8.17 (d, J = 8.5 Hz, 1H), 8.11 – 8.02 (m, 6H), 7.74 – 7.58 (m, 2H), 5.71 (d, J = 11.8 Hz, 1H), 5.23 – 5.14 (m, 1H), 3.54 (t, J = 9.6 Hz, 1H), 3.43 (s, 1H), 2.63 (s, 3H), 2.38 (dt, J = 13.5, 6.7 Hz, 1H), 2.04 – 1.93 (m, 1H), 1.50 (d, J = 3.0 Hz, 9H), ¹³C NMR (101 MHz, DMSO-*d*₆) δ 202.2, 198.0, 163.4, 153.6, 144.8, 136.0, 135.9, 129.4, 129.3, 127.8, 127.7, 127.2, 127.0, 126.8, 126.3, 125.9, 123.9, 121.7, 80.5, 42.3, 28.5, 27.9, 27.3. HR-MS (ESI) *m/z*, calculated for [M+Na]⁺: 518.1938; found: 518.1933.

2.16. Synthesis of PQ-Ph-CN-PY

The title compound was synthesized using the same method as for **PQ-Ph-CF₃-PY** using **PQ-Ph-CN** to obtain **PQ-Ph-CN-PY** as a colourless powder (30 mg, 0.063 mmol, yield 60%). ¹H NMR (400 MHz, CD₃CN-*d*₃) δ 8.93 (d, *J* = 2.0 Hz, 1H), 8.82 (d, *J* = 8.6 Hz, 1H), 8.26 – 8.13 (m, 2H), 8.00 (d, *J* = 8.5 Hz, 2H), 7.96 – 7.90 (m, 1H), 7.86 (s, 2H), 7.73 – 7.59 (m, 2H), 5.72 (d, *J* = 14.4 Hz, 1H), 5.08 (ddt, *J* = 10.6, 6.7, 3.1 Hz, 1H), 3.59 (t, *J* = 9.9 Hz, 1H), 3.55 – 3.43 (m, 1H), 2.44 – 2.35 (m, 1H), 2.16 – 2.07 (m, 1H), 1.57 (s, 9H). ¹³C NMR (101 MHz, CD₃OD-*d*₄) δ 145.3, 135.5, 132.7, 127.9, 127.3, 127.0, 126.9, 126.7, 126.7, 126.5, 126.2, 126.1, 125.8, 125.4, 125.3, 123.00, 121.6, 121.3, 120.5, 118.9, 110.6, 80.4, 29.4, 27.6, 27.0. HR-MS (ESI) *m/z*, calculated for [M+Na]⁺: 501.1784; found: 501.1780.

2.17. Synthesis of PQ-Ph-COOCH₃-PY

The title compound was synthesized using the same method as for **PQ-Ph-CF₃-PY** using **PQ-Ph-COOCH₃** (25 mg, 0.074 mmol) to obtain **PQ-Ph-COOCH₃-PY** as colourless powder (20 mg, 0.049 mmol, yield 66%). ¹H NMR (400 MHz, CD₃CN-*d*₃) δ 8.97 (d, *J* = 1.4 Hz, 1H), 8.84 (d, *J* = 8.3 Hz, 1H), 8.23 (d, *J* = 8.5 Hz, 1H), 8.19 – 8.16 (m, 1H), 8.14 (d, *J* = 8.4 Hz, 2H), 7.97 (d, *J* = 8.4 Hz, 3H), 7.72 – 7.61 (m, 2H), 5.73 (s, 1H), 5.09 (ddd, *J* = 10.6, 6.9, 3.9 Hz, 1H), 3.60 (t, *J* = 9.9 Hz, 1H), 3.51 (s, 1H), 2.40 (ddd, *J* = 9.7, 9.0, 4.5 Hz, 1H), 2.21 – 2.08 (m, 4H), 1.57 (s, 9H). ¹³C NMR (101 MHz, CD₃CN-*d*₃) δ 166.6, 145.4, 136.2, 129.9, 129.1, 127.4, 127.3, 126.9, 126.8, 126.3, 126.0, 125.4, 125.3, 123.0, 121.4, 121.3, 120.6, 80.4, 51.7, 27.6. HR-MS (ESI) *m/z*, calculated for [M+H]⁺: 512.2023; found: 512.2017.

2.18. Synthesis of PQ-Ph-F-PY

The title compound was synthesized using the same method as for **PQ-Ph-CF₃-PY** using **PQ-Ph-F** (23 mg, 0.076 mmol) to obtain **PQ-Ph-F-PY** as colourless powder (25 mg, 0.053 mmol,

yield 70%). ^1H NMR (400 MHz, $\text{DMSO-}d_6$) δ = 9.01 – 8.93 (m, 2H), 8.13 (d, J = 8.5 Hz, 1H), 8.08 (d, J = 7.7 Hz, 1H), 8.00 – 7.92 (m, 3H), 7.66 (d, J = 7.3 Hz, 1H), 7.64 – 7.57 (m, 1H), 7.33 (t, J = 8.8 Hz, 2H), 5.70 (d, J = 12.9 Hz, 1H), 5.16 (ddd, J = 10.4, 6.7, 3.9 Hz, 1H), 3.53 (t, J = 9.6 Hz, 1H), 3.42 (s, 1H), 2.41 – 2.31 (m, 1H), 2.05 – 1.93 (m, 1H), 1.50 (d, J = 2.4 Hz, 9H). ^{13}C NMR (101 MHz, $\text{DMSO-}d_6$) δ 163.6, 161.2, 153.7, 137.0, 136.4, 136.3, 129.6, 129.5, 127.7, 127.2, 127.1, 126.9, 126.8, 126.2, 126.0, 125.8, 125.7, 123.9, 121.5, 121.1, 120.7, 120.2, 116.3, 116.1, 112.6, 80.5, 28.5. ^{19}F NMR (376 MHz, $\text{DMSO-}d_6$) δ -111.5. HR-MS (ESI) m/z , calculated for $[\text{M}+\text{Na}]^+$: 494.1738; found: 494.1724.

2.19. Synthesis of PQ-Ph-Br-PY

The title compound was synthesized using the same method as for **PQ-Ph-CF₃-PY** using **PQ-Ph-Br** (30 mg, 0.081 mmol) to obtain **PQ-Ph-Br-PY** as colourless powder (30 mg, 0.056 mmol, yield 69%). ^1H NMR (400 MHz, $\text{DMSO-}d_6$) δ 9.01 (s, 1H), 8.96 (d, J = 8.2 Hz, 1H), 8.14 (d, J = 8.3 Hz, 1H), 8.08 (d, J = 7.7 Hz, 1H), 7.95 (d, J = 8.6 Hz, 1H), 7.89 (d, J = 8.1 Hz, 2H), 7.69 (d, J = 8.2 Hz, 3H), 7.65 – 7.57 (m, 1H), 5.70 (d, J = 11.2 Hz, 1H), 5.18 (dd, J = 8.7, 5.2 Hz, 1H), 3.53 (t, J = 9.3 Hz, 1H), 3.42 (s, 1H), 2.37 (dd, J = 11.9, 6.4 Hz, 1H), 2.04 – 1.93 (m, 1H), 1.50 (s, 9H). ^{13}C NMR (101 MHz, $\text{DMSO-}d_6$) δ 153.6, 139.6, 132.3, 132.2, 129.6, 129.5, 129.1, 127.7, 127.2, 127.1, 126.8, 126.0, 125.8, 123.9, 121.6, 121.4, 121.2, 120.2, 112.6, 80.5, 28.5, 27.9. HR-MS (ESI) m/z , calculated for $[\text{M}+\text{H}]^+$: 532.1118; found: 532.1147.

2.20. Synthesis of PQ-Ph-PY

The title compound was synthesized using the same method as for **PQ-Ph-CF₃-PY** using **PQ-Ph** (30 mg, 0.106 mmol) to obtain **PQ-Ph-PY** as colourless powder (35 mg, 0.077 mmol, yield 73%). ^1H NMR (400 MHz, $\text{DMSO-}d_6$) δ 8.99 (s, 1H), 8.96 (d, J = 8.3 Hz, 1H), 8.15 (d, J = 8.4 Hz, 1H), 8.08 (d, J = 7.8 Hz, 1H), 7.96 (dd, J = 8.6, 1.6 Hz, 1H), 7.91 (d, J = 7.2 Hz, 2H), 7.63 (dddd, J = 8.3, 6.2, 4.9, 4.4 Hz, 2H), 7.52 (t, J = 7.6 Hz, 2H), 7.43 – 7.37 (m, 1H), 5.70 (d, J =

11.2 Hz, 1H), 5.17 (ddd, $J = 10.4, 6.8, 3.9$ Hz, 1H), 3.53 (t, $J = 9.6$ Hz, 1H), 3.42 (s, 1H), 2.37 (dt, $J = 17.2, 6.1$ Hz, 1H), 2.05 – 1.93 (m, 1H), 1.51 (s, 10H). ^{13}C NMR (101 MHz, DMSO- d_6) δ 153.7, 140.5, 137.4, 129.4, 127.9, 127.7, 127.6, 127.2, 127.1, 126.8, 126.3, 125.7, 123.9, 121.5, 121.1, 120.8, 80.5, 28.5. HR-MS (ESI) m/z , calculated for $[\text{M}+\text{Na}]^+$: 476.1819; found: 476.1832.

2.21. Synthesis of PQ-Ph-CH₃-PY

The title compound was synthesized using the same method as for **PQ-Ph-CF₃-PY** using **PQ-Ph-CH₃** (34 mg, 0.113 mmol) to obtain **PQ-Ph-CH₃-PY** as colourless powder (40 mg, 0.086 mmol, yield 76%). ^1H NMR (400 MHz, DMSO- d_6) δ = 8.98 – 8.91 (m, 2H), 8.12 (d, $J = 8.4$ Hz, 1H), 8.08 (d, $J = 7.8$ Hz, 1H), 7.94 (dd, $J = 9.8, 5.0$ Hz, 1H), 7.81 (d, $J = 8.0$ Hz, 2H), 7.71 – 7.58 (m, 2H), 7.32 (d, $J = 8.0$ Hz, 2H), 5.70 (d, $J = 12.4$ Hz, 1H), 5.16 (ddd, $J = 10.3, 6.7, 3.9$ Hz, 1H), 3.53 (t, $J = 9.6$ Hz, 1H), 3.42 (s, 1H), 2.36 (s, 4H), 1.97 (dd, $J = 20.7, 10.1$ Hz, 1H), 1.50 (s, 9H). ^{13}C NMR (101 MHz, DMSO- d_6) δ 153.7, 137.6, 137.4, 137.3, 137.2, 130.0, 127.6, 127.4, 127.2, 127.1, 126.9, 126.8, 126.1, 125.8, 125.7, 123.8, 121.5, 120.7, 120.2, 112.6, 84.1, 80.5, 28.5, 27.9, 21.2. HR-MS (ESI) m/z , calculated for $[\text{M}+\text{H}]^+$: 467.2091; found: 467.2089.

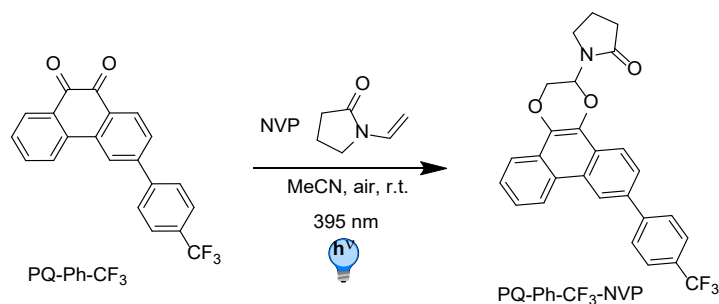
2.22. Synthesis of PQ-Ph-OCH₃-PY

The title compound was synthesized using the same method as for **PQ-Ph-CF₃-PY** using **PQ-Ph-OCH₃** (20 mg, 0.064 mmol) to obtain **PQ-Ph-OCH₃-PY** as colourless powder (20 mg, 0.041 mmol, yield 65%). ^1H NMR (400 MHz, DMSO- d_6) δ = 8.94 (d, $J = 7.3$ Hz, 2H), 8.09 (dd, $J = 16.3, 7.7$ Hz, 2H), 7.93 (dd, $J = 8.6, 1.6$ Hz, 1H), 7.86 (d, $J = 8.8$ Hz, 2H), 7.70 – 7.56 (m, 2H), 7.07 (d, $J = 8.8$ Hz, 2H), 5.70 (d, $J = 10.5$ Hz, 1H), 5.17 (s, 1H), 3.82 (s, 3H), 3.53 (t, $J = 9.6$ Hz, 1H), 3.42 (d, $J = 5.3$ Hz, 1H), 2.42 – 2.33 (m, 1H), 2.05 – 1.91 (m, 1H), 1.50 (s, 9H). ^{13}C NMR (151 MHz, DMSO- d_6) δ = 159.5, 153.7, 137.1, 132.9, 128.7, 127.6, 127.3, 126.9,

126.8, 126.0, 125.7, 123.9, 121.5, 120.8, 120.4, 114.9, 80.6, 55.7, 28.5. HR-MS (ESI) m/z , calculated for $[M+Na]^+$: 506.1938; found: 506.1922.

2.23. Synthesis of PQ-Ph-Amide-PY

The title compound was synthesized using the same method as for **PQ-Ph-CF₃-PY** using **PQ-Ph-Amide** (23 mg, 0.068 mmol) to obtain **PQ-Ph-Amide-PY** as colourless powder (22 mg, 0.043 mmol, yield 63%). ¹H NMR (400 MHz, DMSO-*d*₆) δ = 10.06 (s, 1H), 8.95 (d, J = 10.9 Hz, 2H), 8.10 (dd, J = 17.4, 8.1 Hz, 2H), 8.00 – 7.92 (m, 1H), 7.87 (d, J = 8.7 Hz, 2H), 7.73 (d, J = 8.6 Hz, 2H), 7.69 – 7.57 (m, 2H), 5.70 (d, J = 11.0 Hz, 1H), 5.20 – 5.13 (m, 1H), 3.53 (t, J = 9.4 Hz, 1H), 3.42 (s, 1H), 2.37 (dt, J = 11.5, 5.8 Hz, 1H), 2.07 (d, J = 2.6 Hz, 3H), 2.02 – 1.95 (m, 1H), 1.50 (s, 9H). ¹³C NMR (101 MHz, DMSO-*d*₆) δ 168.8, 153.7, 139.3, 136.9, 134.9, 127.7, 127.6, 127.2, 126.8, 125.9, 125.7, 123.4, 121.5, 120.5, 119.8, 80.5, 28.5, 28.1, 27.9, 24.5. HR-MS (ESI) m/z , calculated for $[M+H]^+$: 511.2227; found: 511.2215.



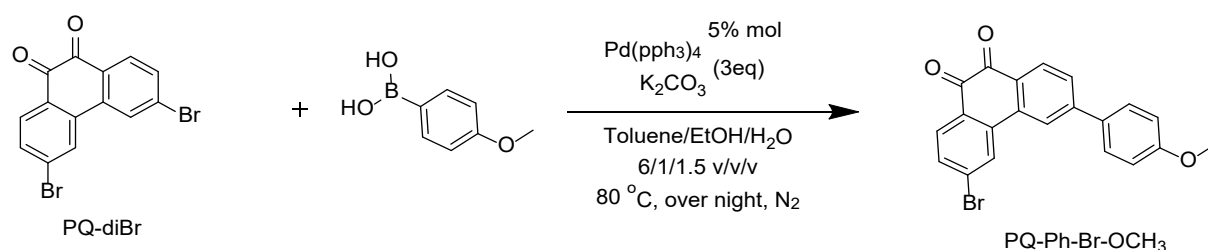
Scheme S4. Synthesis of **PQ-Ph-CF₃-NVP** compounds.

2.24. Synthesis of PQ-Ph-CF₃-NVP

The title compound was synthesized using the same method as for **PQ-Ph-CF₃-PY** using **PQ-Ph-CF₃** (45 mg, 0.128 mmol) to obtain **PQ-Ph-CF₃-NVP** as colourless solid (40 mg, 0.086 mmol, yield 67%). ¹H NMR (400 MHz, DMSO-*d*₆) δ 9.09 (d, J = 1.2 Hz, 1H), 8.99 (d, J = 7.9 Hz, 1H), 8.17 – 8.12 (m, 3H), 8.11 – 7.99 (m, 2H), 7.85 (d, J = 8.4 Hz, 2H), 7.70 – 7.60 (m, 2H), 6.08 (dd, J = 6.7, 2.5 Hz, 1H), 4.67 (dd, J = 11.3, 2.5 Hz, 1H), 4.54 (ddd, J = 11.3, 6.7, 2.2 Hz, 1H), 3.62 – 3.48 (m, 2H), 2.39 (t, J = 8.1 Hz, 2H), 2.04 – 1.96 (m, 2H). ¹³C NMR (101 MHz,

DMSO-*d*₆) δ 176.1, 144.5, 135.8, 135.8, 133.3, 133.3, 132.6, 132.5, 127.9, 127.8, 127.2, 127.0, 126.9, 126.7, 126.4, 126.2, 126.2, 126.1, 126.0, 125.5, 125.5, 124.0, 121.9, 121.8, 121.7, 120.9, 120.8, 75.5, 75.4, 65.6, 43.4, 30.8, 18.3. ¹⁹F NMR (376 MHz, DMSO-*d*₆) δ -60.8. HR-MS (ESI) *m/z*, calculated for [M+H]⁺: 464.1468; found: 464.1456.

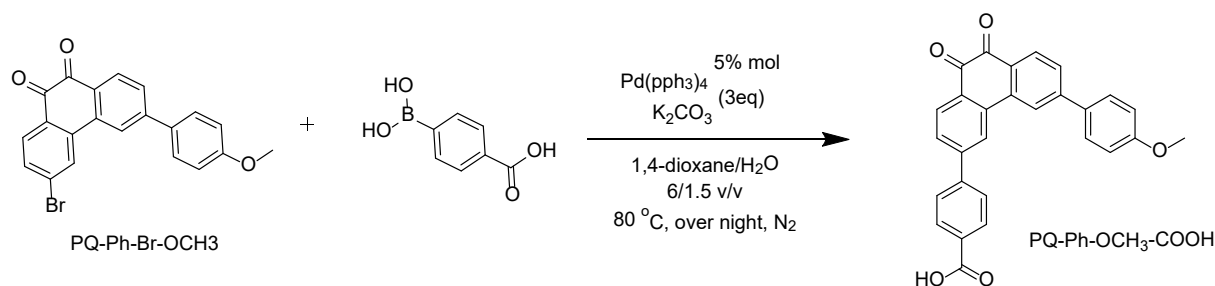
2.25. Synthesis of PQ-Ph-Br-OCH₃



Scheme S5. Synthesis of PQ-Ph-Br-OCH₃.

A Schlenk tube containing **PQ-diBr** (200 mg, 0.55 mmol), (4-methoxyphenyl)boronic acid (84 mg, 0.55 mmol), and Pd(PPh₃)₄ (32 mg, 0.0275 mmol) was evacuated and backfilled with N₂ three times. After the addition of degassed K₂CO₃ (228 mg in 3 mL H₂O), ethanol (2 mL), and toluene (12 mL), the tube was sealed under N₂ atmosphere and heated at 80 °C for 12 h. After being cooled to room temperature, the reaction mixture was diluted with dichloromethane, the phases were separated and the organic phase was washed with water and dried over anhydrous Na₂SO₄. Upon removal of solvents in vacuo, the residual was purified with column chromatography over silica gel eluting with EtOAc/DCM (1/5, v/v) to afford **PQ-Ph-Br-OCH₃** as a red solid (86 mg, 0.22 mmol, yield 40%). ¹H NMR (400 MHz, CDCl₃) δ 8.25 – 8.20 (m, 2H), 8.05 (dd, *J* = 5.9, 5.1 Hz, 2H), 7.68 – 7.60 (m, 4H), 7.05 (d, *J* = 8.8 Hz, 2H), 3.89 (s, 3H). ¹³C NMR (101 MHz, CDCl₃) δ 179.7, 179.1, 160.7, 148.6, 137.3, 134.8, 132.7, 131.8, 131.4, 129.8, 129.4, 128.6, 128.2, 127.1, 122.0, 114.7, 55.5. HR-MS (ESI) *m/z*, calculated for [M+H]⁺: 393.0121; found: 393.0119.

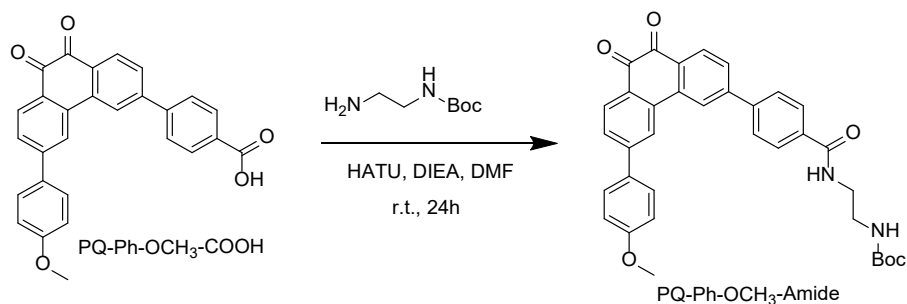
2.26. Synthesis of PQ-Ph-OCH₃-COOH



Scheme S6. Synthesis of PQ-Ph-OCH₃-Ph-COOH.

A Schlenk tube containing **PQ-Ph-Br-OCH₃** (80 mg, 0.55 mmol), 4-carboxyphenylboronic acid (84 mg, 0.55 mmol), and Pd(PPh₃)₄ (32 mg, 0.0275 mmol) was evacuated and backfilled with N₂ for three times. After the addition of degassed K₂CO₃ (228 mg in 3 mL H₂O), 1,4-dioxane (12 mL), the tube was sealed under N₂ atmosphere and heated at 80 °C for 12 h. After being cooled to room temperature, the reaction mixture was poured into 50 mL of distilled water, and then acidified to pH 2 with HCl (37%, aqueous). The yellow precipitated was filtered off, washed with acetone and DCM, and then dried under vacuum to obtain **PQ-Ph-OCH₃-Ph-COOH** (48 mg, 0.11 mmol, yield 55%). ¹H NMR (400 MHz, DMSO-*d*₆) δ 13.09 (s, 1H), 8.71 (s, 1H), 8.61 (s, 1H), 8.05 (dt, J = 8.5, 6.8 Hz, 6H), 7.89 (d, J = 8.7 Hz, 2H), 7.84 (d, J = 8.0 Hz, 1H), 7.77 (d, J = 8.2 Hz, 1H), 7.07 (d, J = 8.8 Hz, 2H), 3.82 (s, 3H). ¹³C NMR (101 MHz, DMSO-*d*₆) δ 179.4, 179.0, 167.5, 160.5, 147.1, 146.1, 143.3, 136.4, 136.1, 131.3, 131.2, 131.1, 130.5, 130.3, 130.0, 129.3, 128.4, 128.2, 127.6, 127.5, 123.8, 122.7, 114.9, 55.7, 31.2. HR-MS (ESI) *m/z*, calculated for [M+H]⁺: 435.1227; found: 435.1221

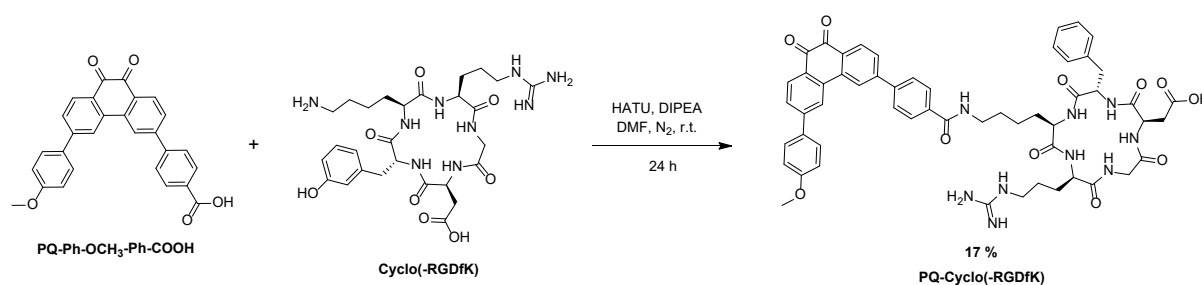
2.27. Synthesis of PQ-Ph-OCH₃-Ph-Amide



Scheme S7. Synthesis procedure of **PQ-Ph-OCH₃-Ph-Amide**.

A Schlenk tube containing **PQ-Ph-OCH₃-Ph-COOH** (100 mg, 0.23 mmol), HATU (87 mg, 0.23 mmol), and *N,N*-Diisopropylethylamine (DIPEA, 60 mg, 0.46 mmol) and 5 mL dry DMF was evacuated and backfilled with N₂ for three times. After stirring for 15 min, *N*-Boc-ethylenediamine (44 mg, 0.28 mmol) was added to the reaction mixture and stirring overnight under room temperature. The reaction progress was followed by UPLC-MS, and after full conversion, the reaction mixture was poured into 50 mL of brine, the yellow precipitate was filtered off and purified by column chromatography over silica gel eluted with EtOAc/DCM (1/5, v/v) to obtain **PQ-Ph-OCH₃-Ph-Amide** (70 mg, 0.13 mmol, yield 55%). ¹H NMR (400 MHz, CDCl₃) δ 8.20 (d, *J* = 8.8 Hz, 2H), 8.14 (s, 1H), 7.98 (d, *J* = 7.9 Hz, 2H), 7.71 (d, *J* = 7.8 Hz, 2H), 7.62 (t, *J* = 8.3 Hz, 4H), 7.53 (s, 1H), 7.03 (d, *J* = 8.4 Hz, 2H), 5.15 (t, *J* = 5.6 Hz, 1H), 3.88 (s, 3H), 3.65 – 3.57 (m, 2H), 3.45 (d, *J* = 4.4 Hz, 2H), 1.44 (s, 9H). ¹³C NMR (101 MHz, CDCl₃) δ 180.0, 179.6, 167.0, 160.6, 148.4, 147.5, 142.3, 136.2, 135.8, 134.5, 131.6, 131.3, 131.1, 130.2, 129.3, 128.6, 128.3, 127.9, 127.8, 127.4, 122.6, 121.9, 114.6, 80.1, 55.5, 42.5, 39.9, 28.4. HR-MS (ESI) *m/z*, calculated for [M+Na]⁺: 599.2152; found: 599.2134.

2.28. Synthesis of PQ-Cyclo(-RGDfK)



Scheme S8. Synthesis of PQ-Cyclo(-RGDfK).

A Schlenk tube containing **PQ-Ph-OCH₃-Ph-COOH** (3.5 mg, 0.08 mmol), HATU (3.1 mg, 0.08 mmol), and *N,N*-Diisopropylethylamine (DIPEA, 2.1 mg, 0.16 mmol) and 1 mL dry DMF was evacuated and backfilled with N₂ for three times. After stirring for 15 min, **Cyclo(RGDfK)** solution (5 mg, 0.06 mmol, in 1.5 mL dry DMF) was added to the reaction mixture and stirred overnight under room temperature. The reaction progress was followed by UPLC-MS. After completion, the volatiles were evaporated *in vacuo* and the resulting residue was purified by preparative HPLC (gradient of 10→90% MeCN (with 0.1% formic acid) in water (with 0.1% formic acid) over 35 min) and lyophilized to afford **PQ-Cyclo(RGDfK)** an orange powder (1.04 mg, 17% yield). HR-MS (ESI) *m/z*, calculated for [M+H]⁺: 1020.4250 ; found: 1020.4238.

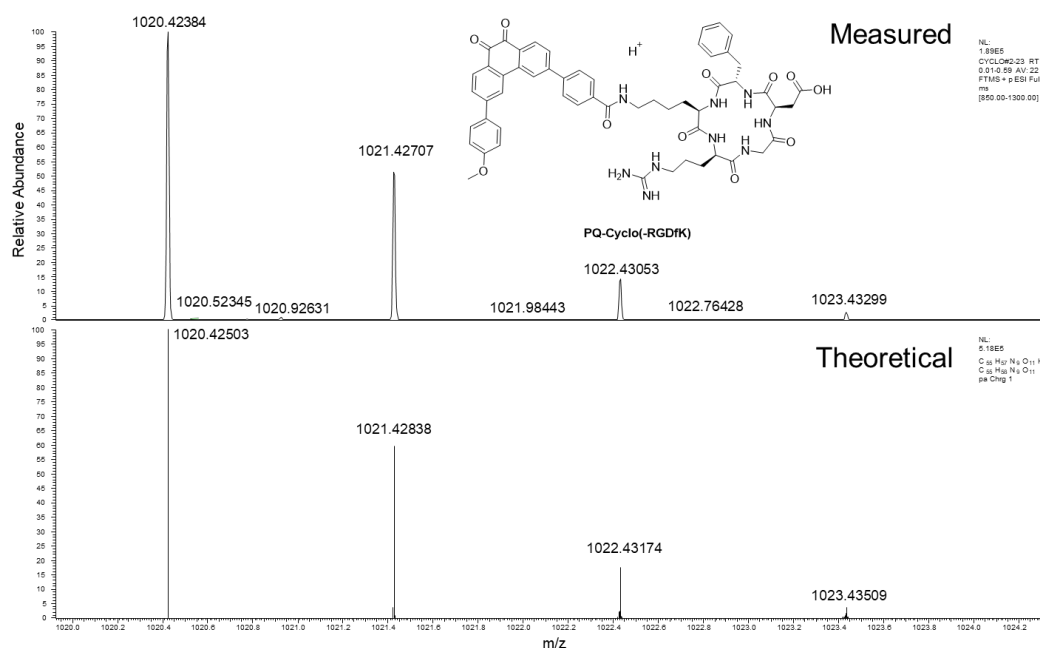
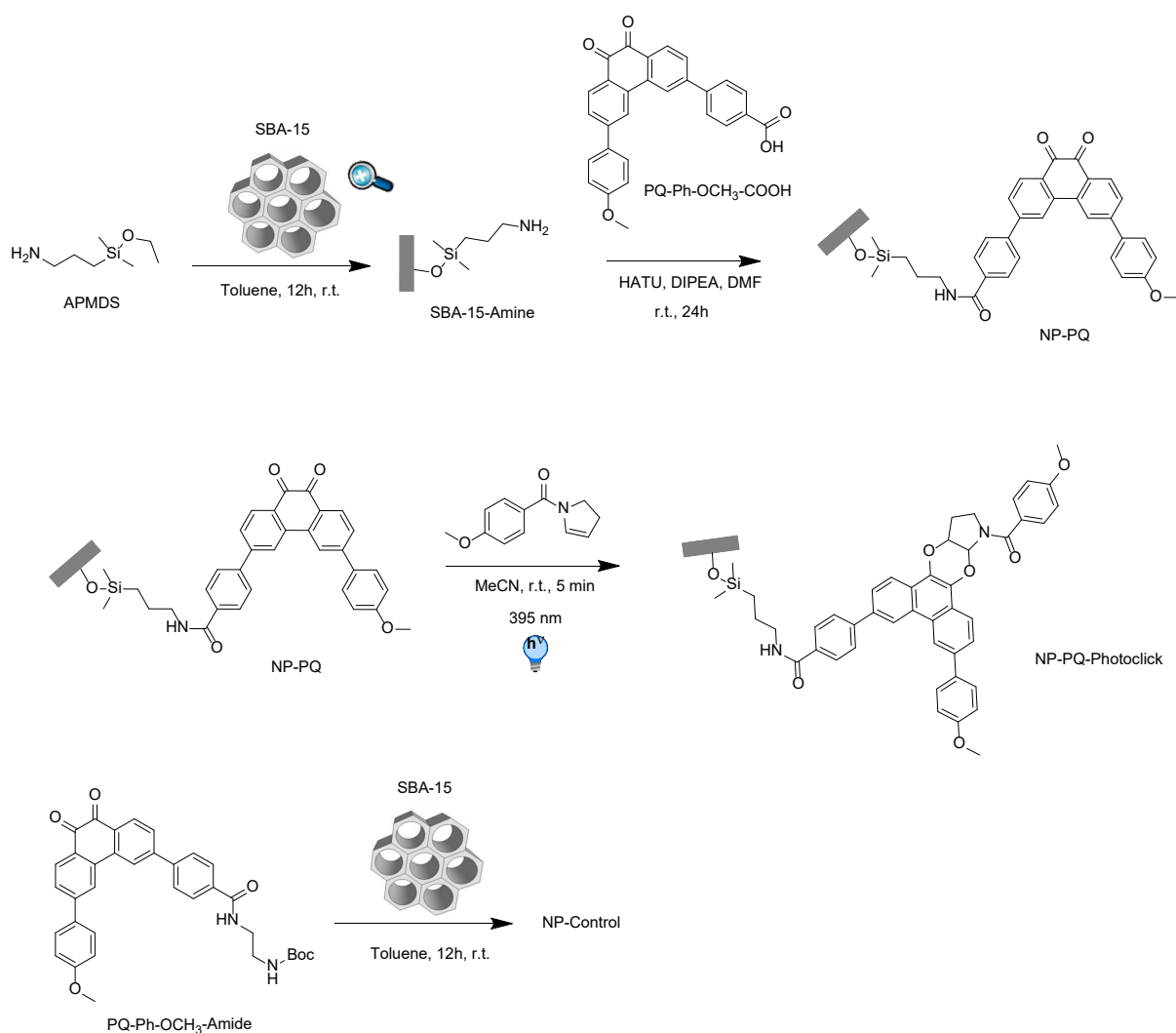


Fig. S2. HR-MS of **PQ-Cyclo(RGDfK)** (top: measured; bottom: simulated).

2.29. Synthesis of NP-PQ and NP-Control



Scheme S9. Synthesis procedure of NP-PQ, NP-Photoclick, and NP-Control.

The functionalization of SBA-15 was based on literature.^[5] SBA-15 nanoparticles (200 mg) were added to a flame-dried schlenk flask, which was subsequently heated at 80 °C overnight to obtain activated SBA-15 nanoparticles. Then, 100 mg of activated nanoparticles was added to 15 mL dry toluene (containing wt 0.02% of 3-(ethoxydimethylsilyl)propylamine (APDMS)), overnight to obtain SBA-15-amine nanoparticle.

A Schlenk tube containing **PQ-Ph-OCH₃-Ph-COOH** (10 mg, 0.023 mmol), HATU (9 mg, 0.023 mmol), and *N,N*-Diisopropylethylamine (DIPEA, 8 μL, 0.046 mmol) and 5 mL dry DMF was evacuated and backfilled with N₂ three times. After stirring for 15 min, 30 mg SBA-15-amine nanoparticle was added to the reaction mixture and stirred at room temperature overnight.

After the reaction was completed, the nanoparticles were washed with DMF, water, and acetone three times to obtain 25 mg of **NP-PQ**.

For the on-surface photoclick reaction, 15 mg of **NP-PQ** and 10 mg of **OMe-BZPY** were added to 10 mL MeCN. Then, the mixture was irradiated by the hand-held UV light lamp (395 nm, 88 mW cm⁻²) at a fixed distance. The reaction was followed by HPLC till the concentration of **OMe-BZPY** shown no change. Subsequently, the nanoparticles were washed with MeCN, water, and acetone three times to obtain 10 mg of **NP-PQ-Photoclick**. The control, **NP-Control**, was synthesized analogous to **NP-PQ** using **PQ-Ph-OCH₃-Ph-Amide** and SBA-15-Amine.

3. NMR Spectra

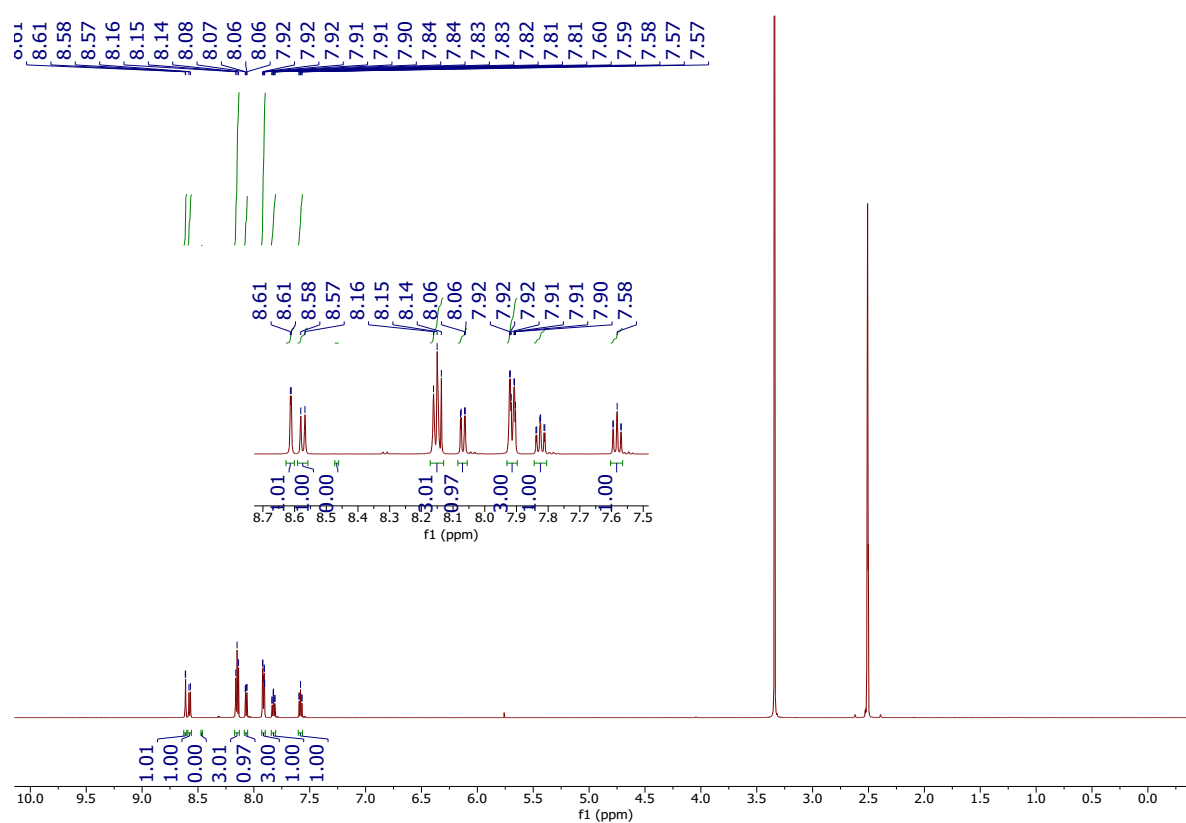


Fig. S3. ¹H NMR of PQ-Ph-CF₃ in DMSO-*d*₆.

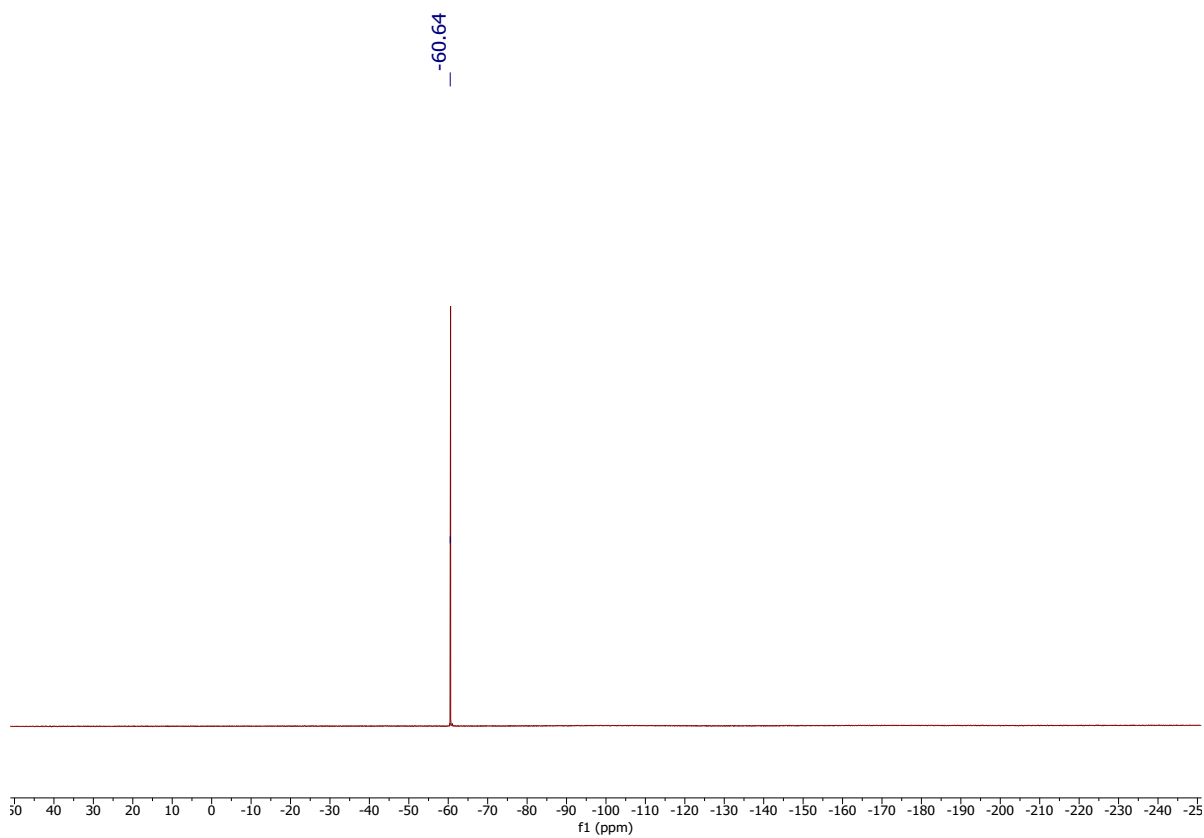


Fig. S4. ¹⁹F NMR of PQ-Ph-CF₃ in DMSO-*d*₆.

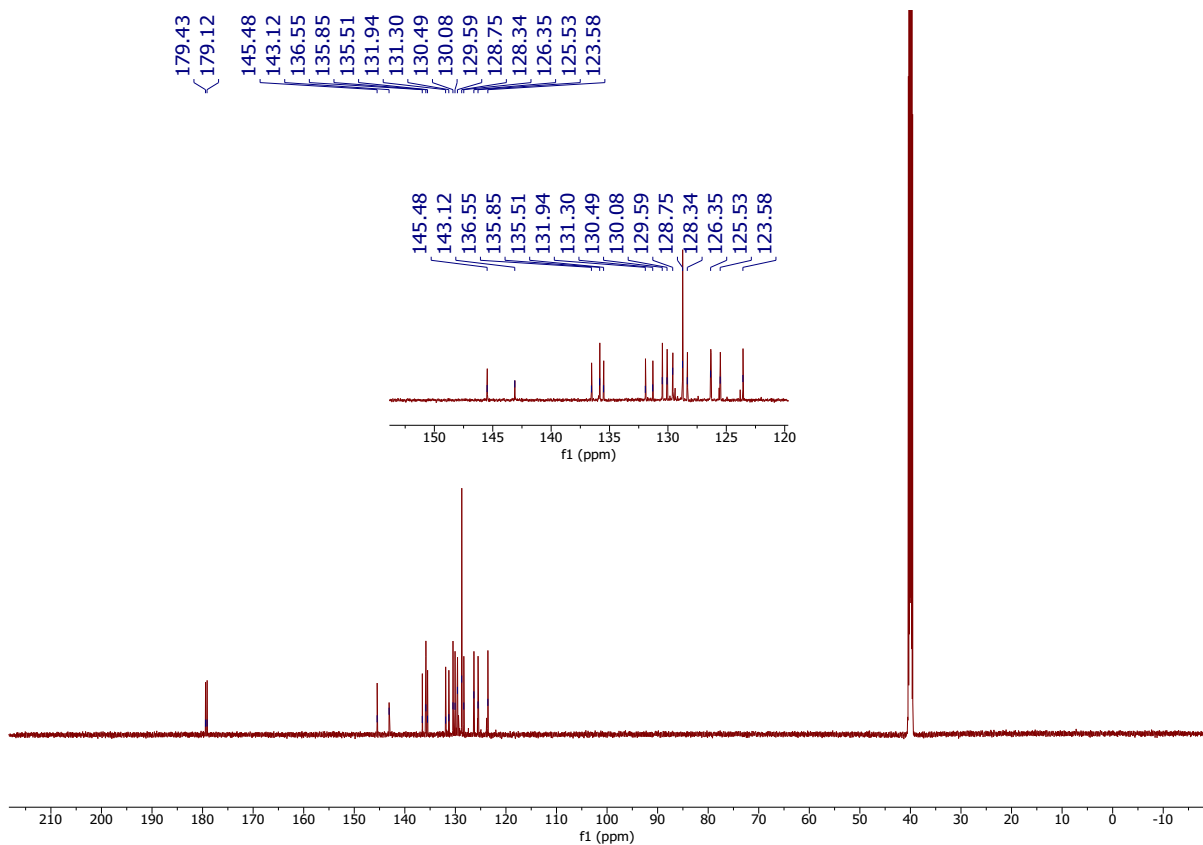


Fig. S5. ^{13}C NMR of PQ-Ph- CF_3 in $\text{DMSO-}d_6$.

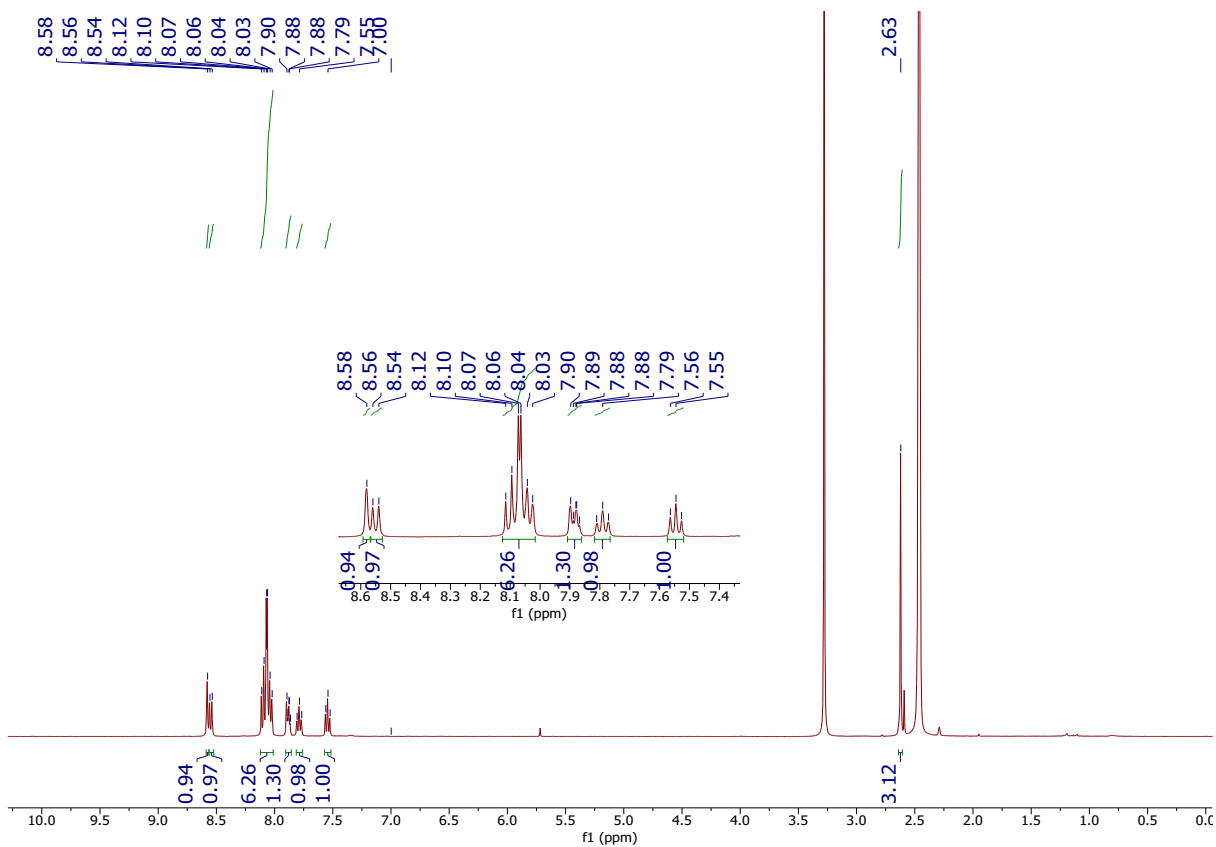


Fig. S6. ^1H NMR of PQ-Ph- COCH_3 in $\text{DMSO-}d_6$.

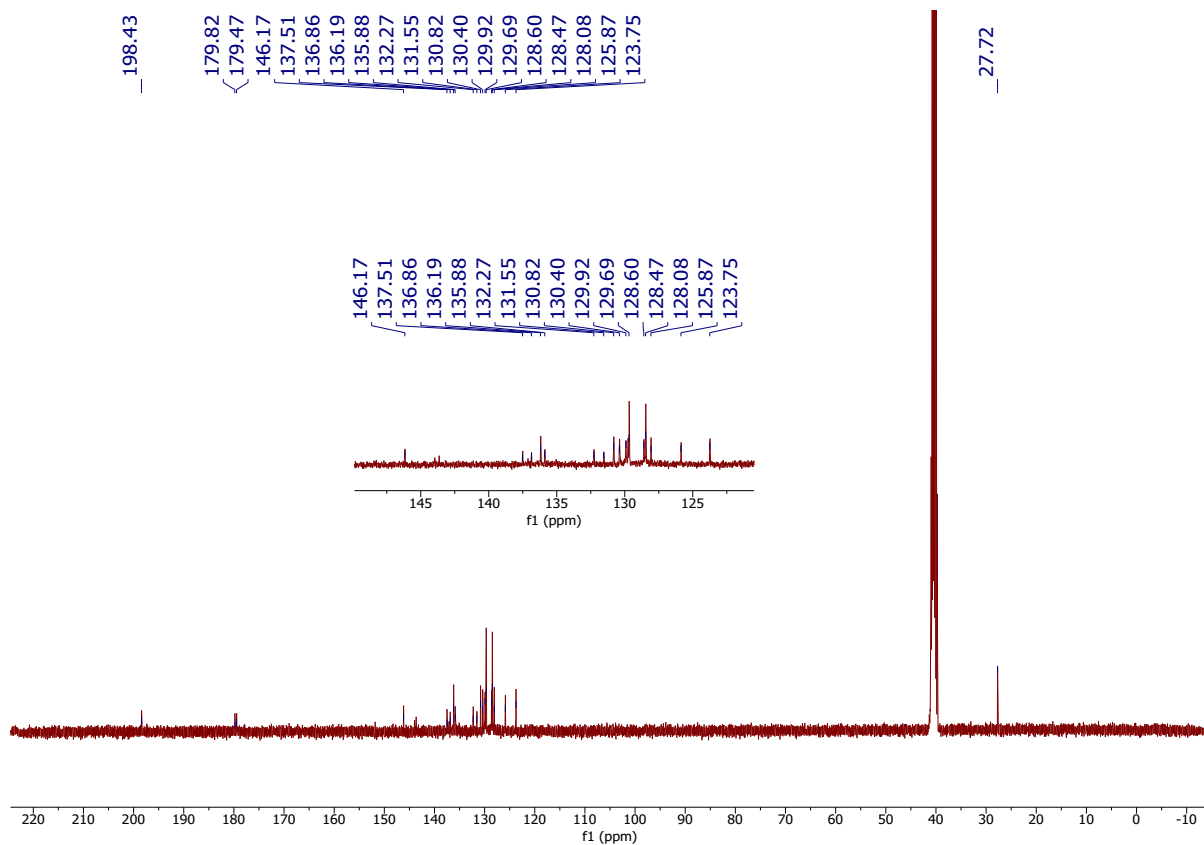


Fig. S7. ^{13}C NMR of PQ-Ph-COCH₃ in DMSO-*d*₆.

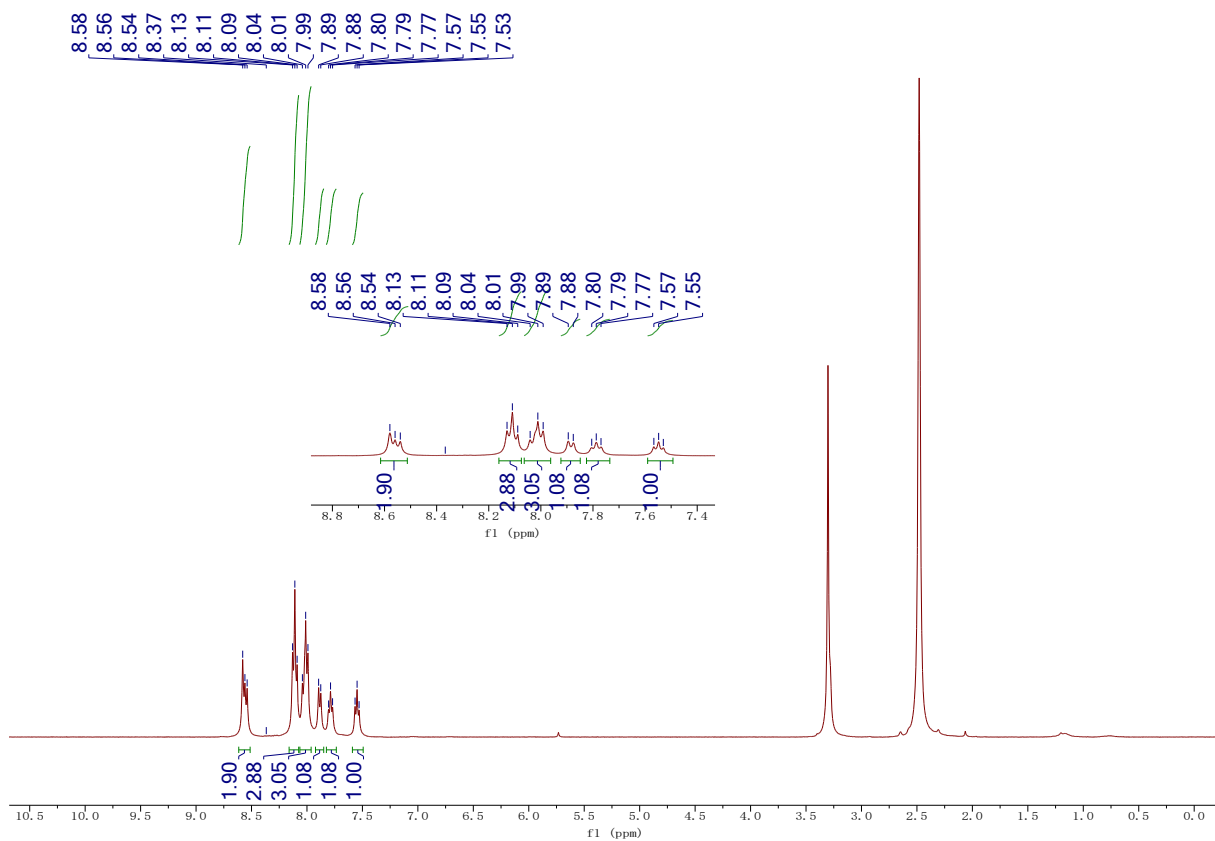


Fig. S8. ^1H NMR of PQ-Ph-CN in DMSO-*d*₆.

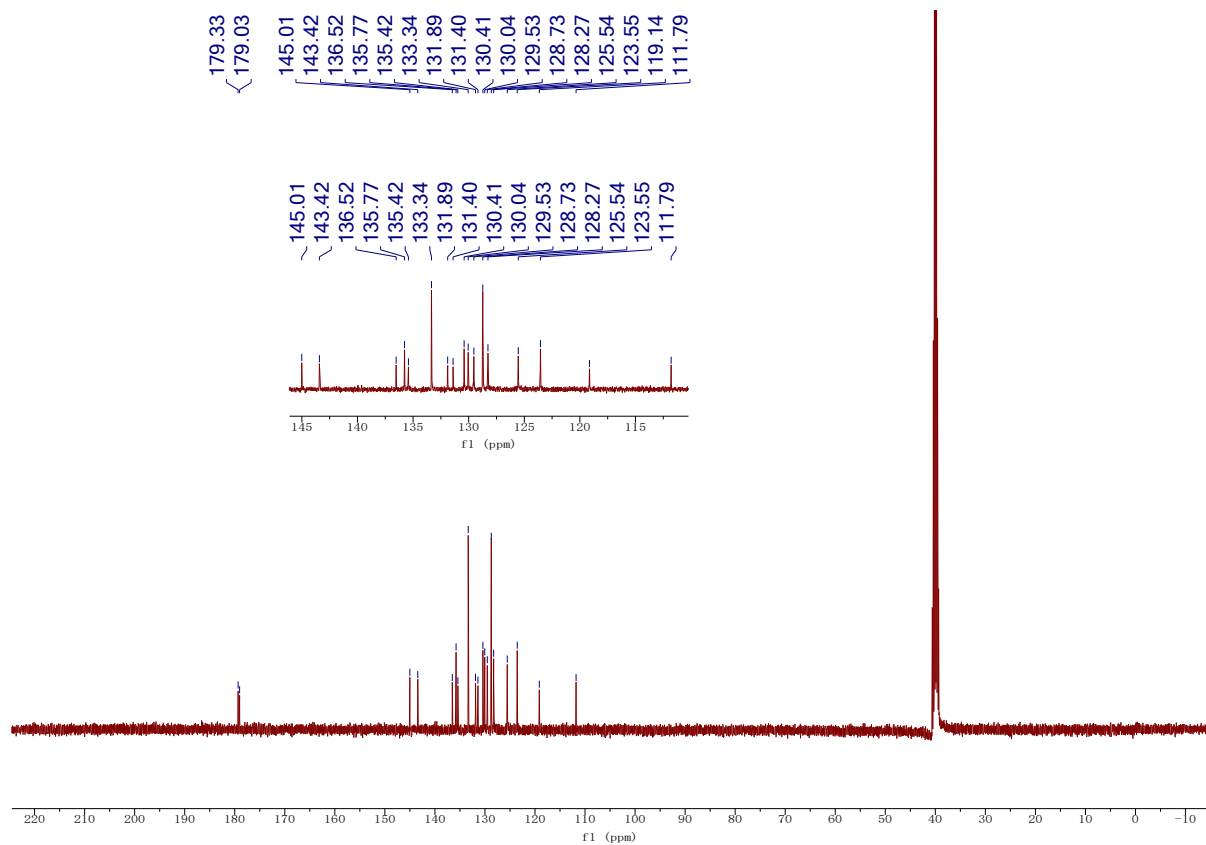


Fig. S9. ^{13}C NMR of PQ-Ph-CN in $\text{DMSO-}d_6$.

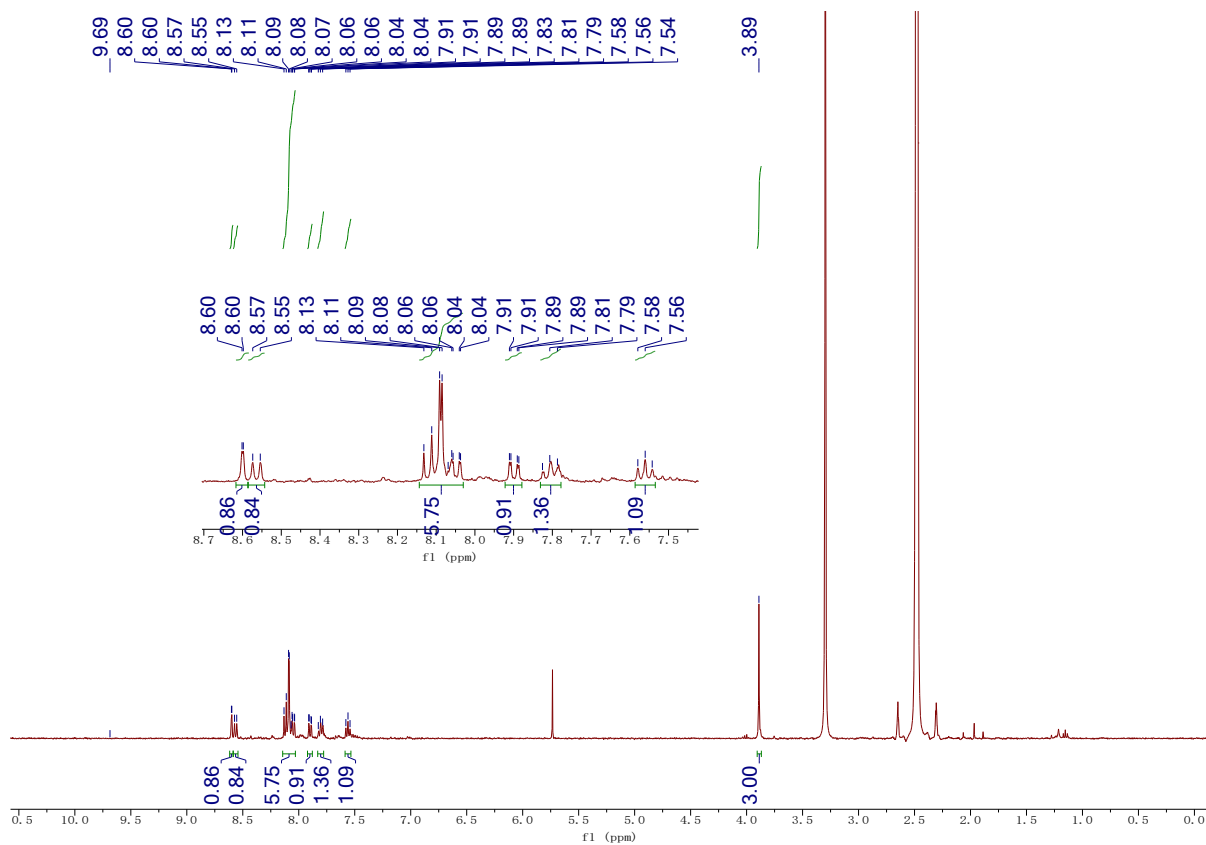


Fig. S10. ^1H NMR of PQ-Ph-COOCH₃ in $\text{DMSO-}d_6$.

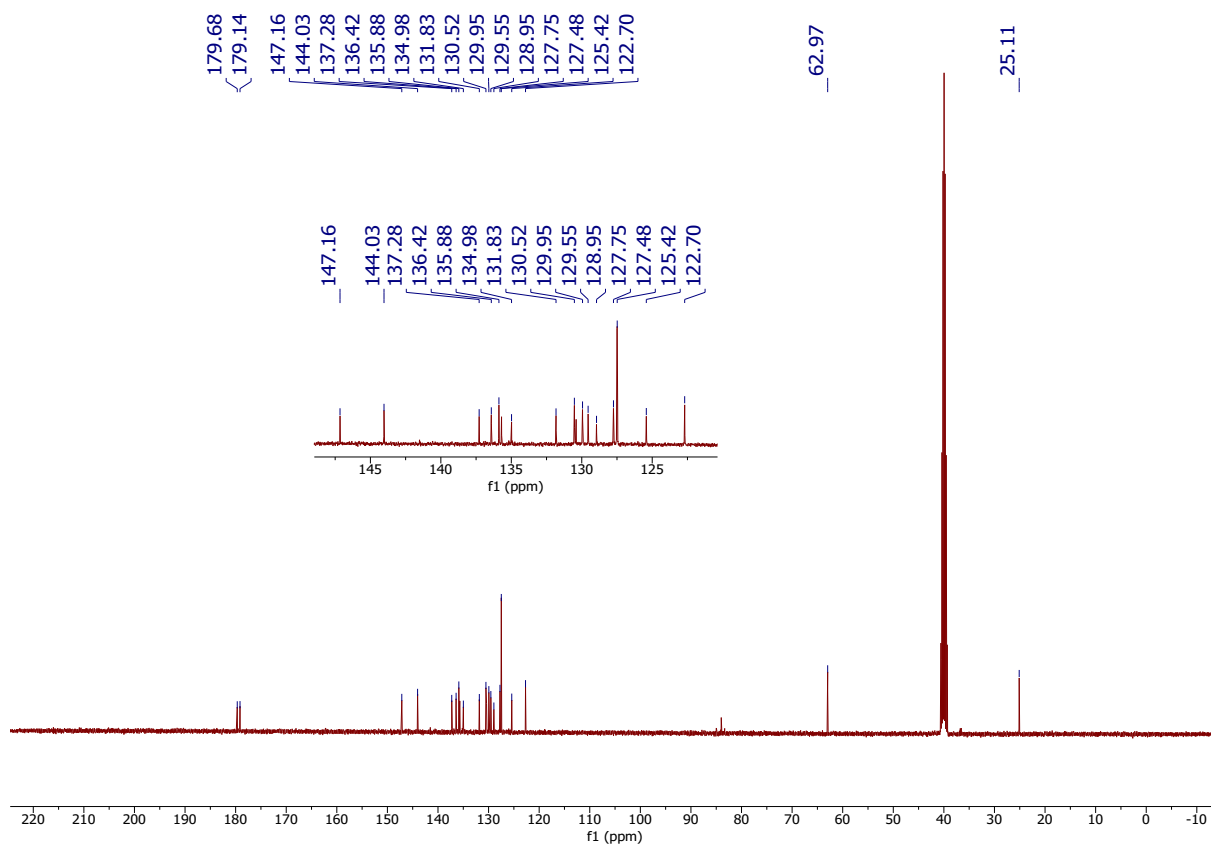


Fig. S11. ^{13}C NMR of PQ-Ph-COOCH₃ in DMSO-*d*₆.

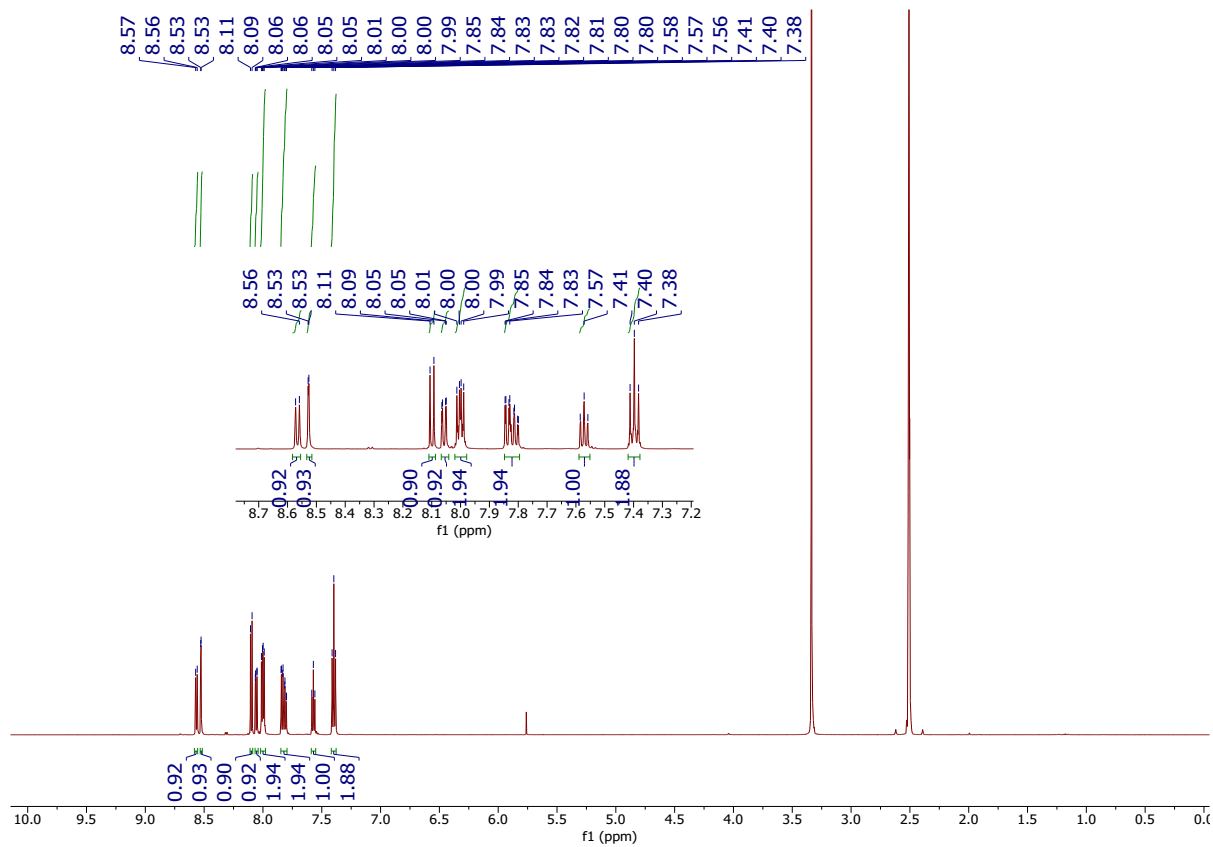


Fig. S12. ^1H NMR of PQ-Ph-F in DMSO-*d*₆.

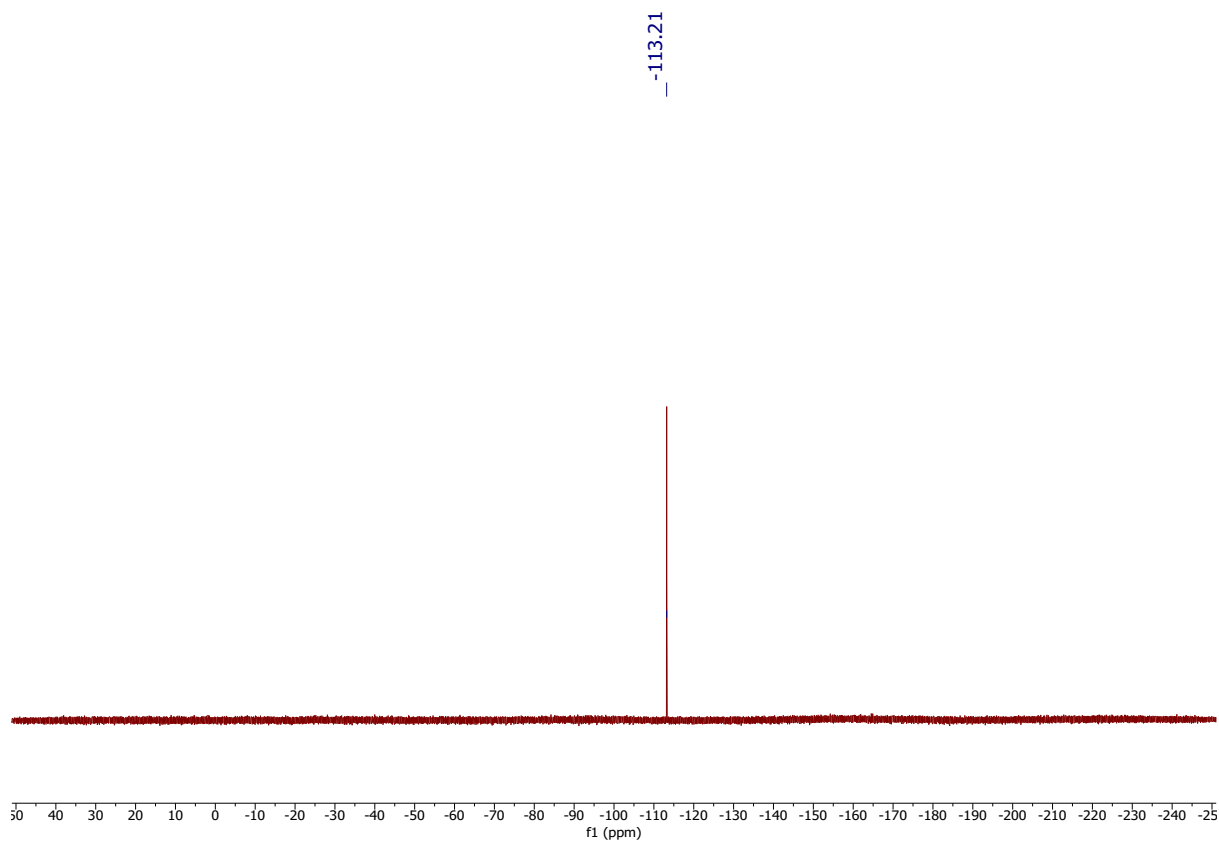


Fig. S13. ¹⁹F NMR of PQ-Ph-F in DMSO-*d*₆.

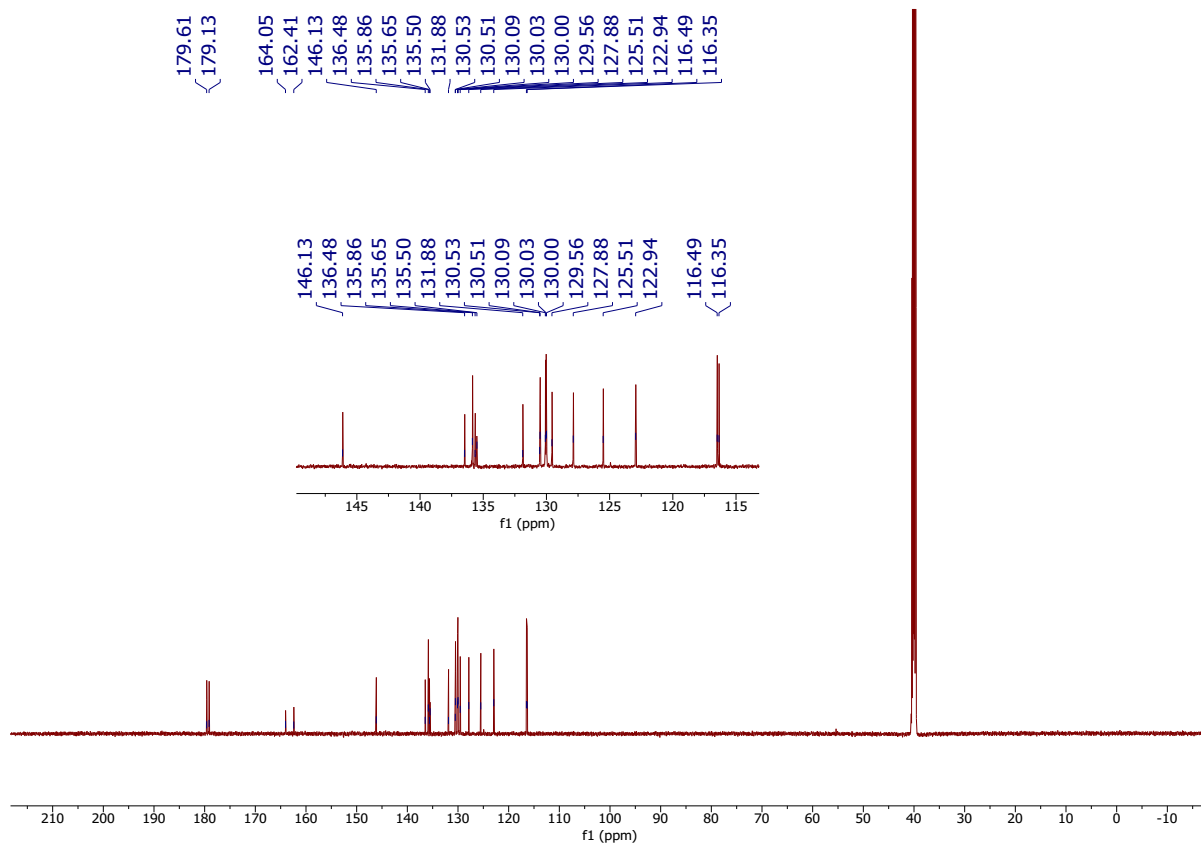


Fig. S14. ¹³C NMR of PQ-Ph-F in DMSO-*d*₆.

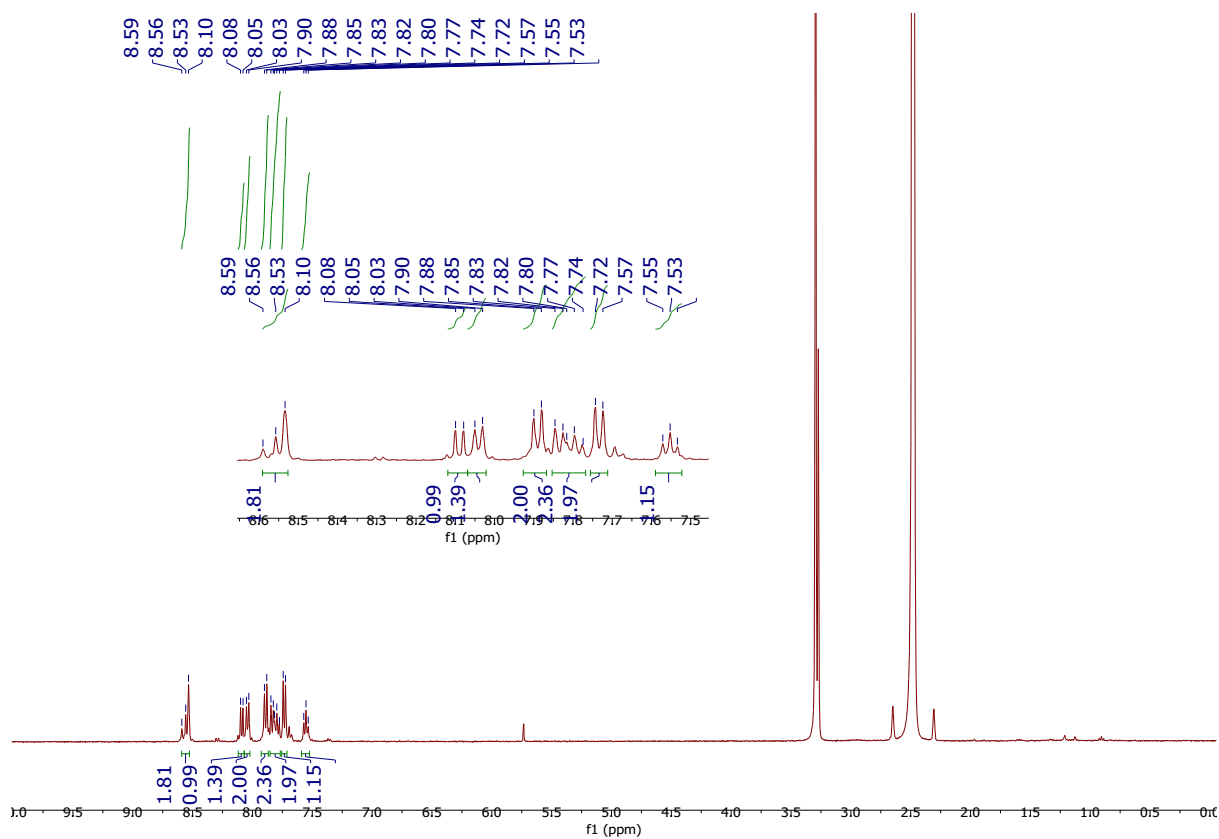


Fig. S15. ^1H NMR of PQ-Ph-Br in $\text{DMSO-}d_6$.

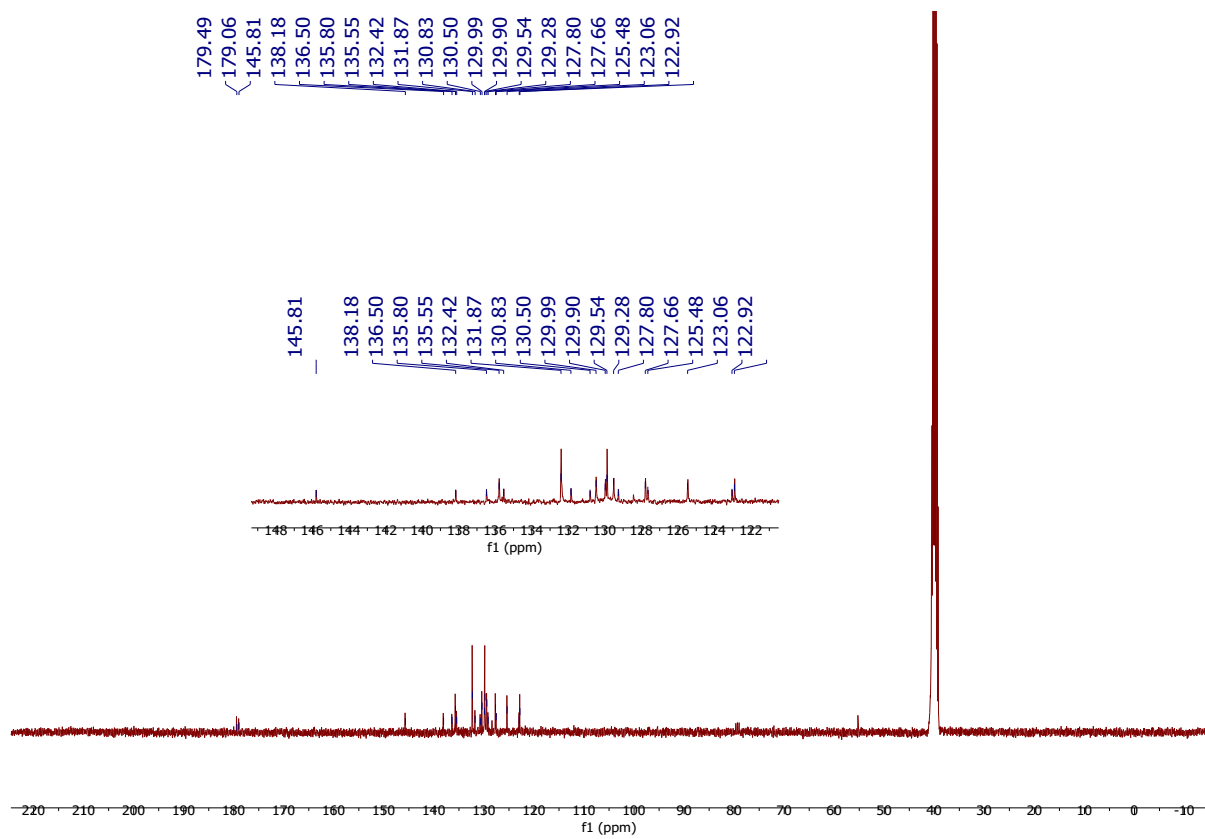


Fig. S16. ^{13}C NMR of PQ-Ph-Br in $\text{DMSO-}d_6$.

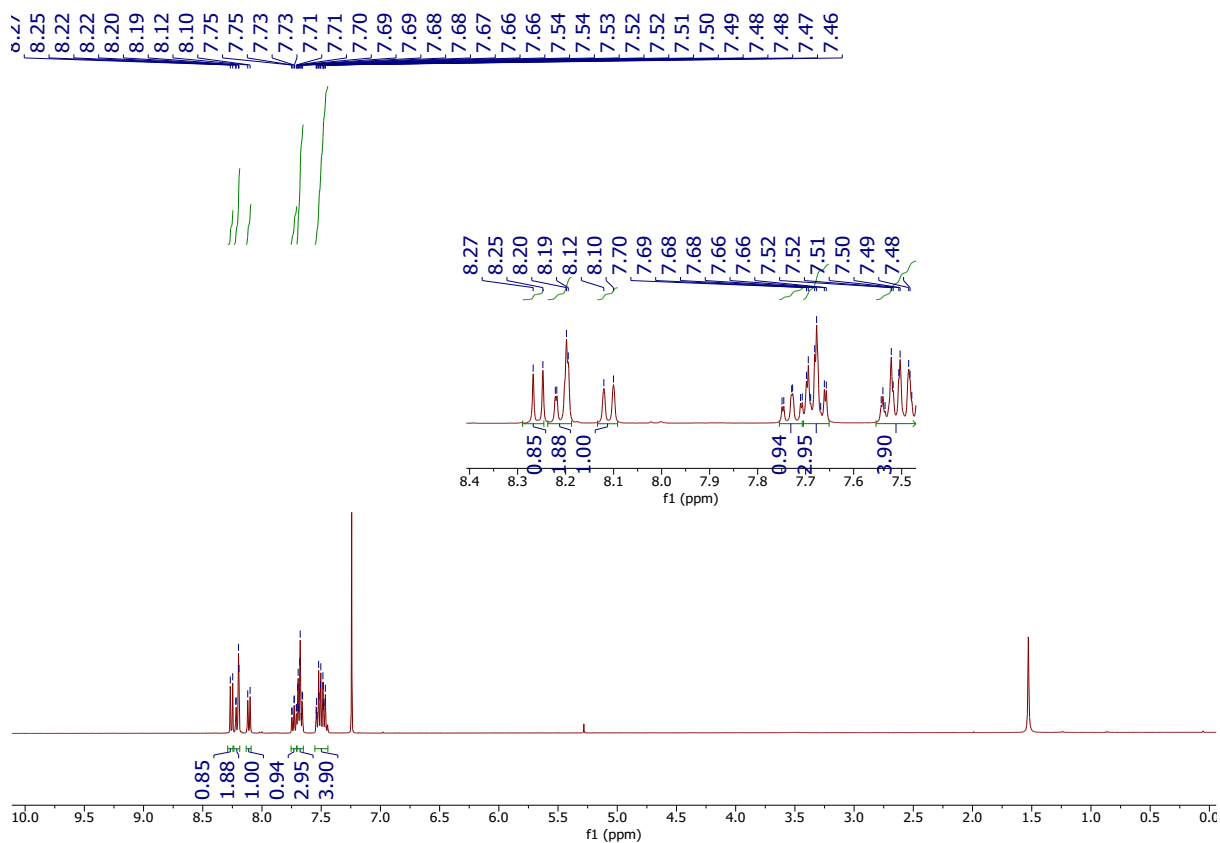


Fig. S17. ^1H NMR of PQ-Ph in CDCl_3 .

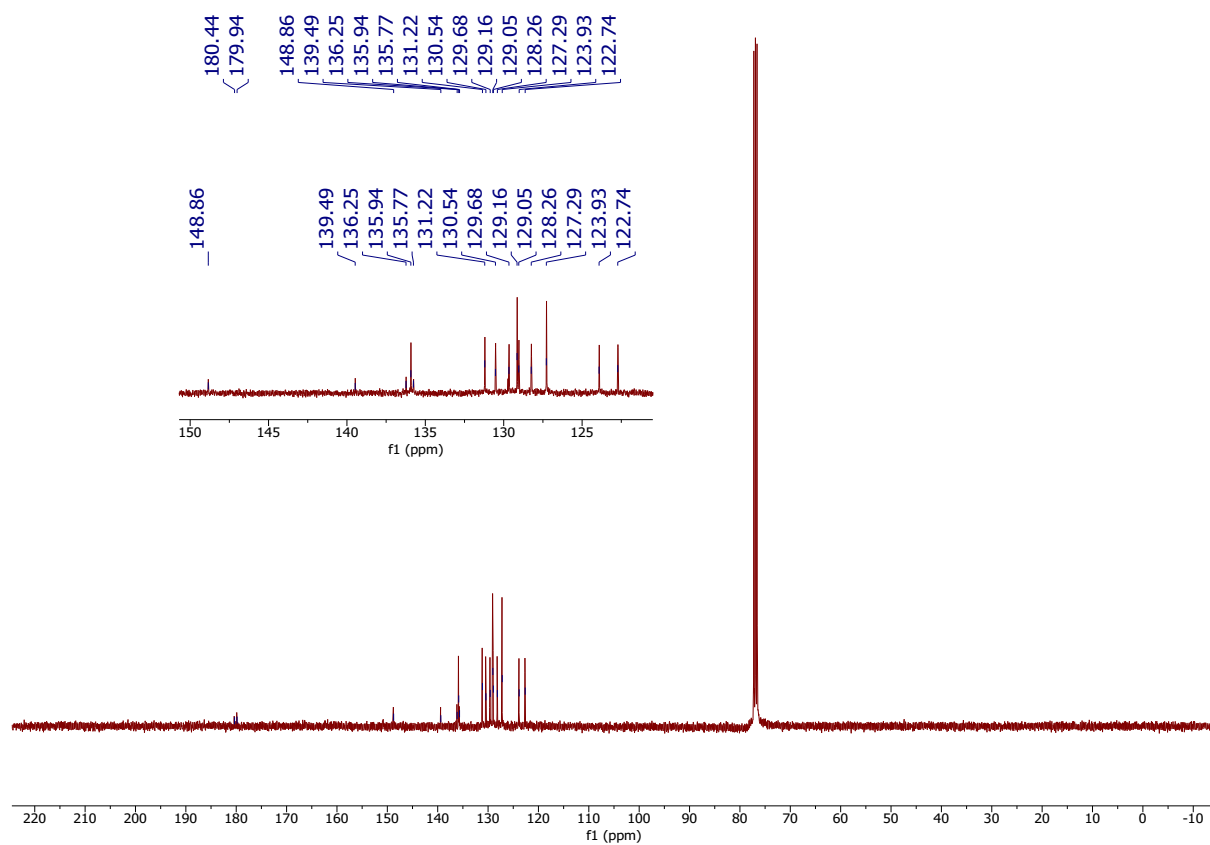


Fig. S18. ^{13}C NMR of PQ-Ph in CDCl_3 .

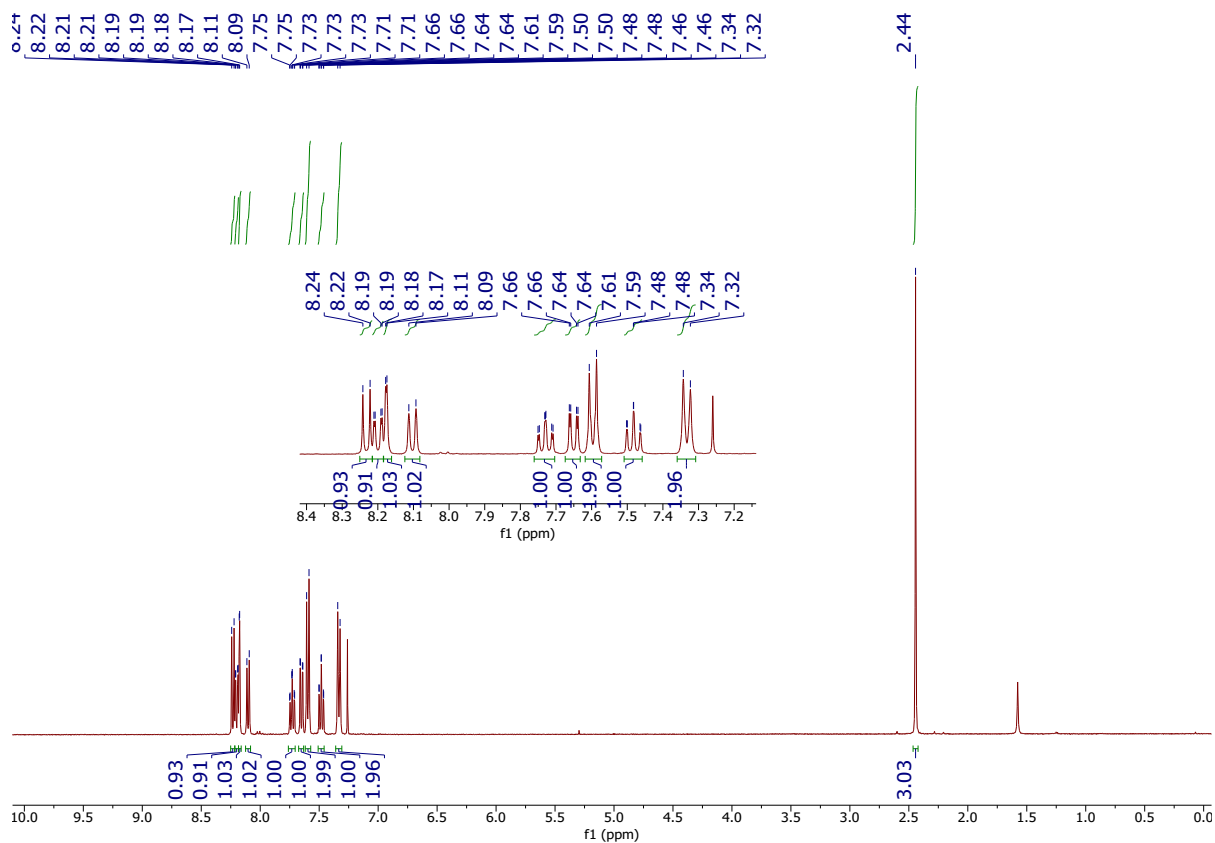


Fig. S19. ^1H NMR of PQ-Ph-CH₃ in CDCl₃.

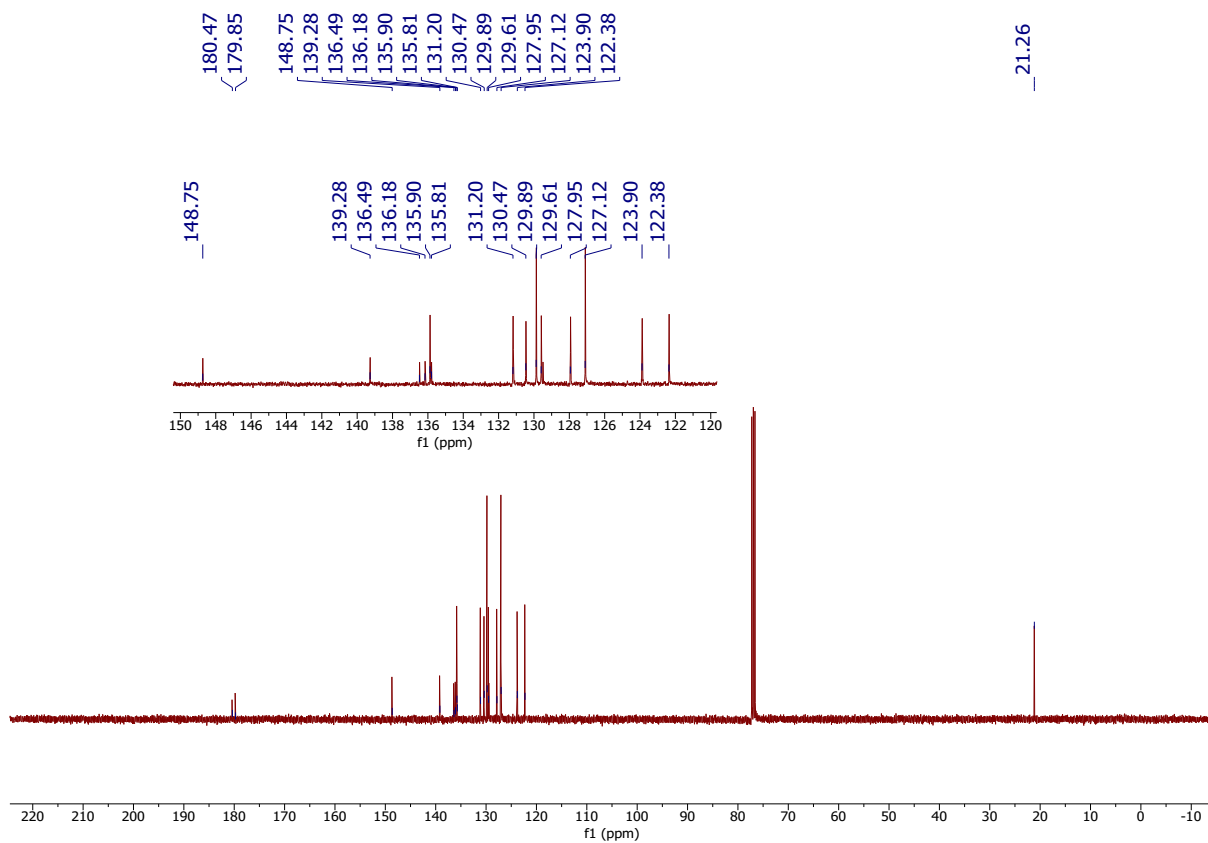


Fig. S20. ^{13}C NMR of PQ-Ph-CH₃ in CDCl₃.

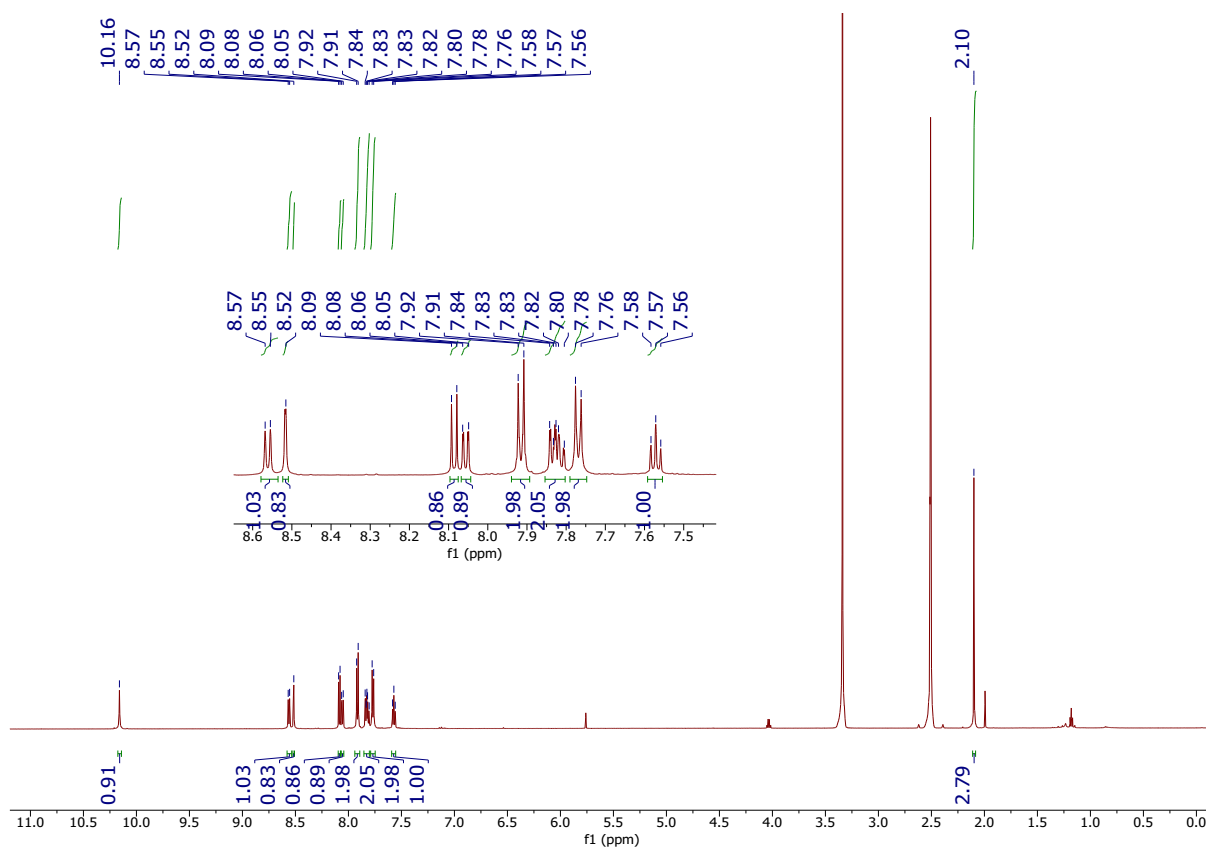


Fig. S21. ^1H NMR of **PQ-Ph-Amide** in $\text{DMSO-}d_6$.

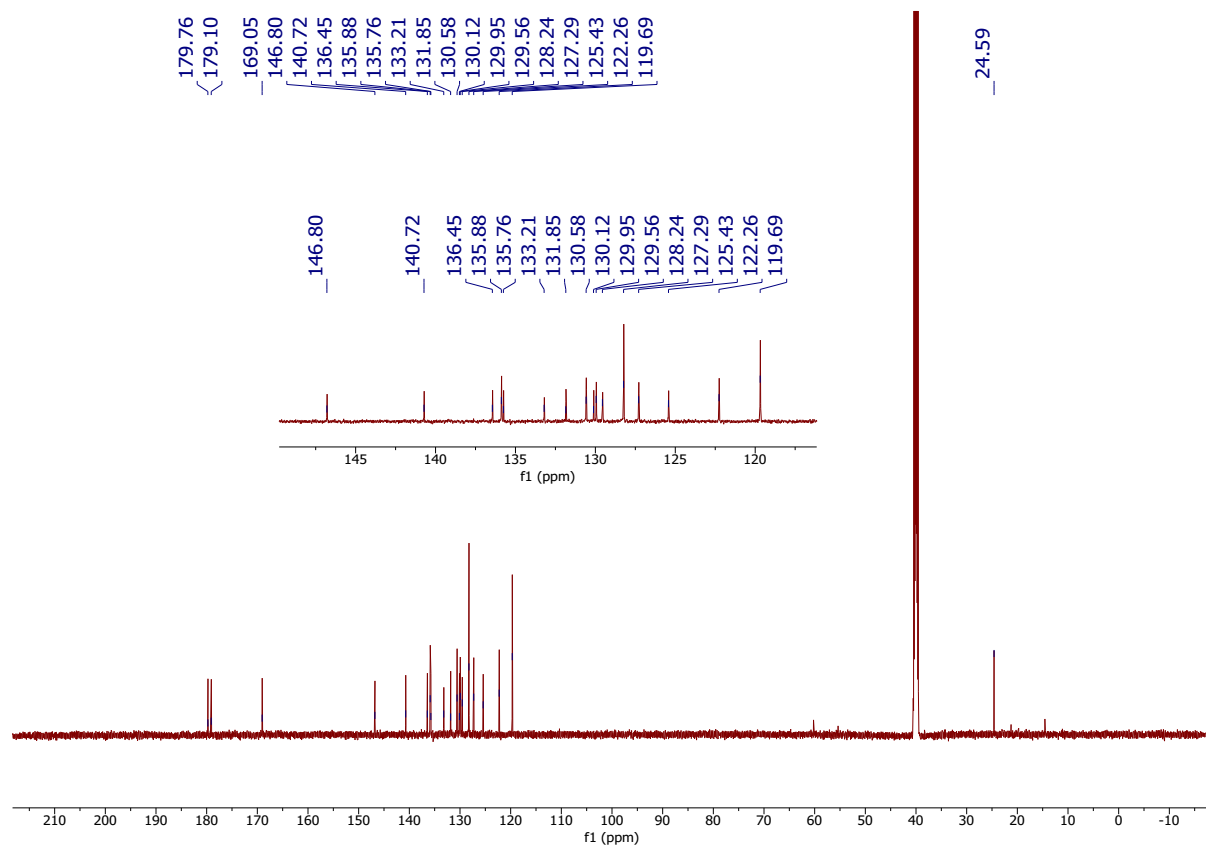


Fig. S22. ^{13}C NMR of **PQ-Ph-Amide** in $\text{DMSO-}d_6$.

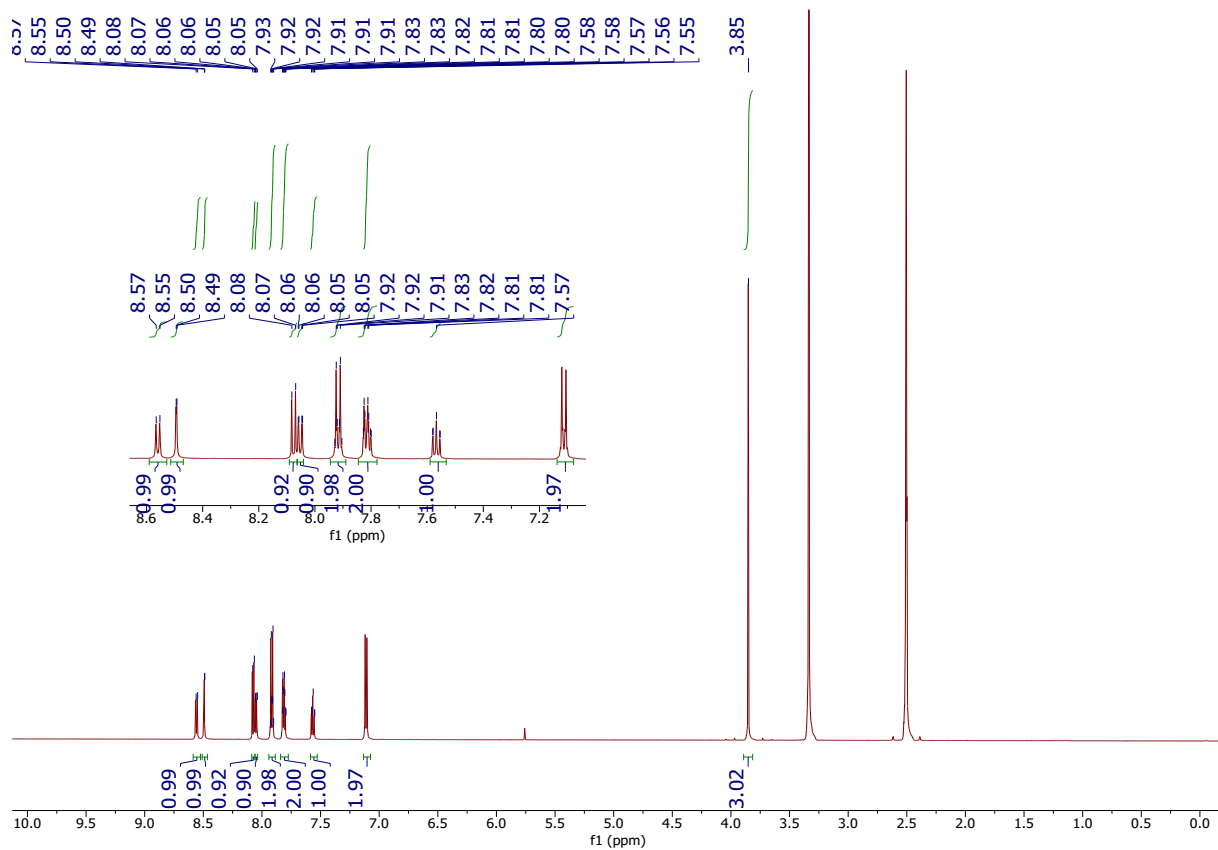


Fig. S23. ^1H NMR of **PQ-Ph-OCH₃** in $\text{DMSO-}d_6$.

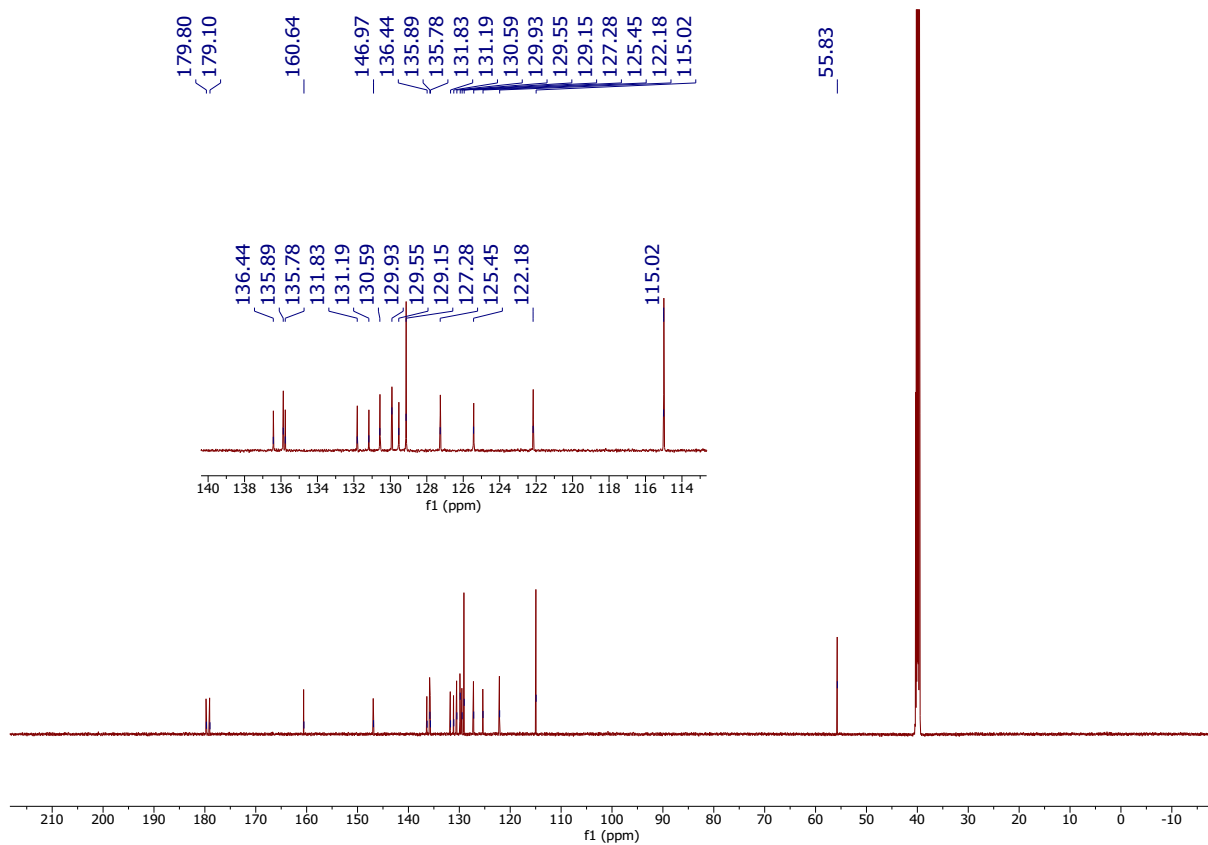


Fig. S24. ^{13}C NMR of **PQ-Ph-OCH₃** in $\text{DMSO-}d_6$.

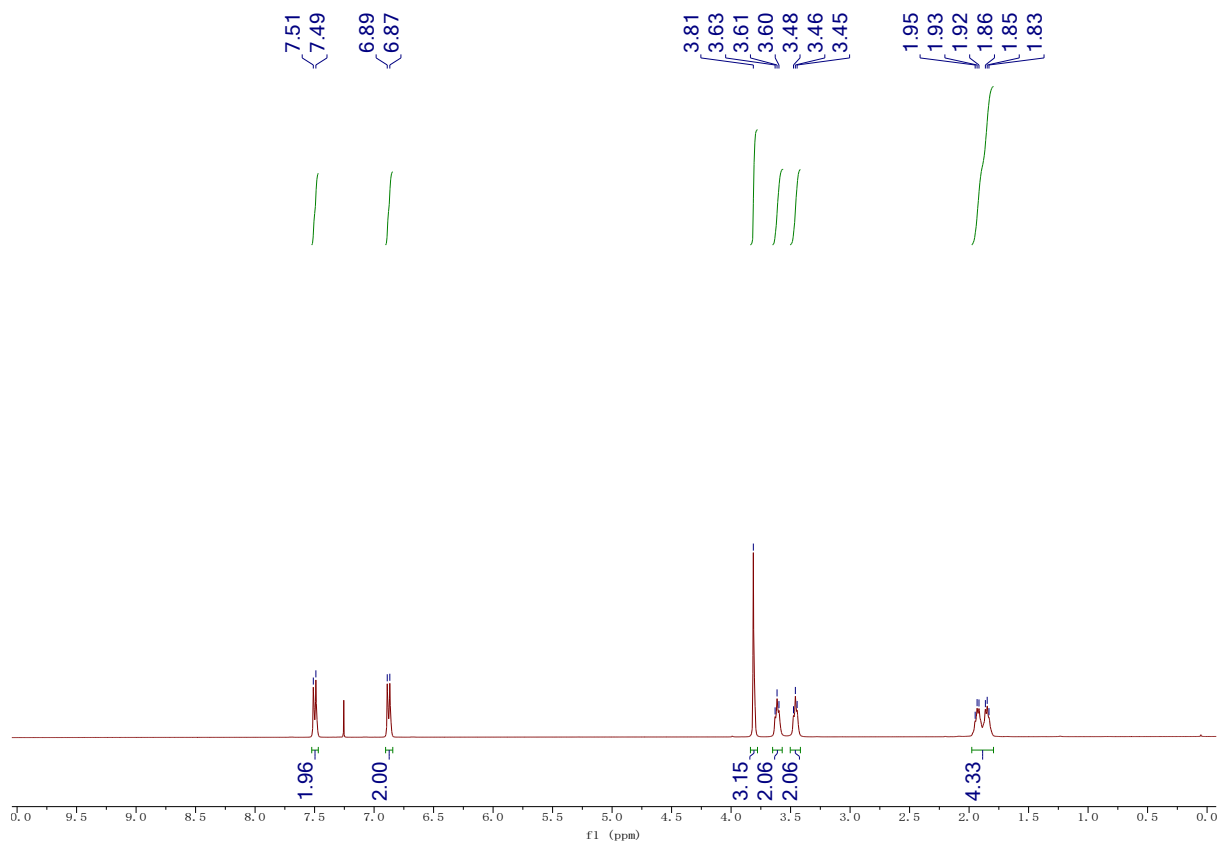


Fig. S25. ^1H NMR of OMe-BZPYD in DMSO- d_6 .

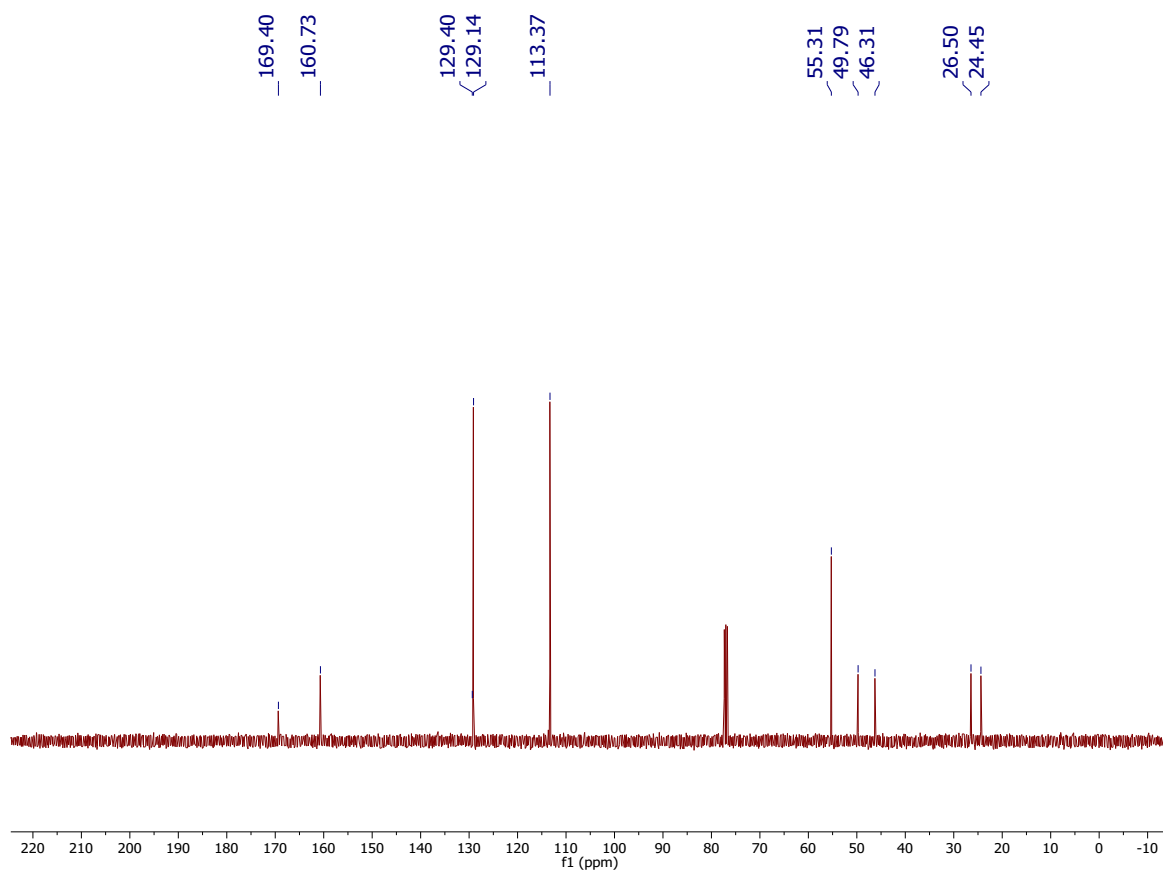


Fig. S26. ^{13}C NMR of OMe-BZPYD in DMSO- d_6 .

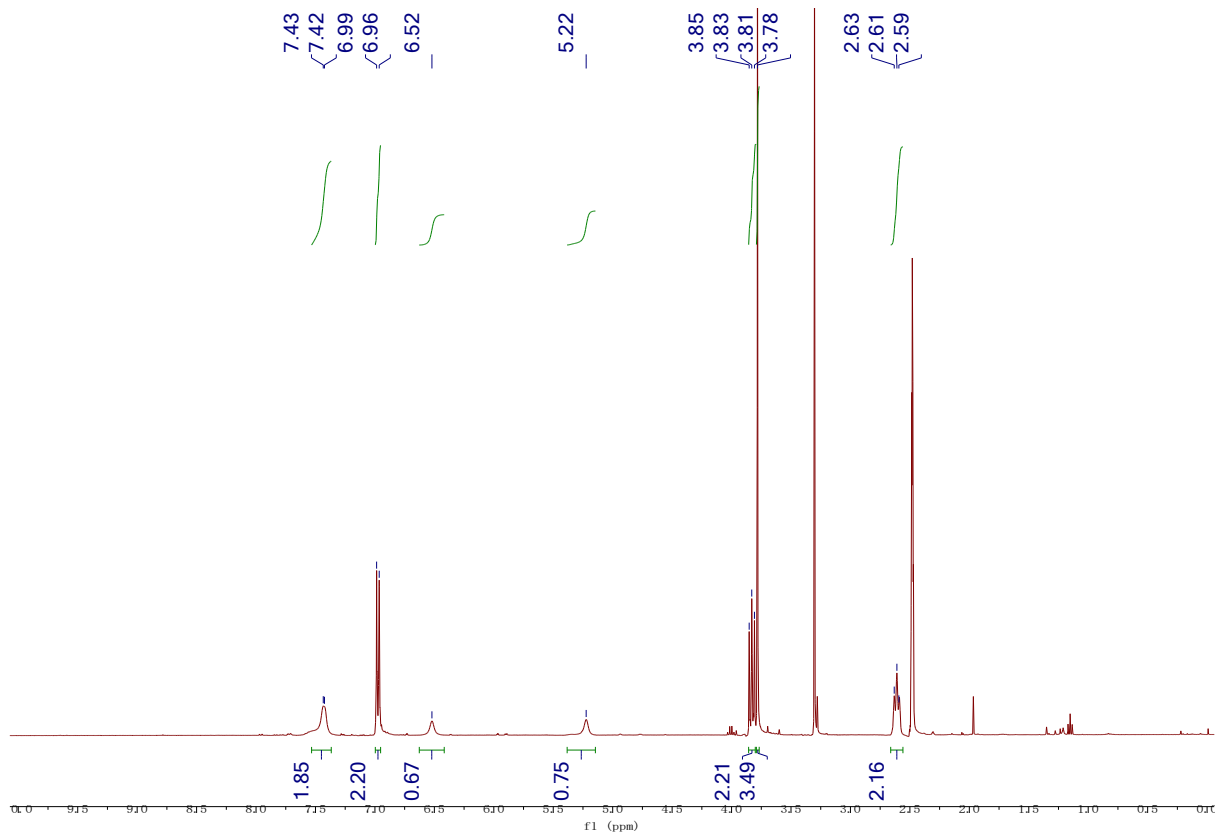


Fig. S27. ^1H NMR of **OMe-BZPY** in $\text{DMSO-}d_6$.

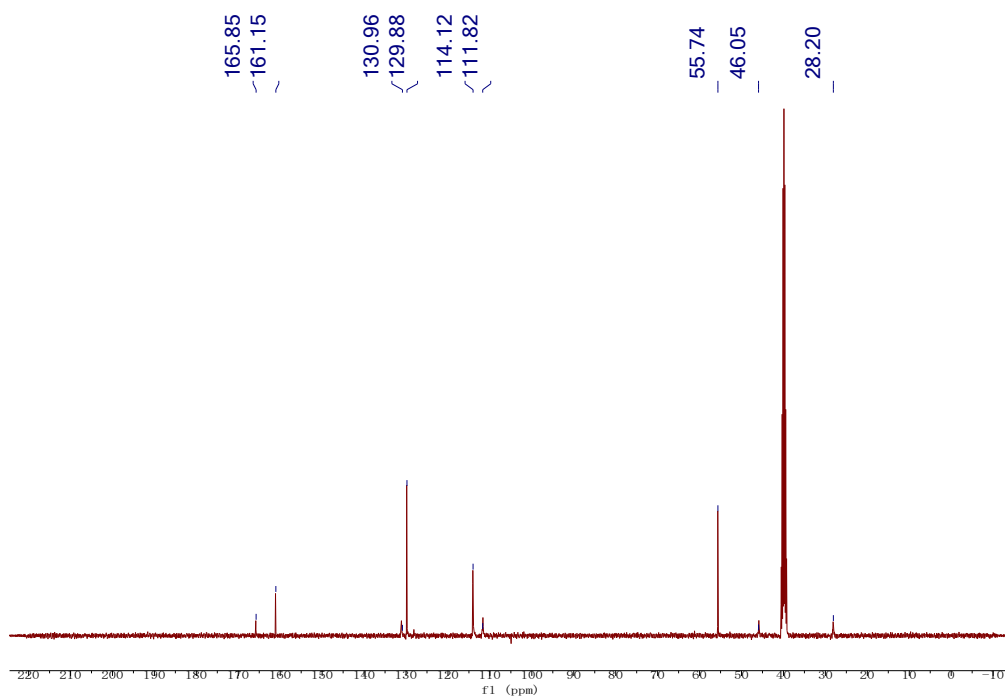


Fig. S28. ^{13}C NMR of **OMe-BZPY** in $\text{DMSO-}d_6$.

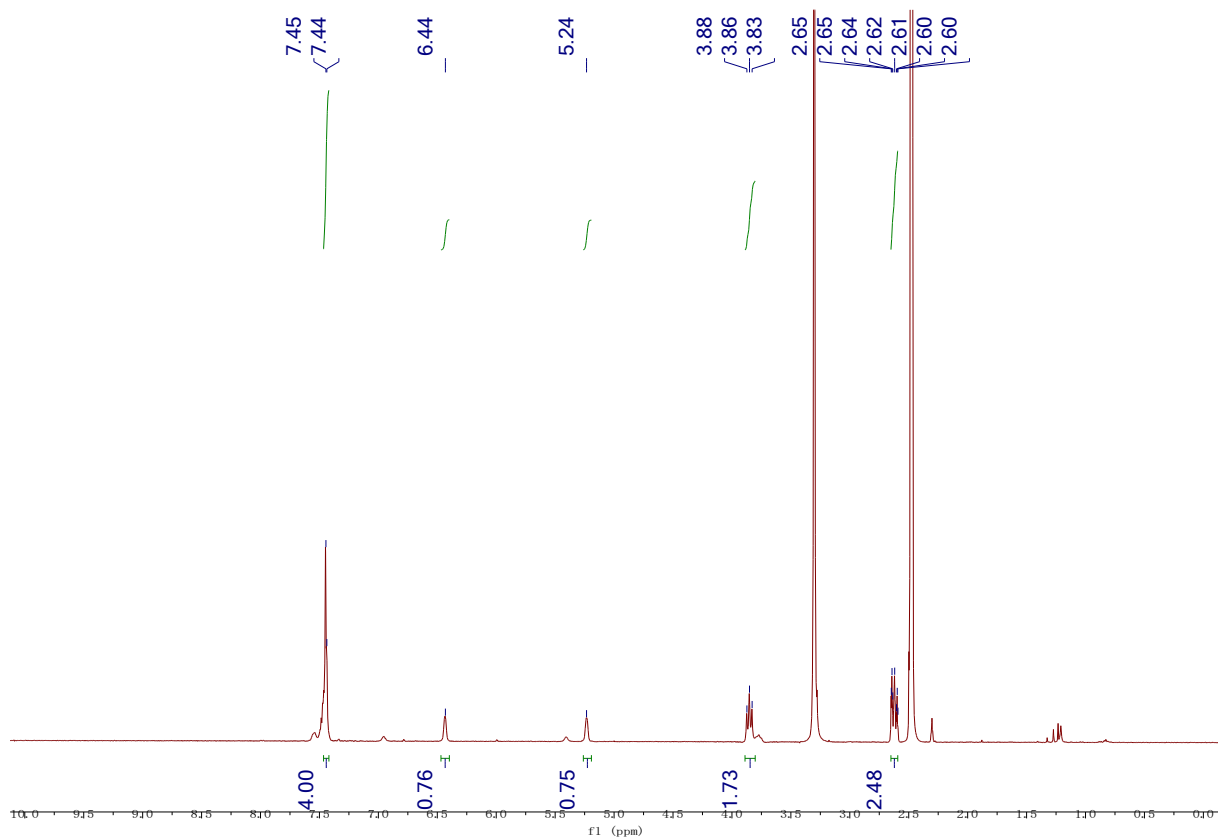


Fig. S29. ^1H NMR of **BZPY** in $\text{DMSO-}d_6$.

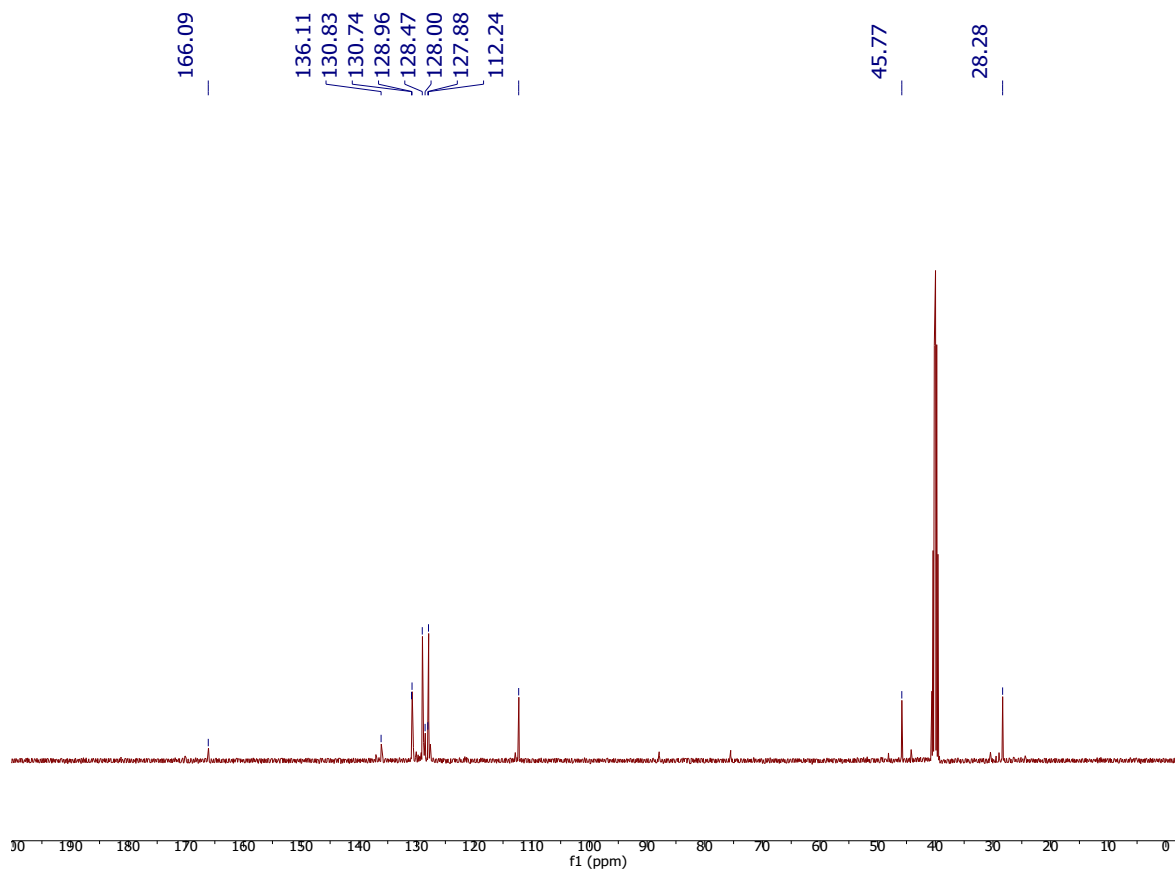


Fig. S30. ^{13}C NMR of **BZPY** in $\text{DMSO-}d_6$.

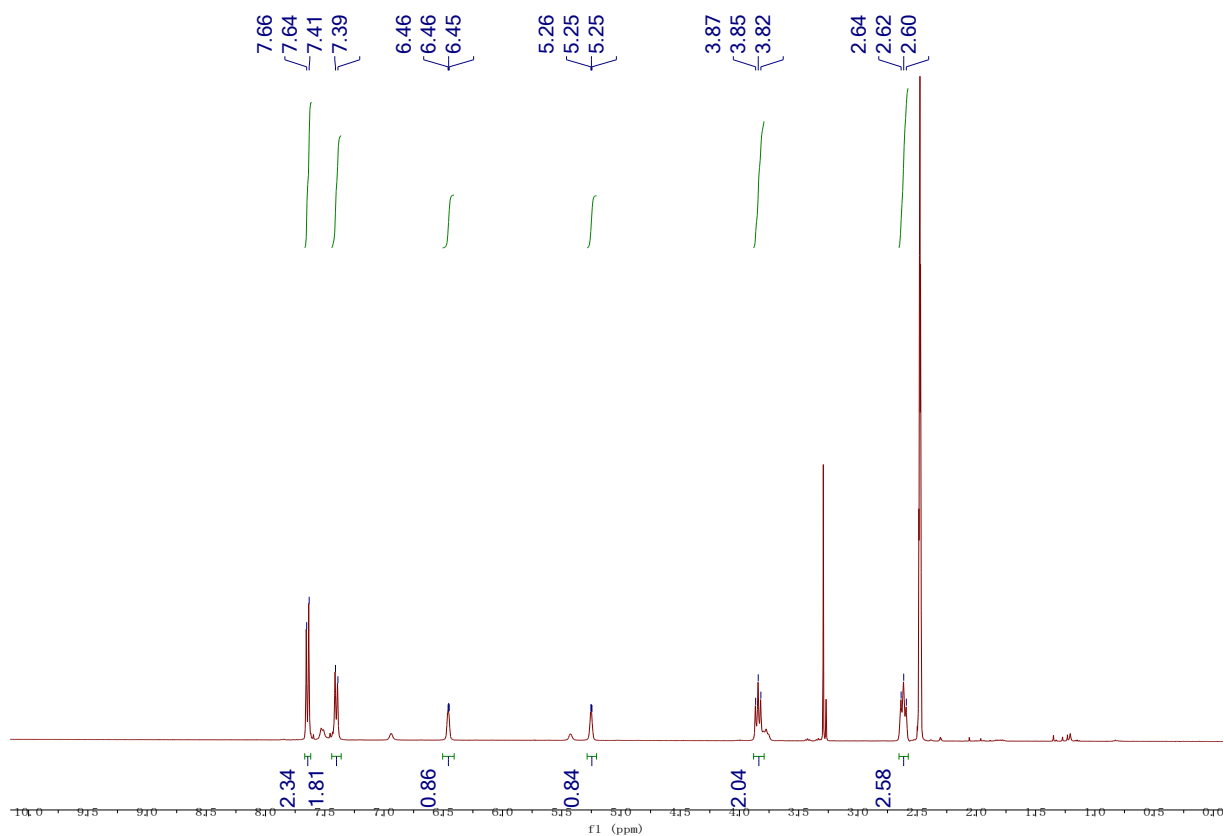


Fig. S31. ^1H NMR of **Br-BZPY** in $\text{DMSO-}d_6$.

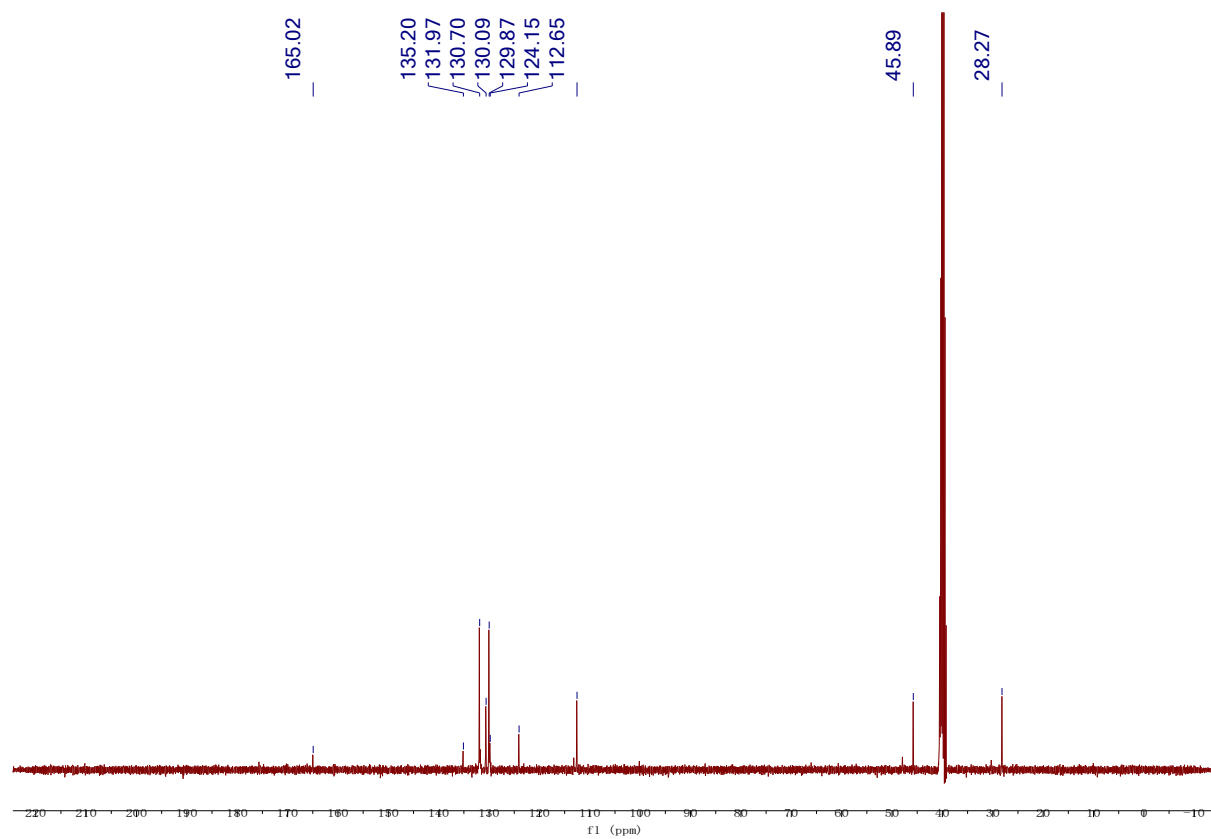


Fig. S32. ^{13}C NMR of **Br-BZPY** in $\text{DMSO-}d_6$.

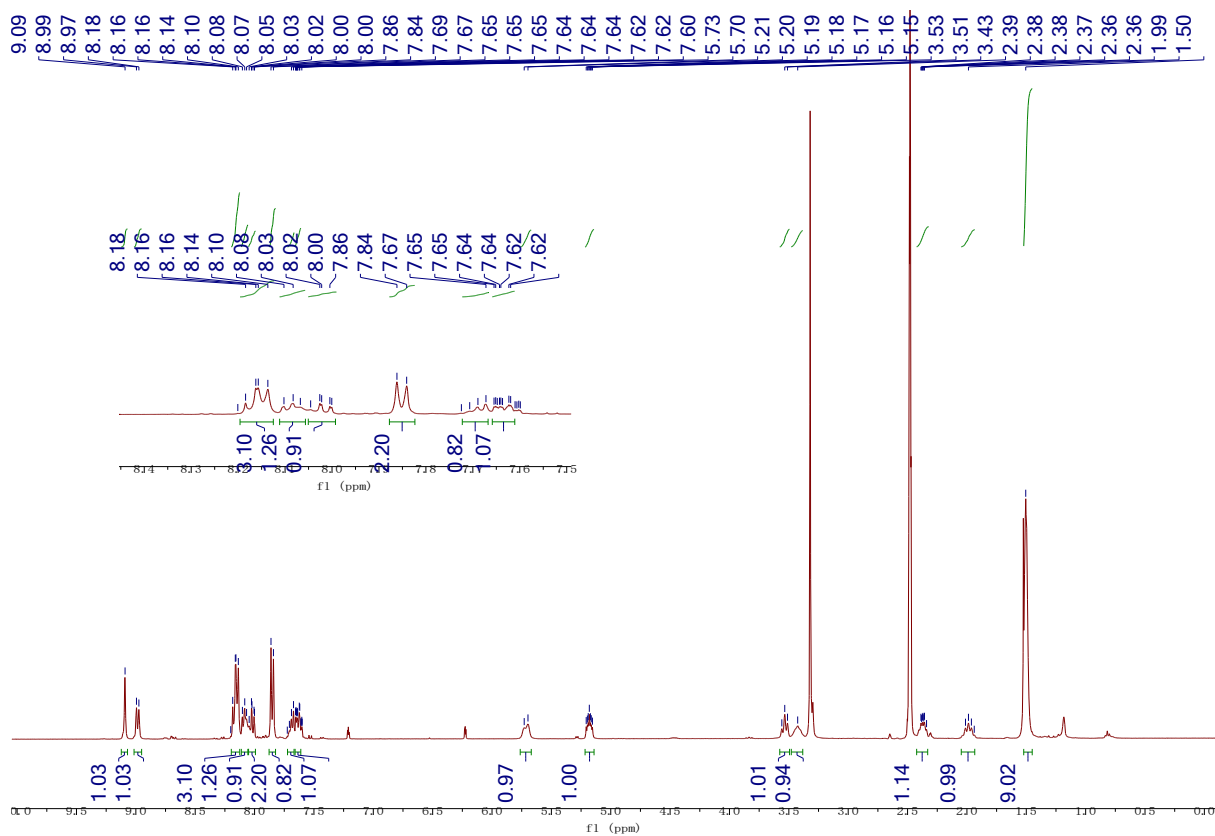


Fig. S33. ^1H NMR of Compound **PQ-Ph-CF₃-PY** in $\text{DMSO-}d_6$.

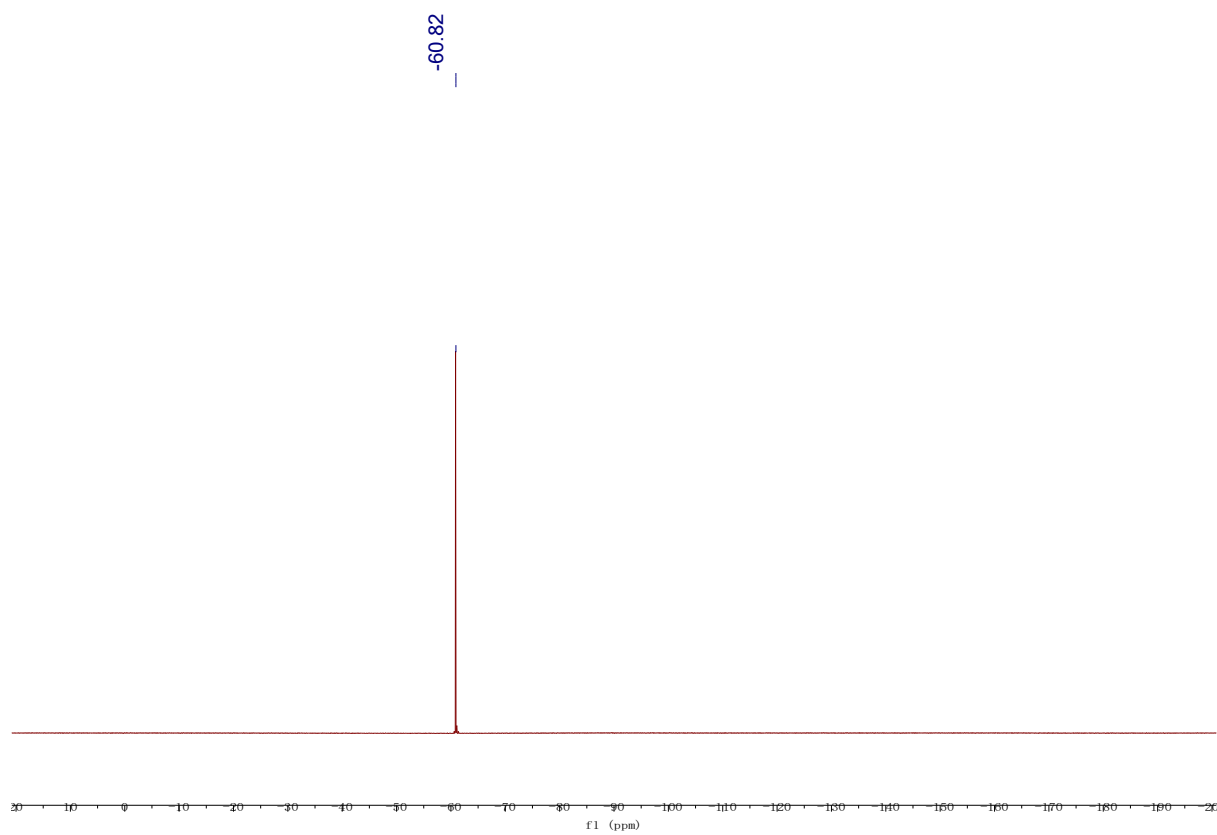


Fig. S34. ^{19}F NMR of Compound **PQ-Ph-CF₃-PY** in $\text{DMSO-}d_6$.

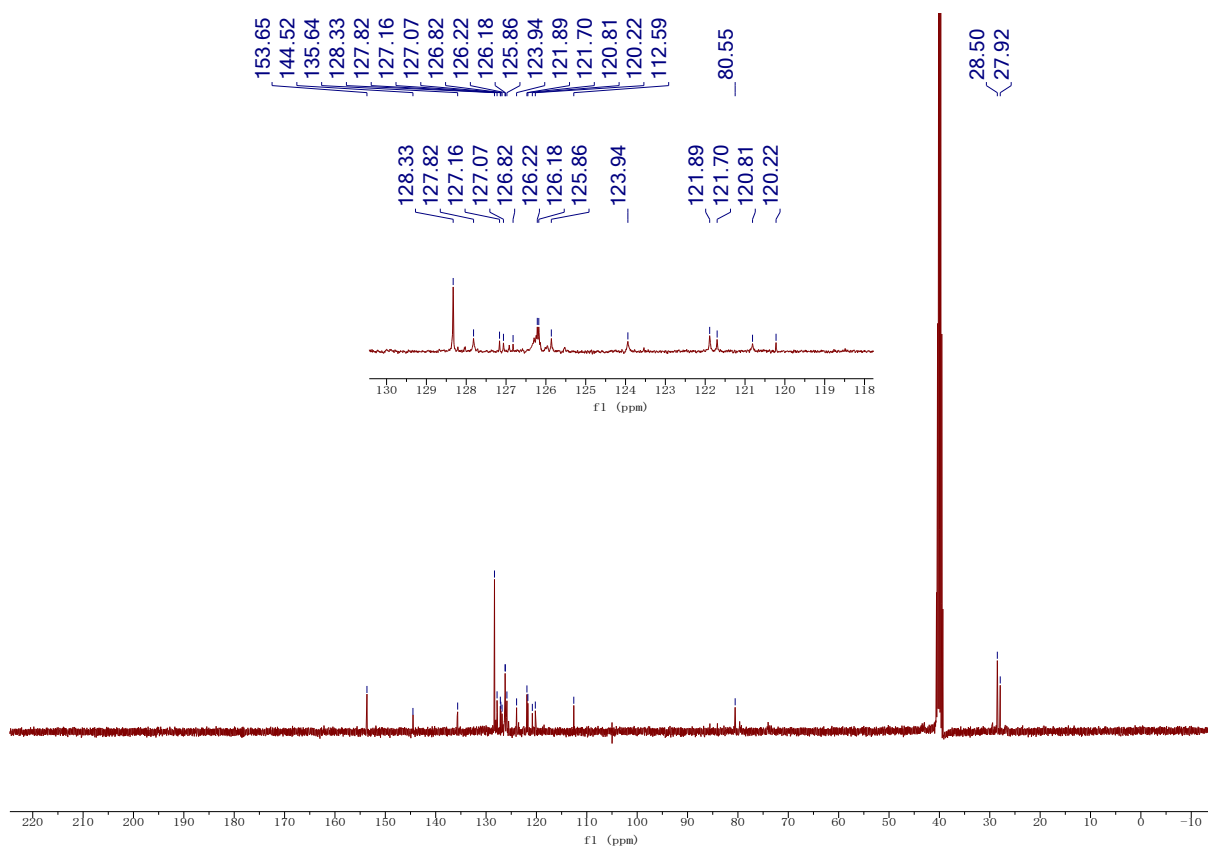


Fig. S35. ^{13}C NMR of Compound **PQ-Ph-CF₃-PY** in $\text{DMSO-}d_6$.

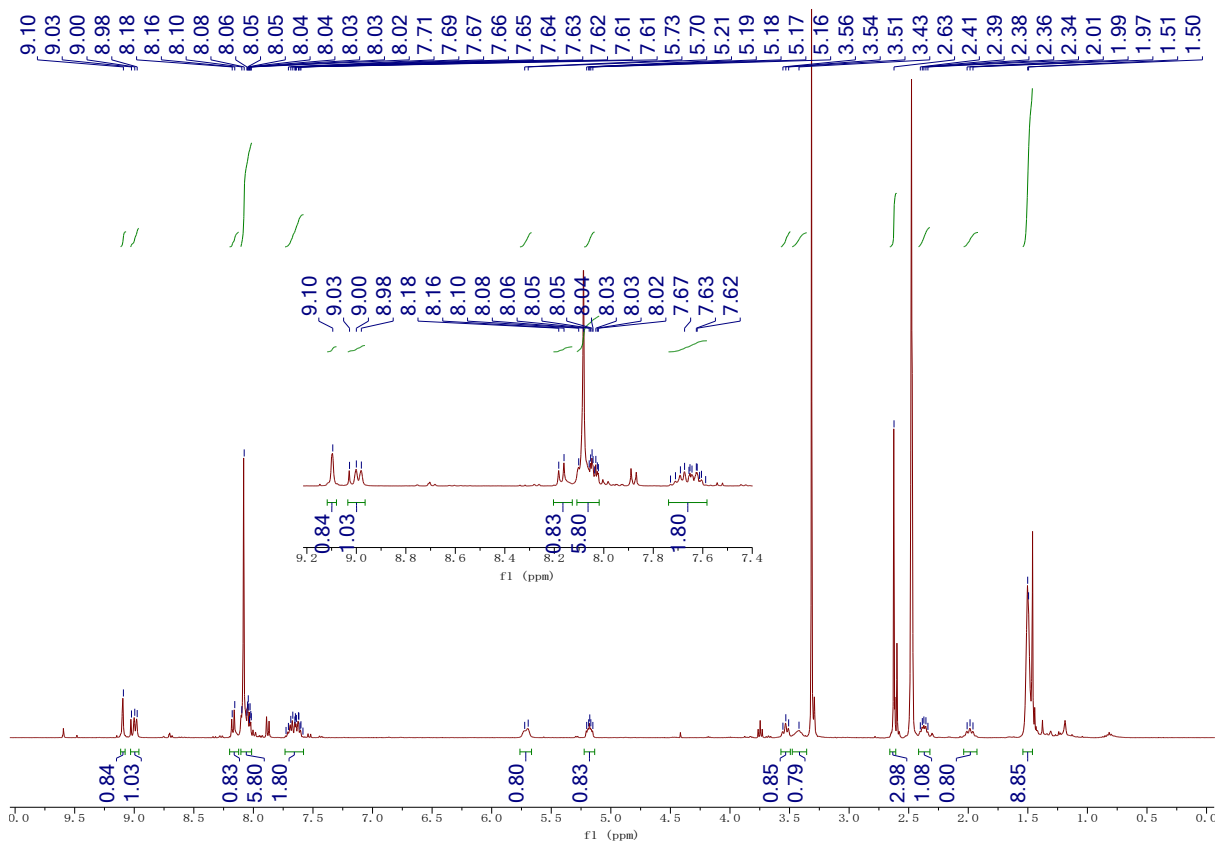


Fig. S36. ^1H NMR of Compound **PQ-Ph-AC-PY** in $\text{DMSO-}d_6$.

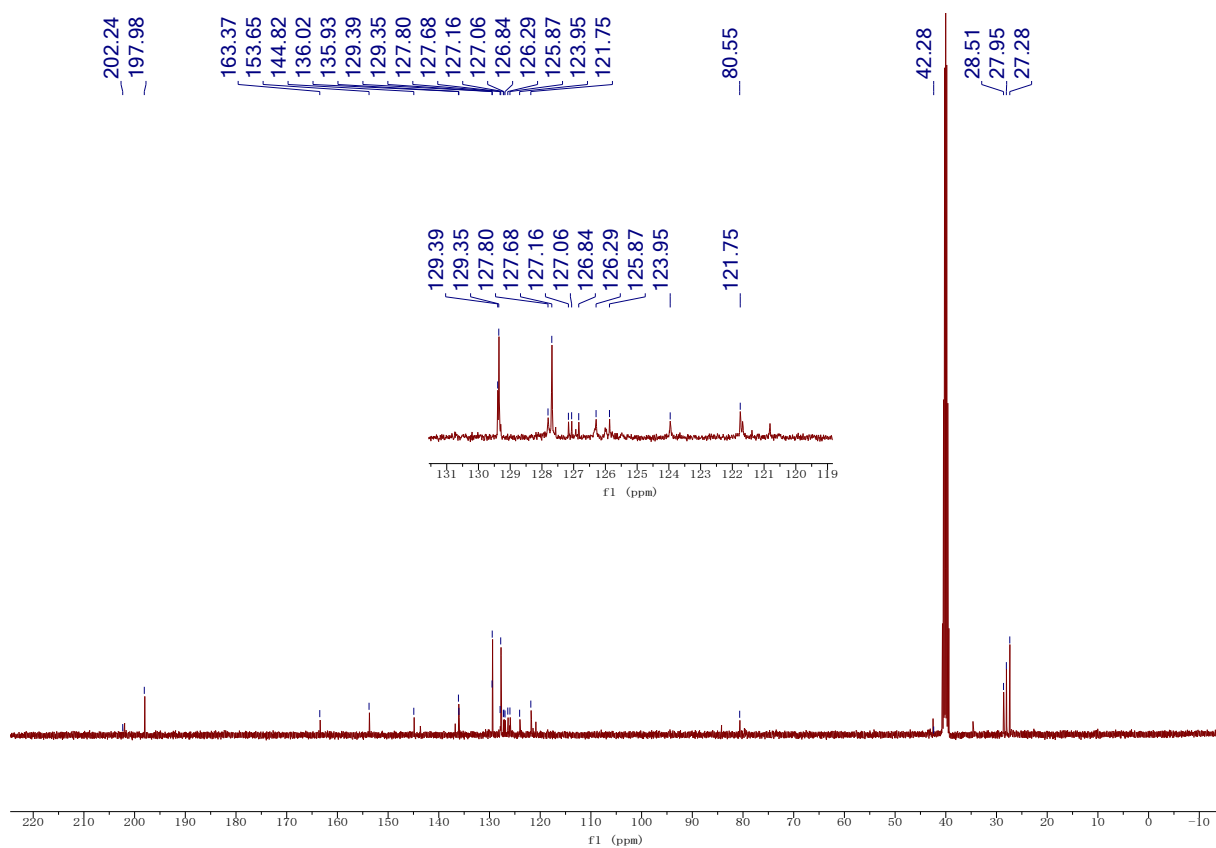


Fig. S37. ^{13}C NMR of Compound **PQ-Ph-AC-PY** in $\text{DMSO-}d_6$.

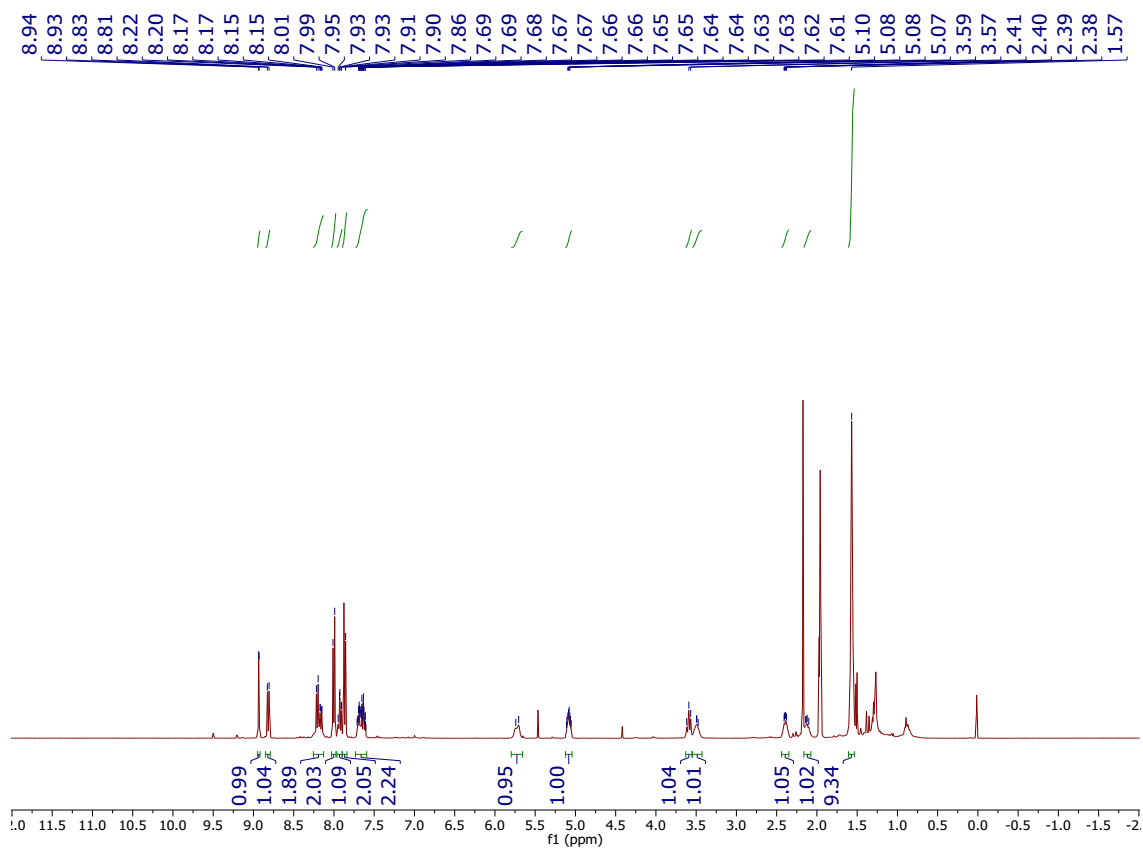


Fig. S38. ^1H NMR of Compound **PQ-Ph-CN-PY** in $\text{CD}_3\text{CN-}d_3$.

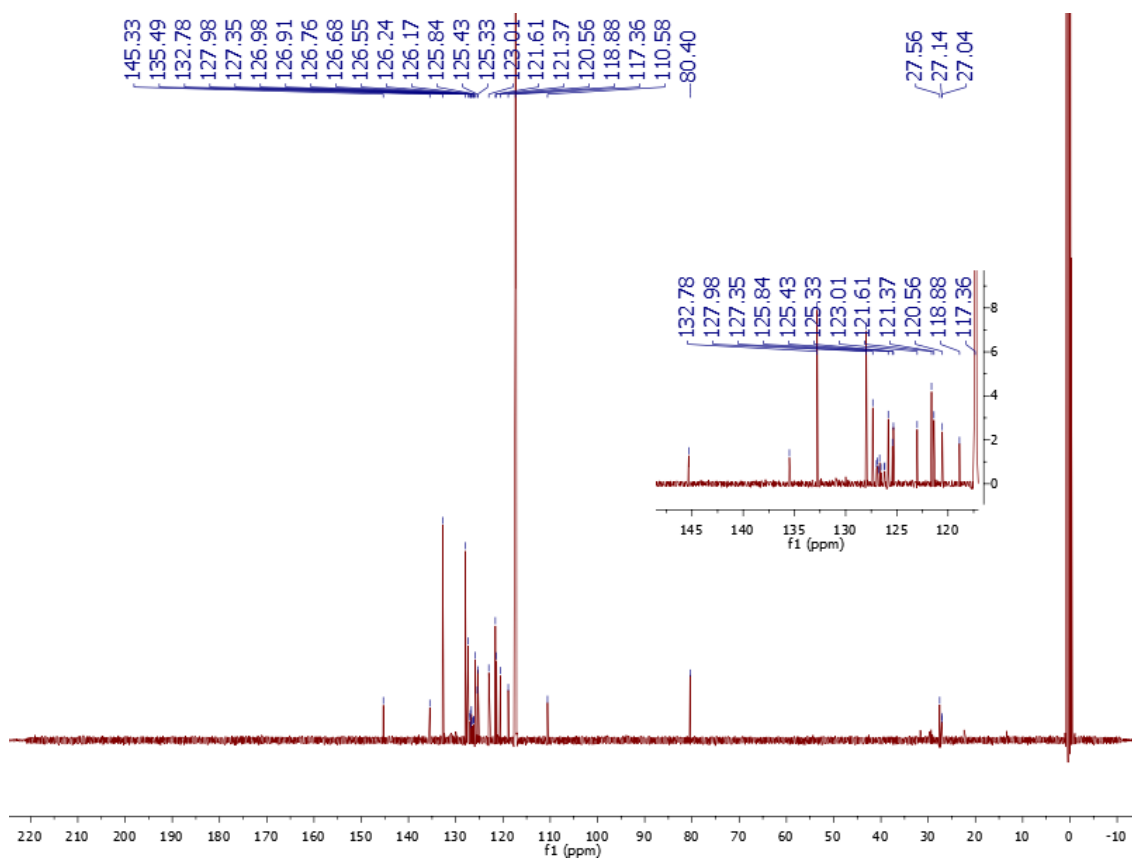


Fig. S39. ¹³C NMR of Compound PQ-Ph-CN-PY in CD₃CN-*d*₃.

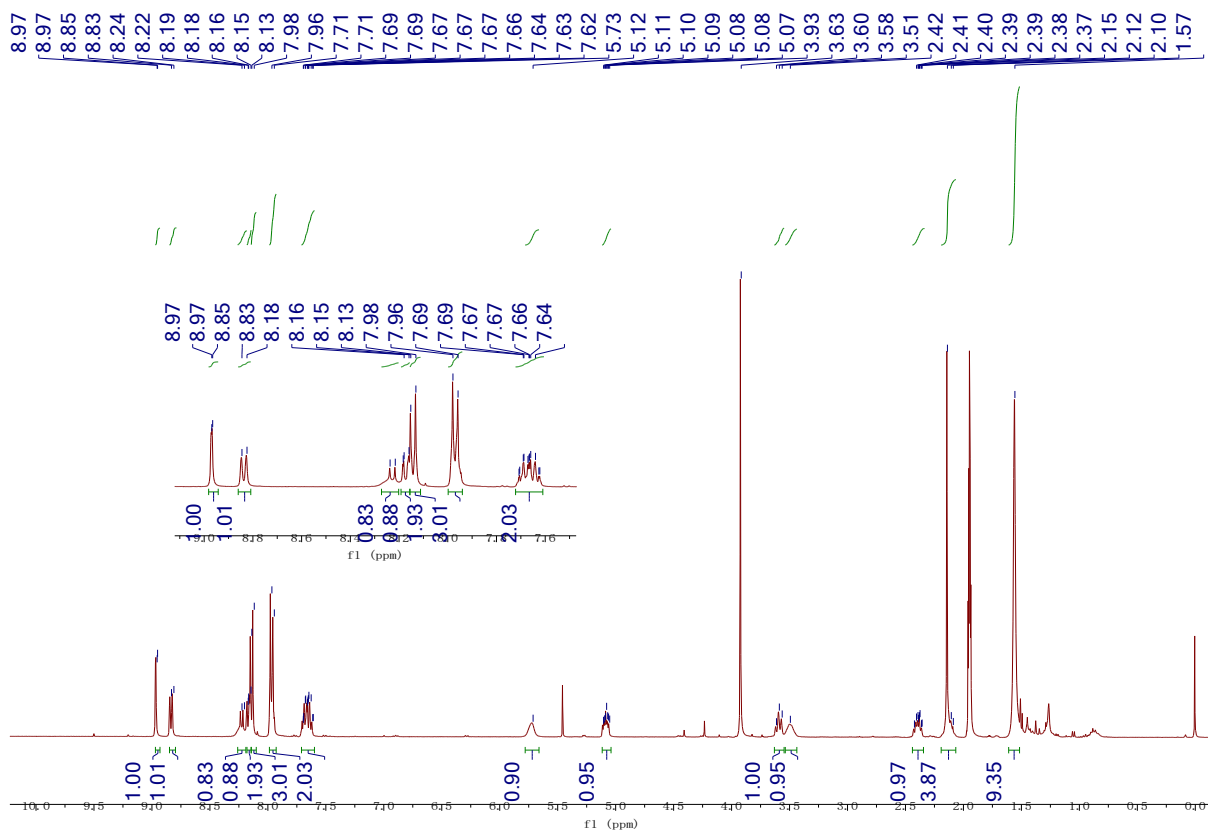


Fig. S40. ¹H NMR of Compound PQ-Ph-COOCH₃-PY in CD₃CN-*d*₃.

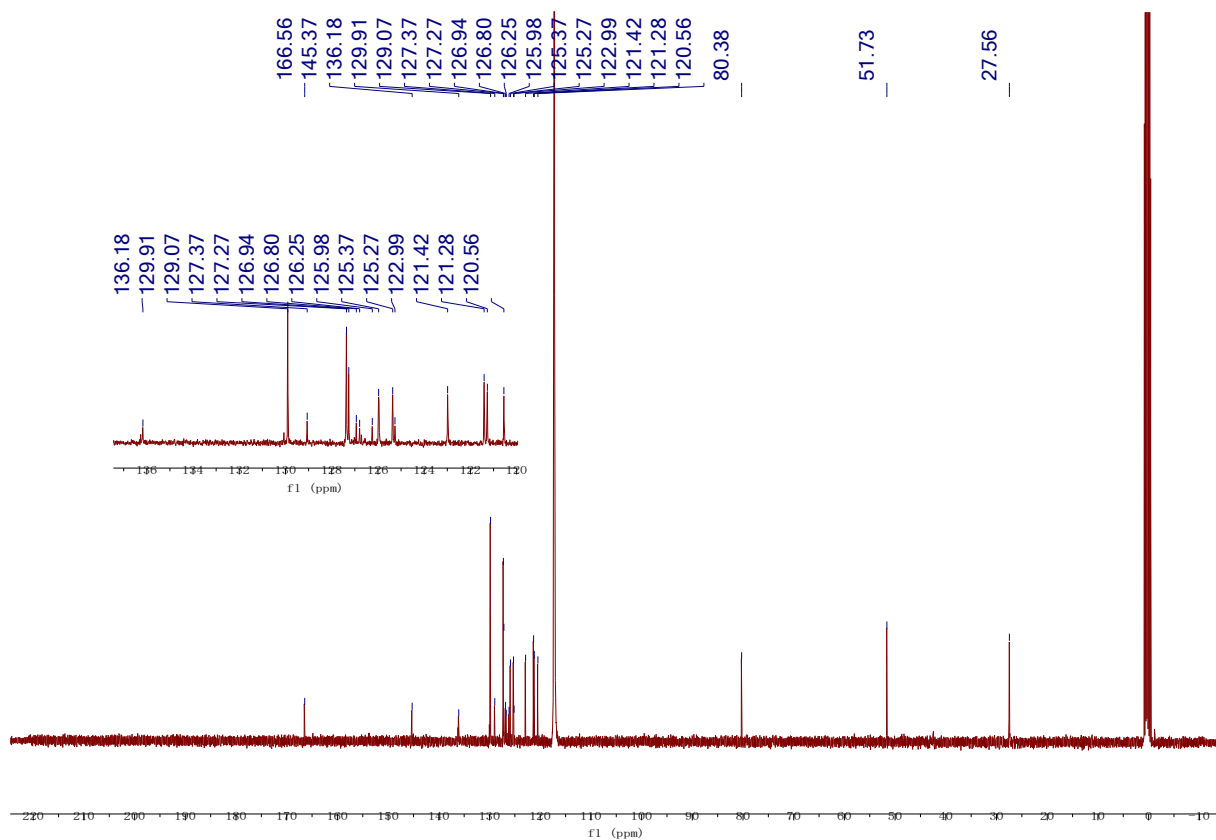


Fig. S41. ^{13}C NMR of Compound PQ-Ph-COOCH₃-PY in CD₃CN-*d*₃.

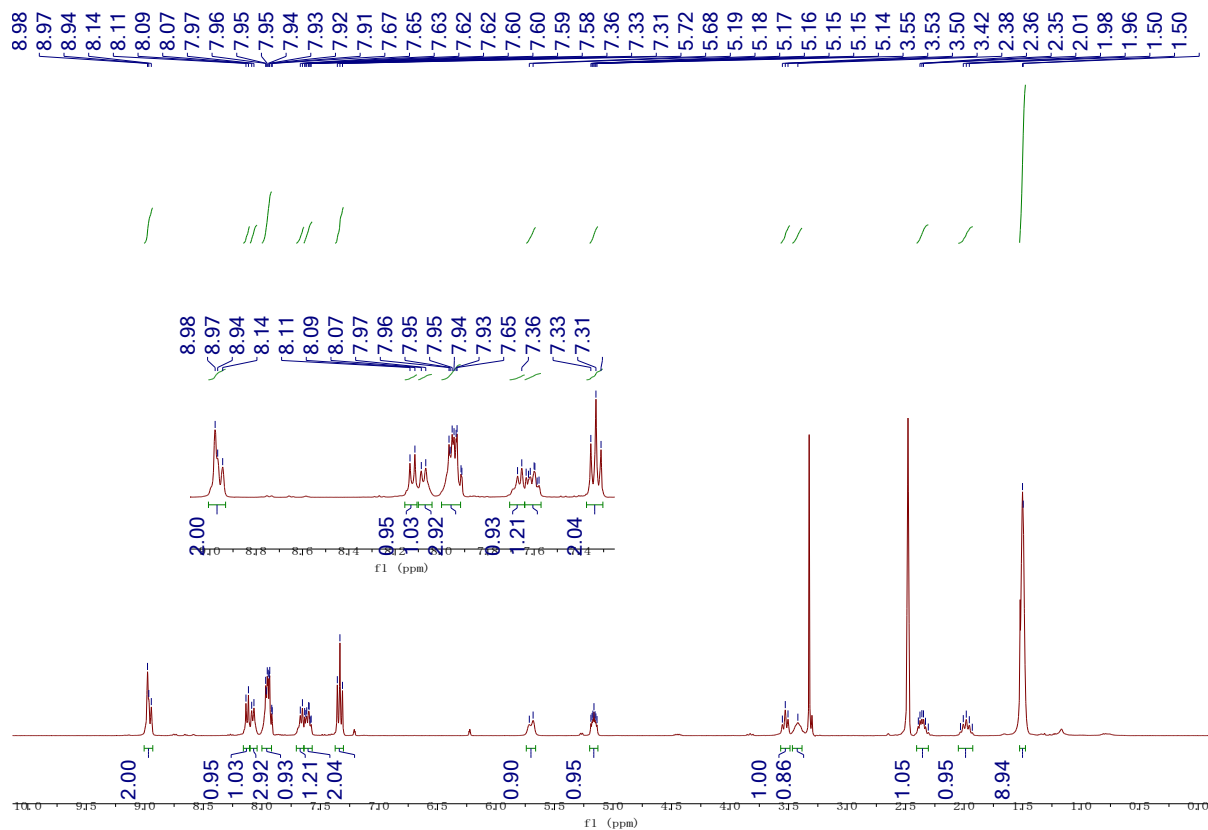


Fig. S42. ^1H NMR of Compound PQ-Ph-F-PY in DMSO-*d*₆.

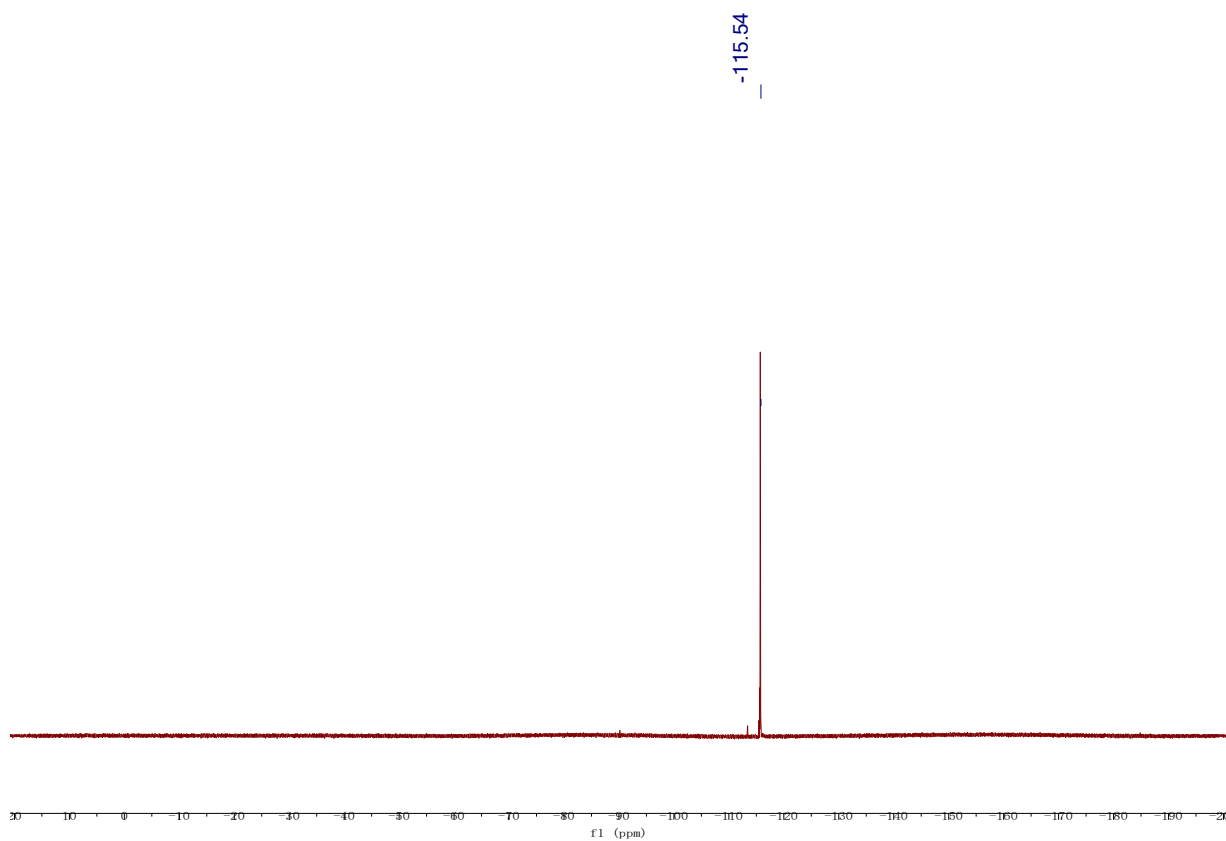


Fig. S43. ¹⁹F NMR of Compound PQ-Ph-F-PY in DMSO-*d*₆.

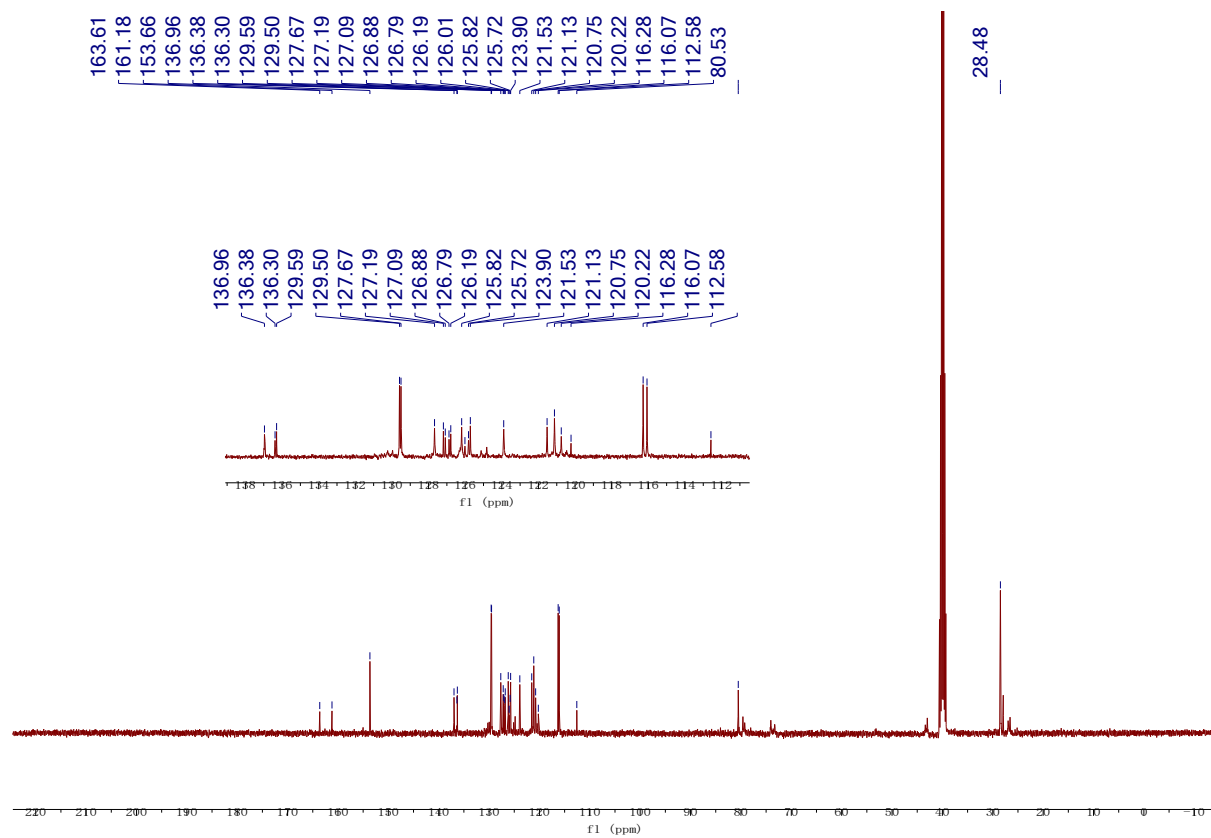


Fig. S44. ¹³C NMR of Compound PQ-Ph-F-PY in DMSO-*d*₆.

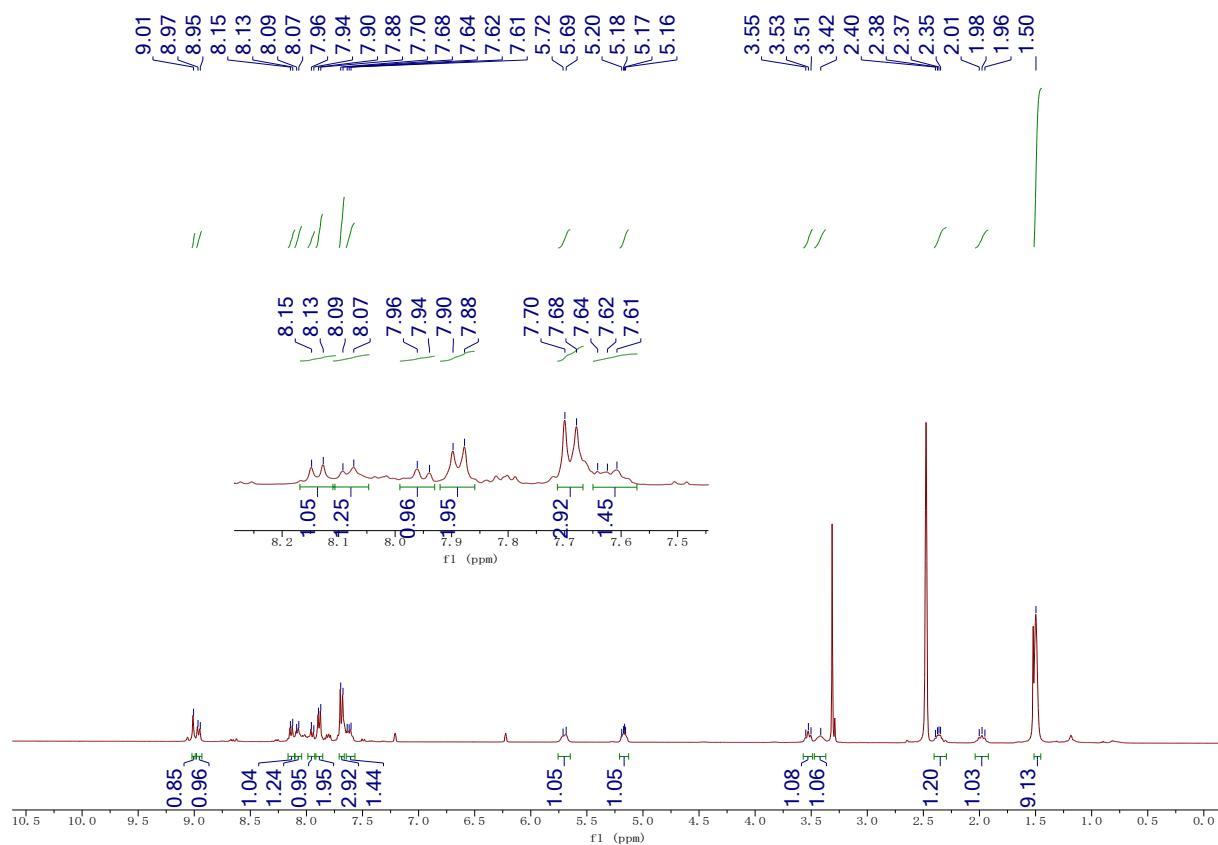


Fig. S45. ^1H NMR of Compound **PQ-Ph-Br-PY** in $\text{DMSO-}d_6$.

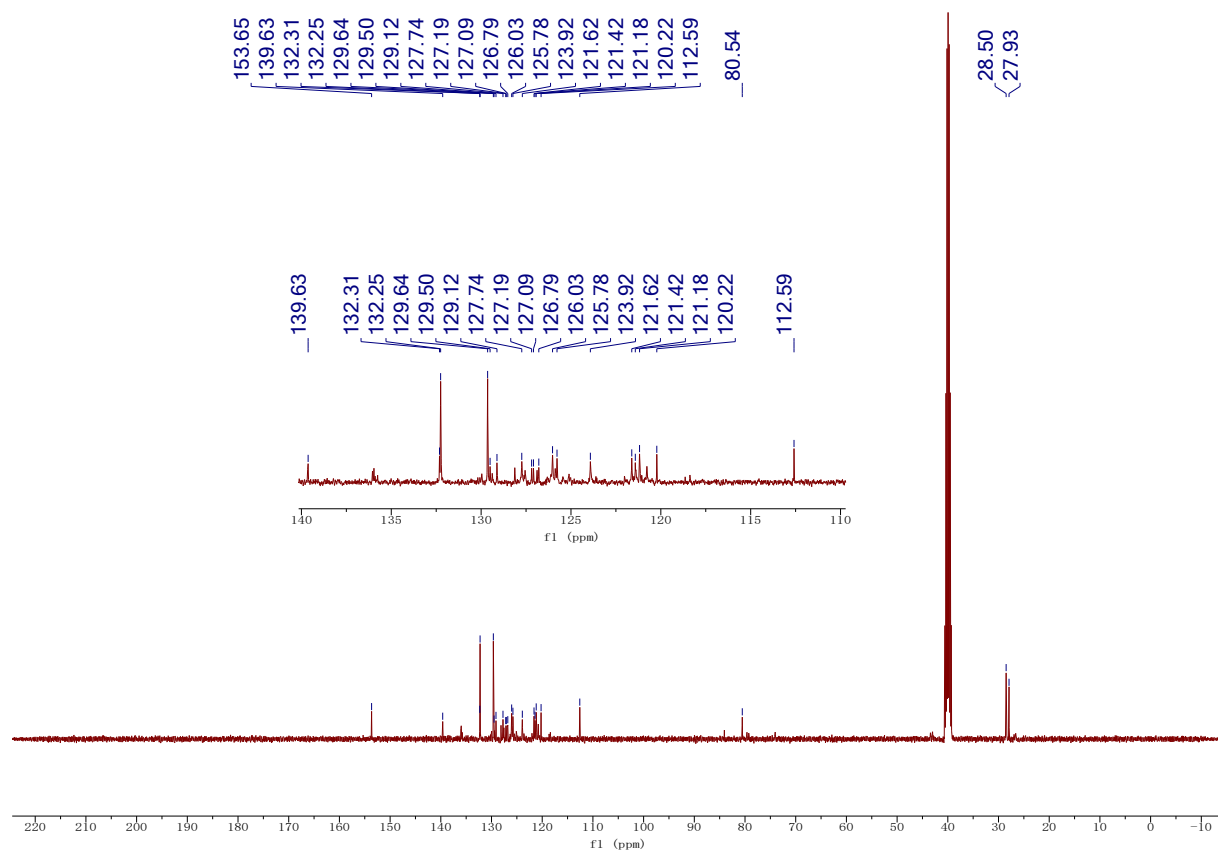


Fig. S46. ^{13}C NMR of Compound **PQ-Ph-Br-PY** in $\text{DMSO-}d_6$.

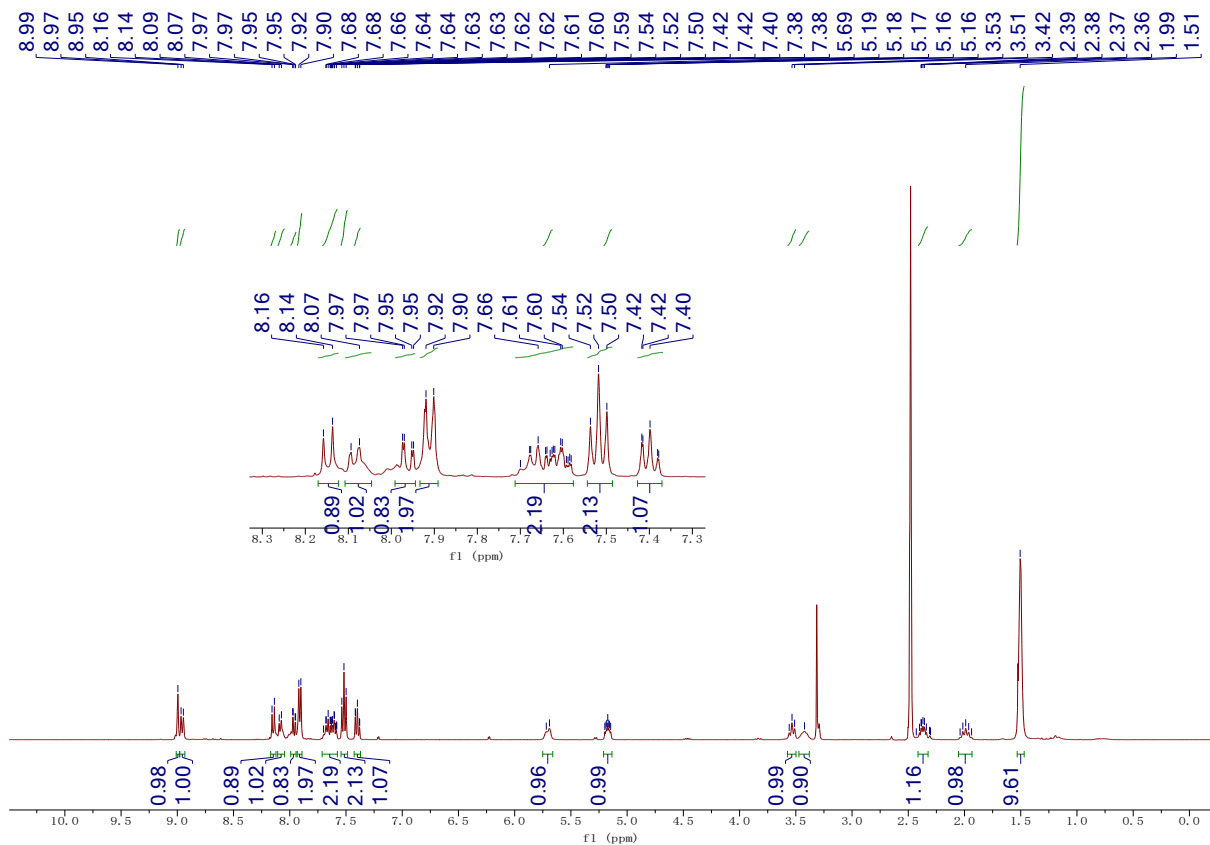


Fig. S47. ^1H NMR of Compound **PQ-Ph-PY** in $\text{DMSO-}d_6$.

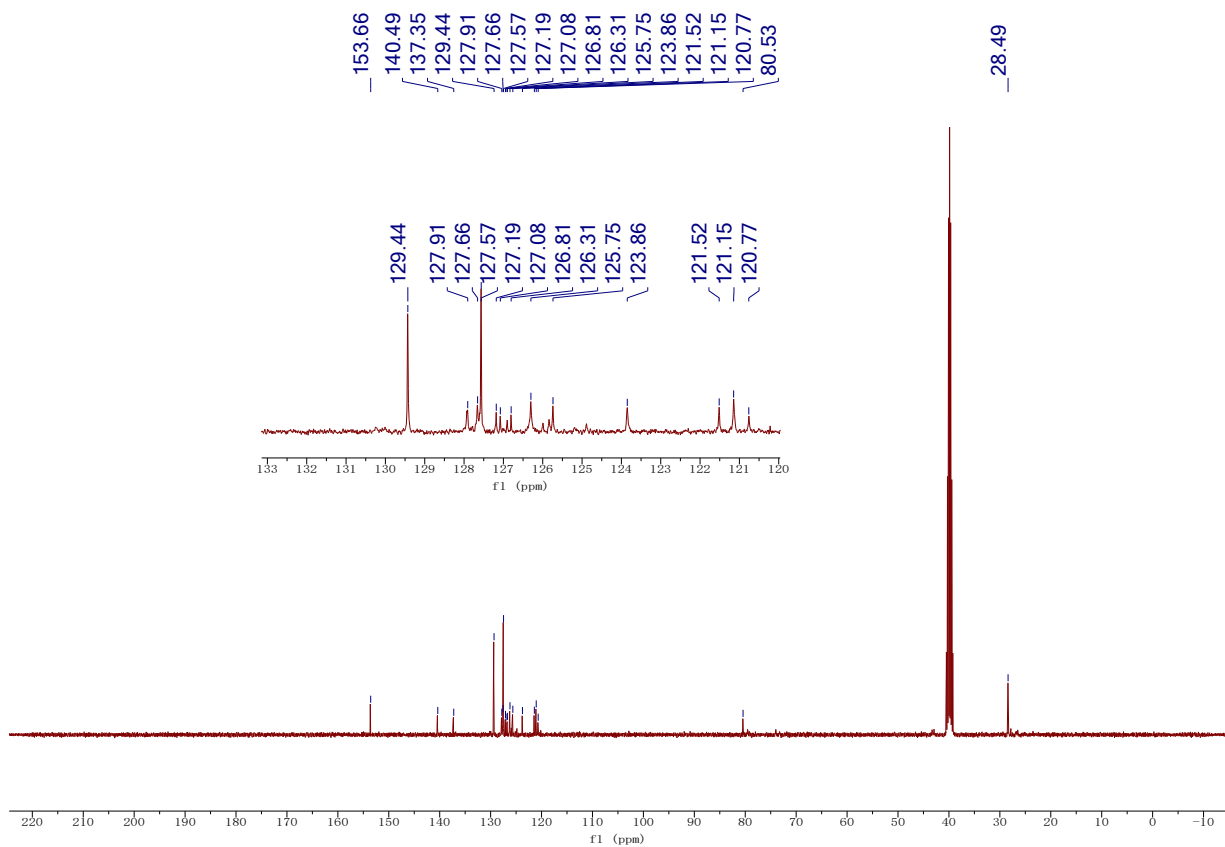


Fig. S48. ^{13}C NMR of Compound **PQ-Ph-PY** in $\text{DMSO-}d_6$.

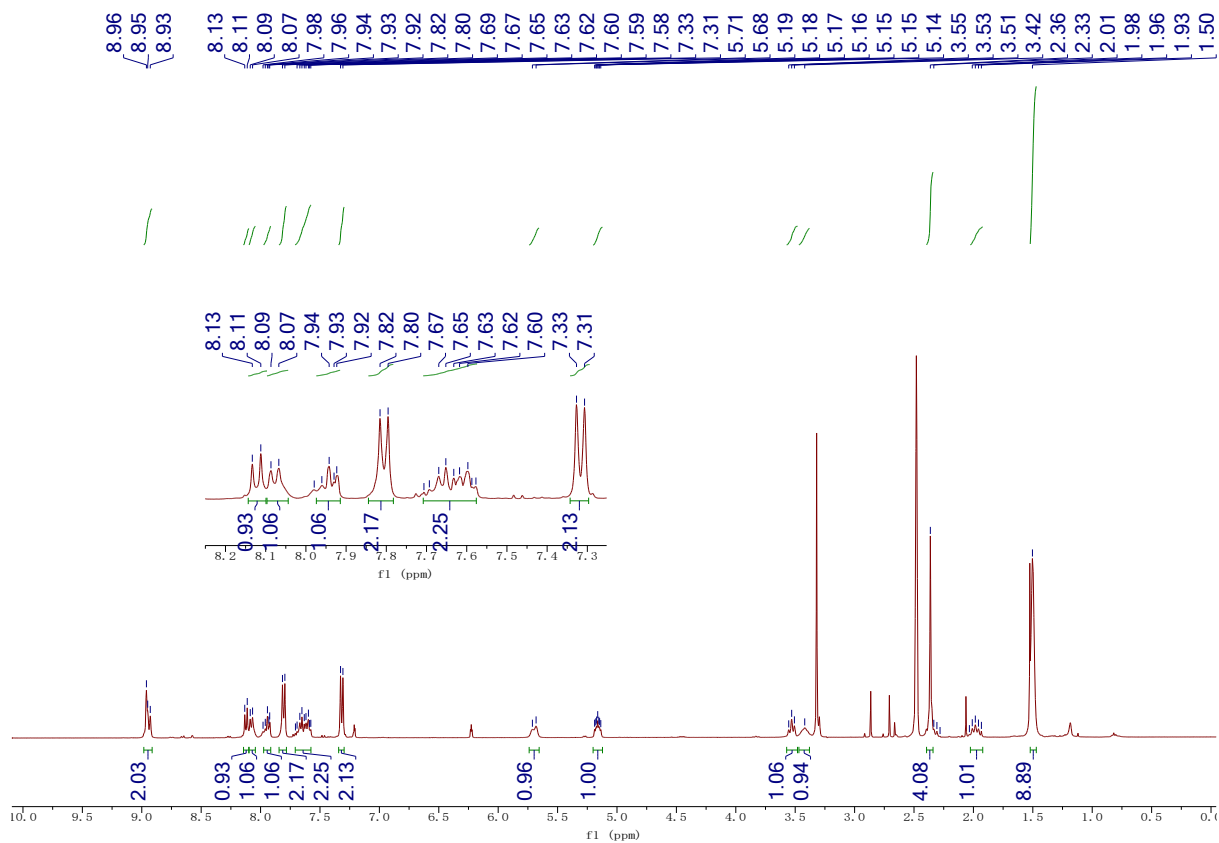


Fig. S49. ^1H NMR of Compound **PQ-Ph-CH₃-PY** in $\text{DMSO-}d_6$.

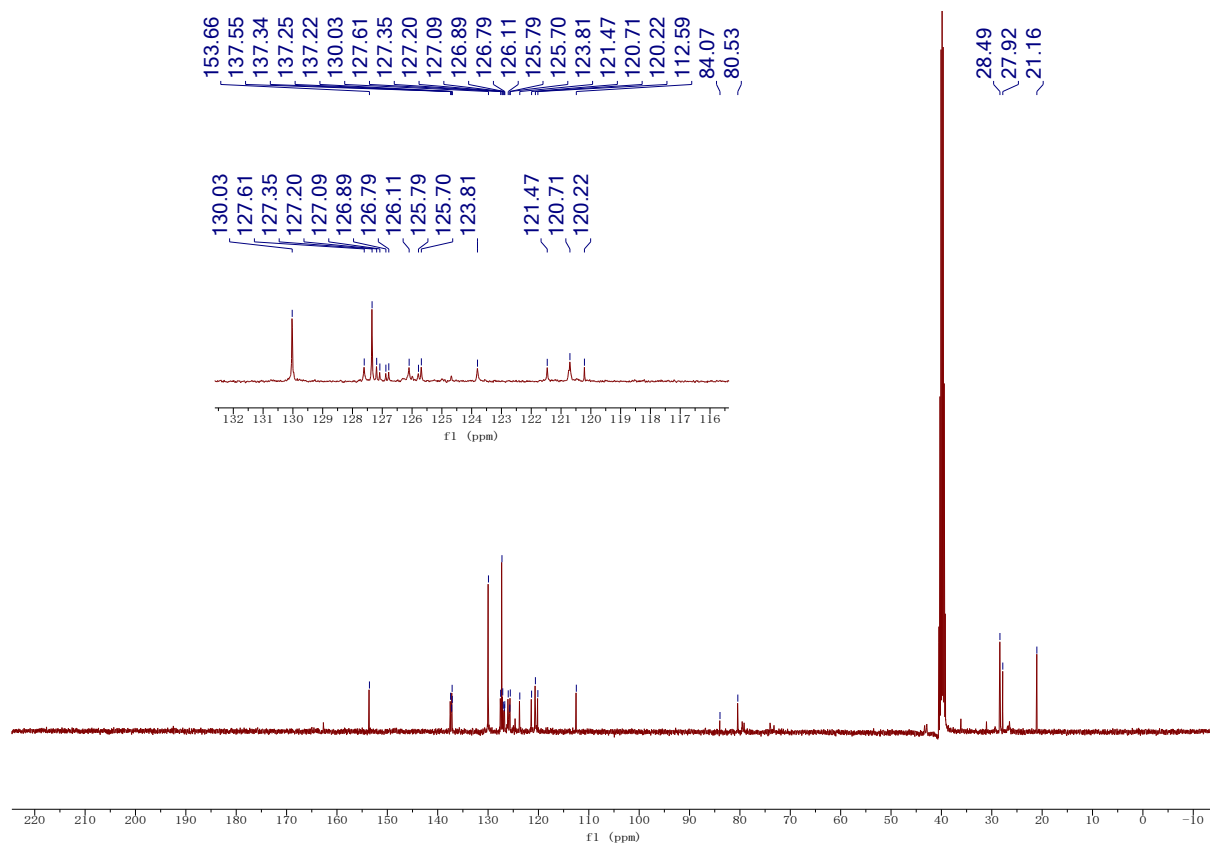


Fig. S50. ^{13}C NMR of Compound **PQ-Ph-CH₃-PY** in $\text{DMSO-}d_6$.

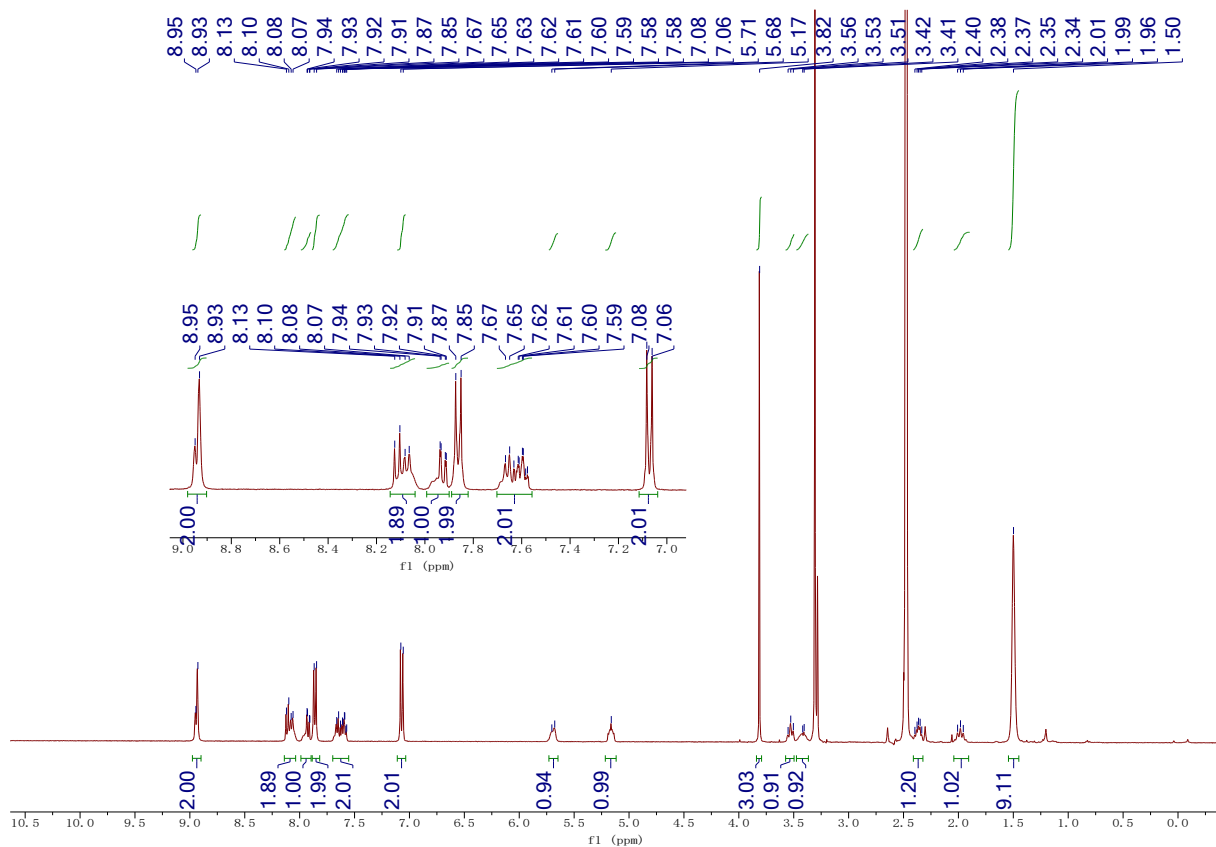


Fig. S51. ^1H NMR of Compound **PQ-Ph-OCH₃-PY** in $\text{DMSO-}d_6$.

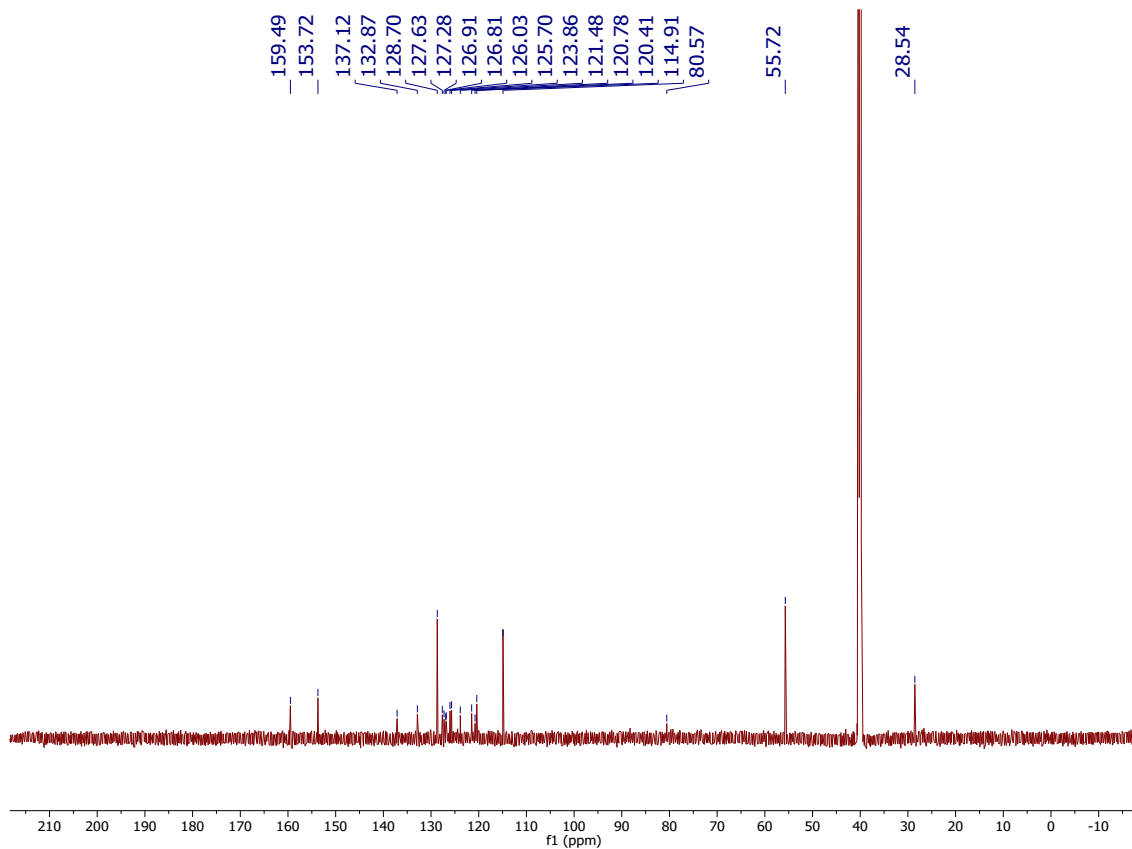


Fig. S52. ^{13}C NMR of Compound **PQ-Ph-OCH₃-PY** in $\text{DMSO-}d_6$.

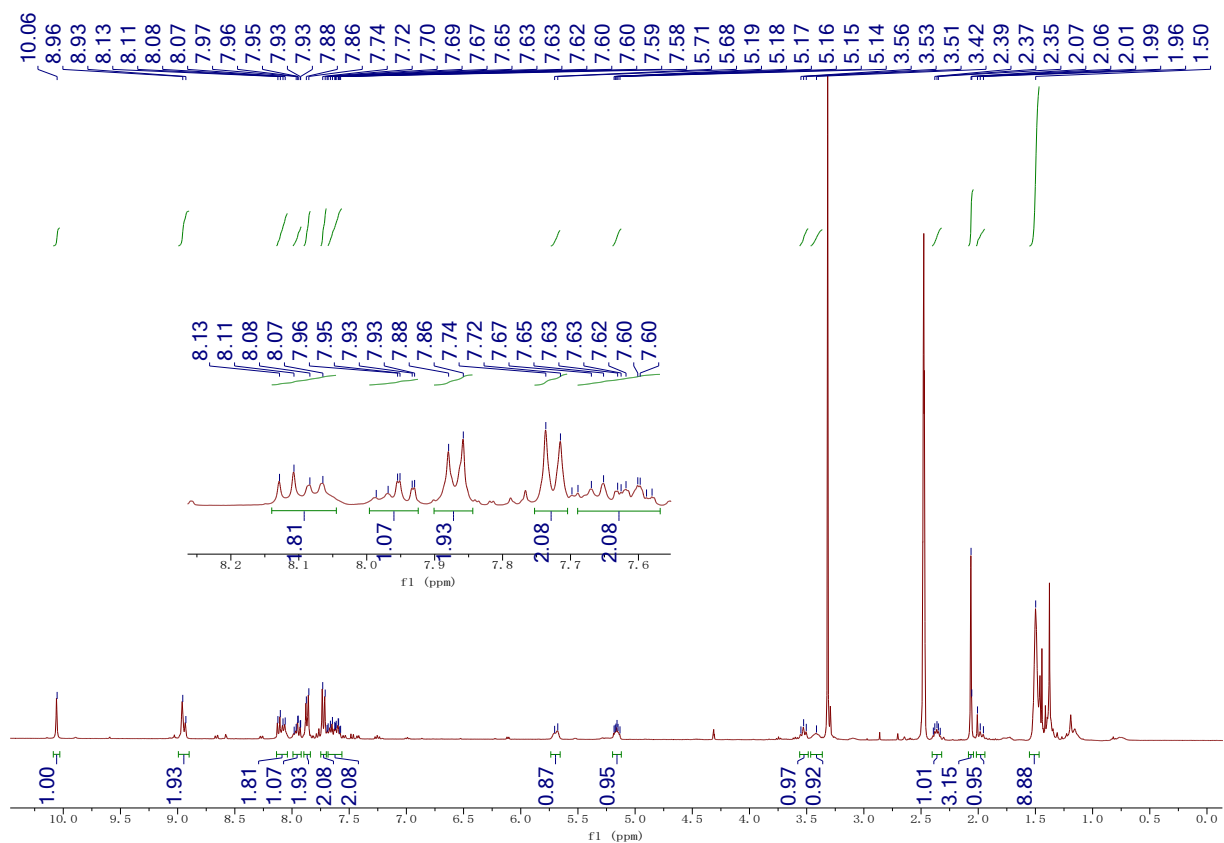


Fig. S53. ^1H NMR of Compound **PQ-Ph-Amide-PY** in $\text{DMSO-}d_6$.

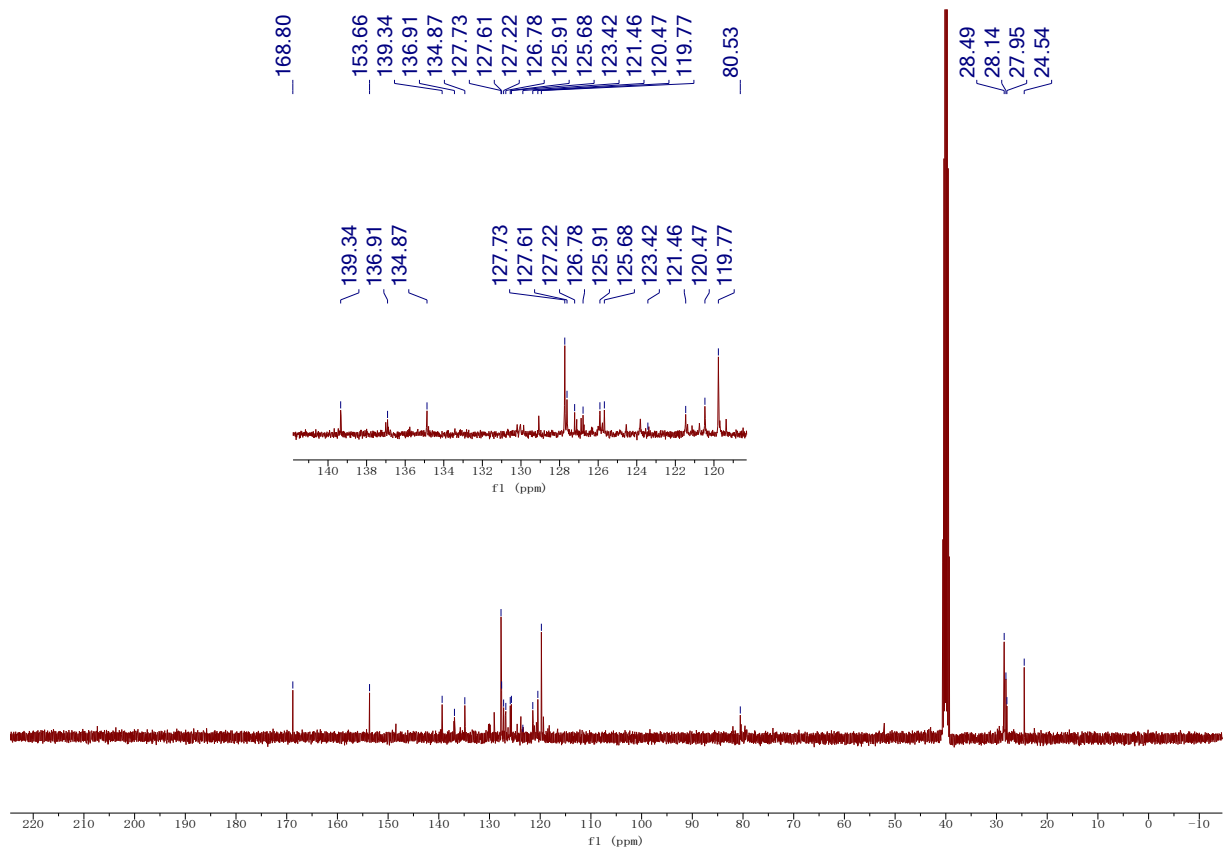


Fig. S54. ^{13}C NMR of Compound **PQ-Ph-Amide-PY** in $\text{DMSO-}d_6$.

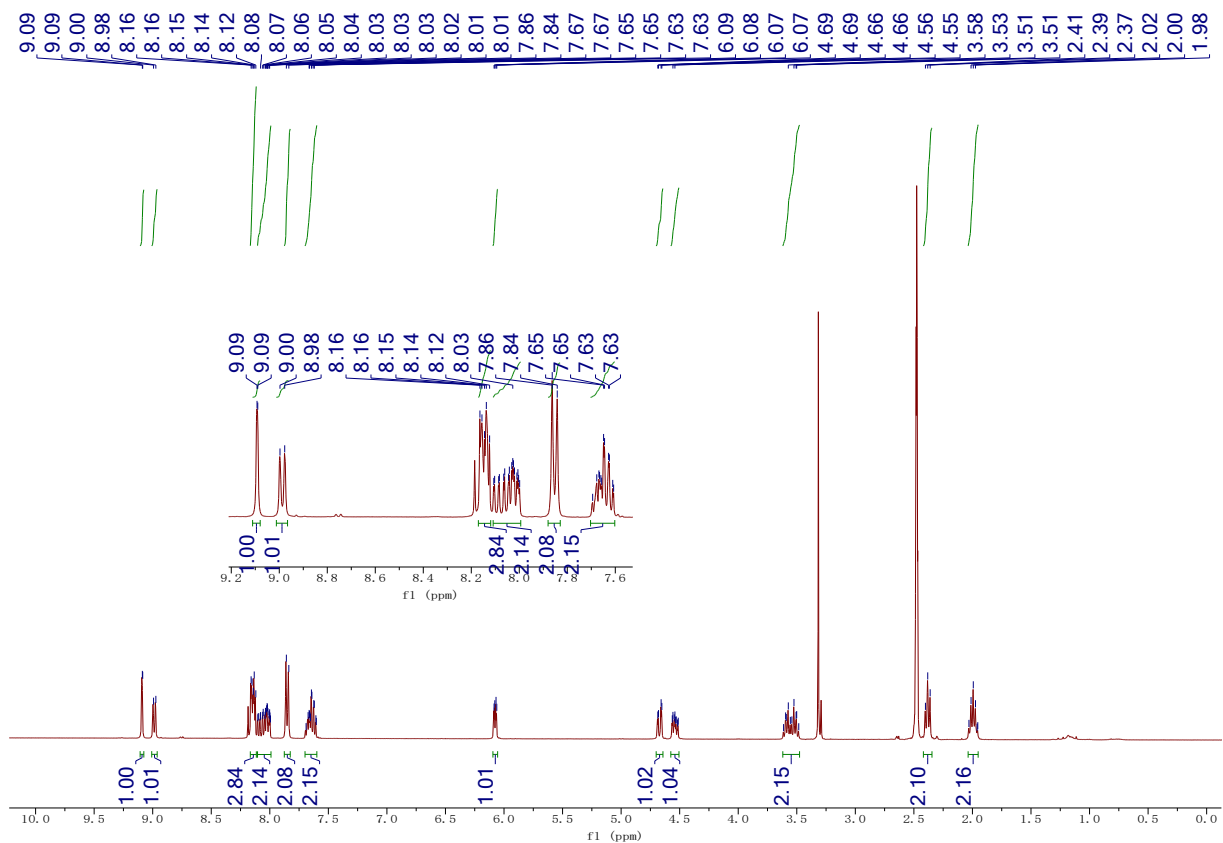


Fig. S55. ^1H NMR of Compound **PQ-Ph-CF₃-NVP** in $\text{DMSO-}d_6$.

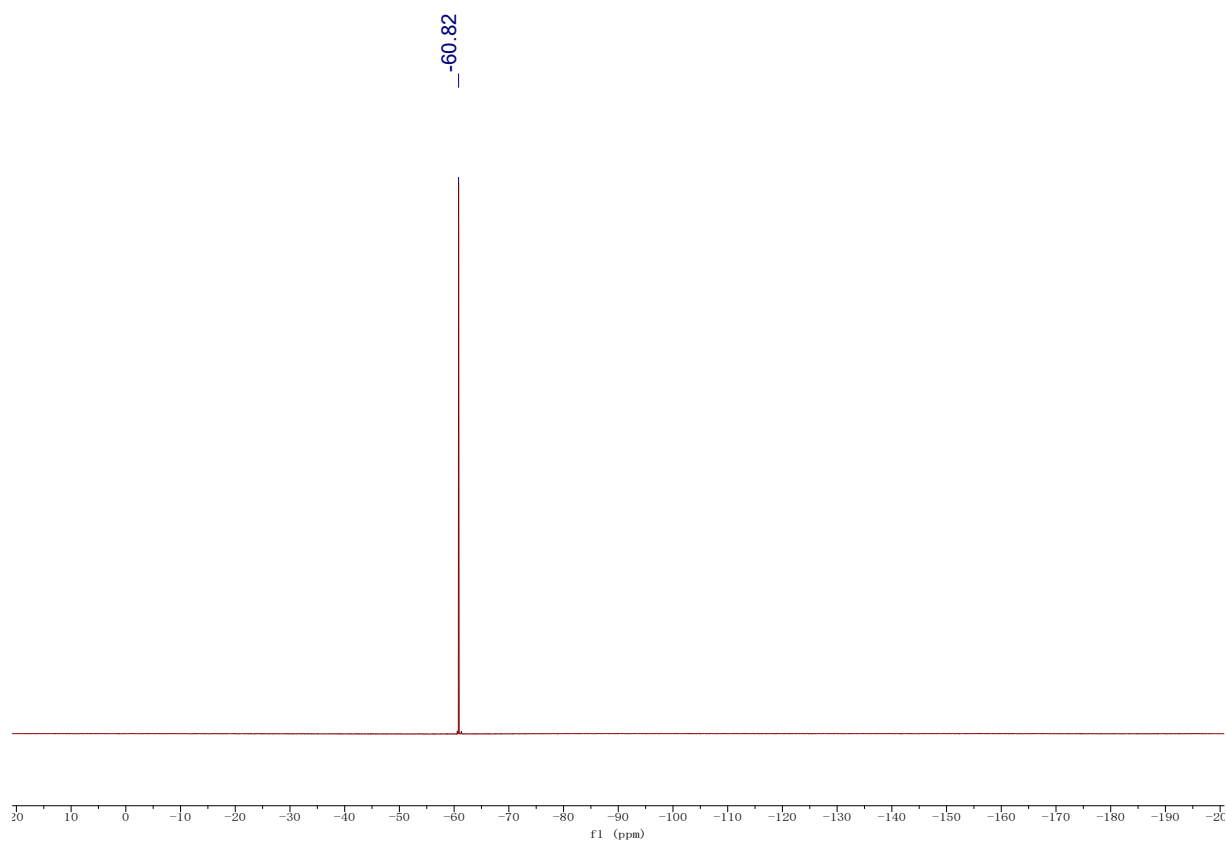


Fig. S56. ^{19}F NMR of Compound **PQ-Ph-CF₃-NVP** in $\text{DMSO-}d_6$.

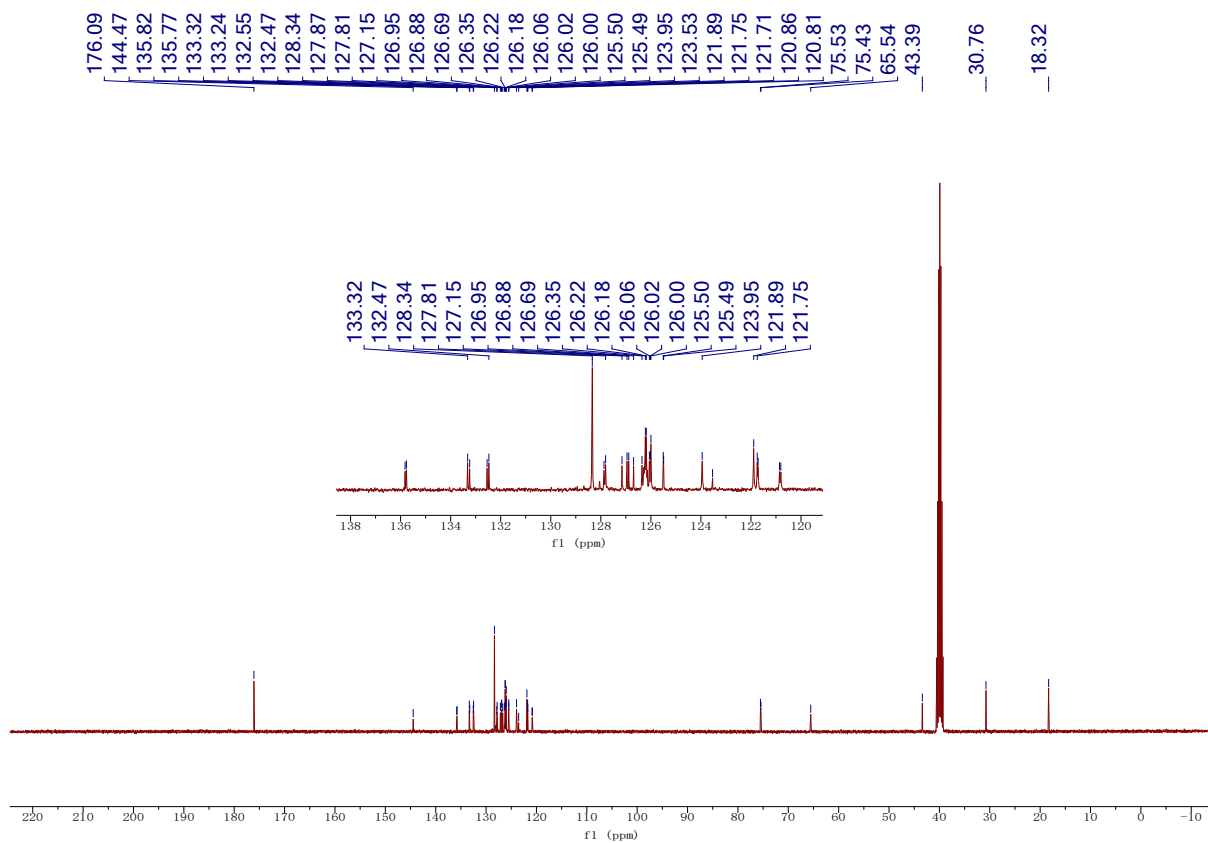


Fig. S57. ^{13}C NMR of Compound **PQ-Ph-CF₃-NVP** in $\text{DMSO-}d_6$.

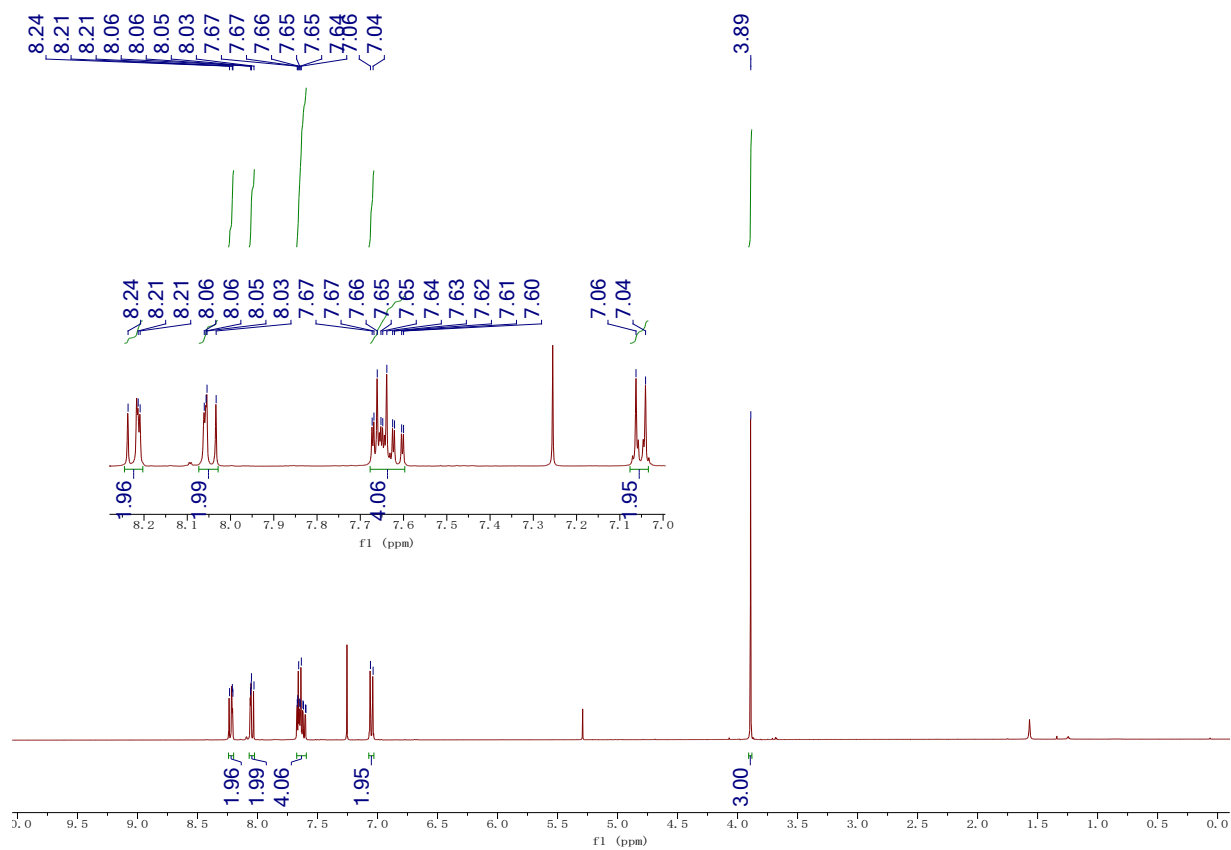


Fig. S58. ^1H NMR of Compound **PQ-Ph-OCH₃-Br** in CDCl_3 .

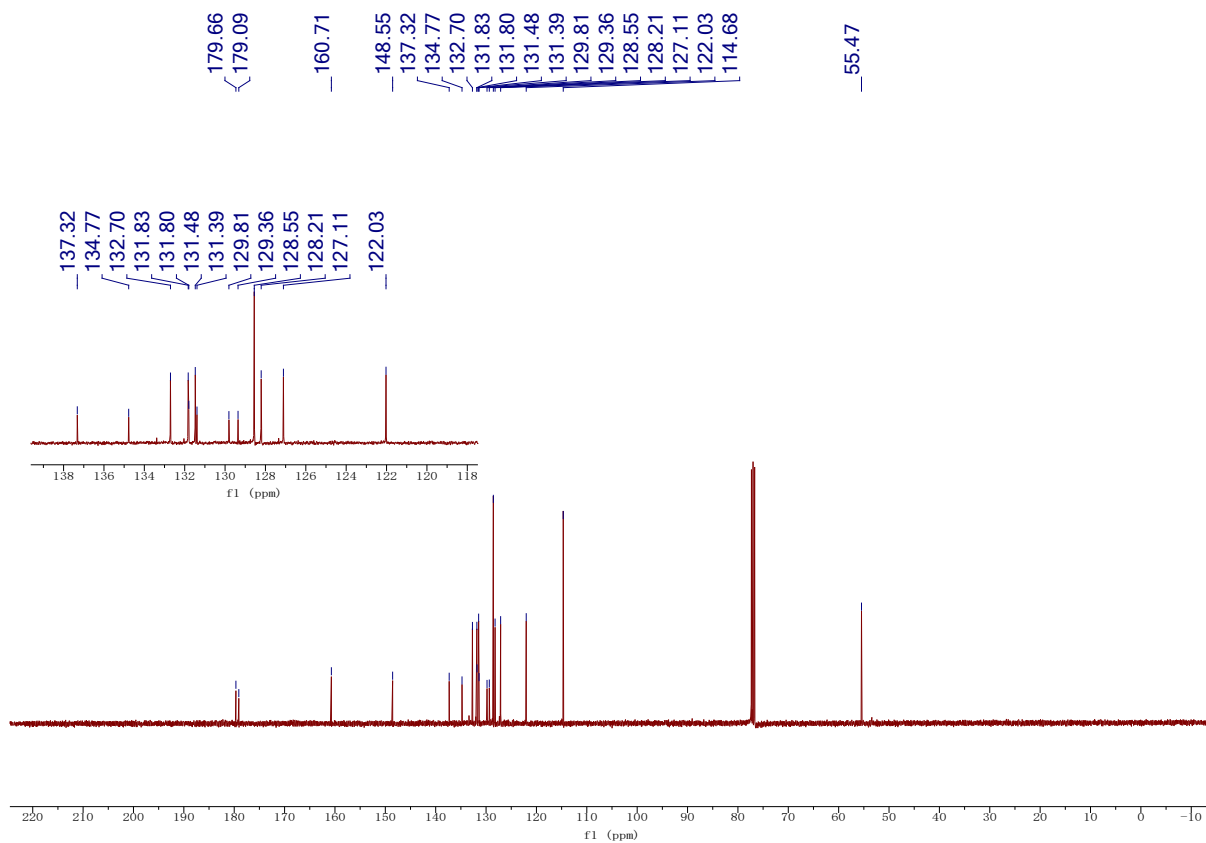


Fig. S59. ^{13}C NMR of Compound **PQ-Ph-OCH₃-Br** in CDCl_3 .

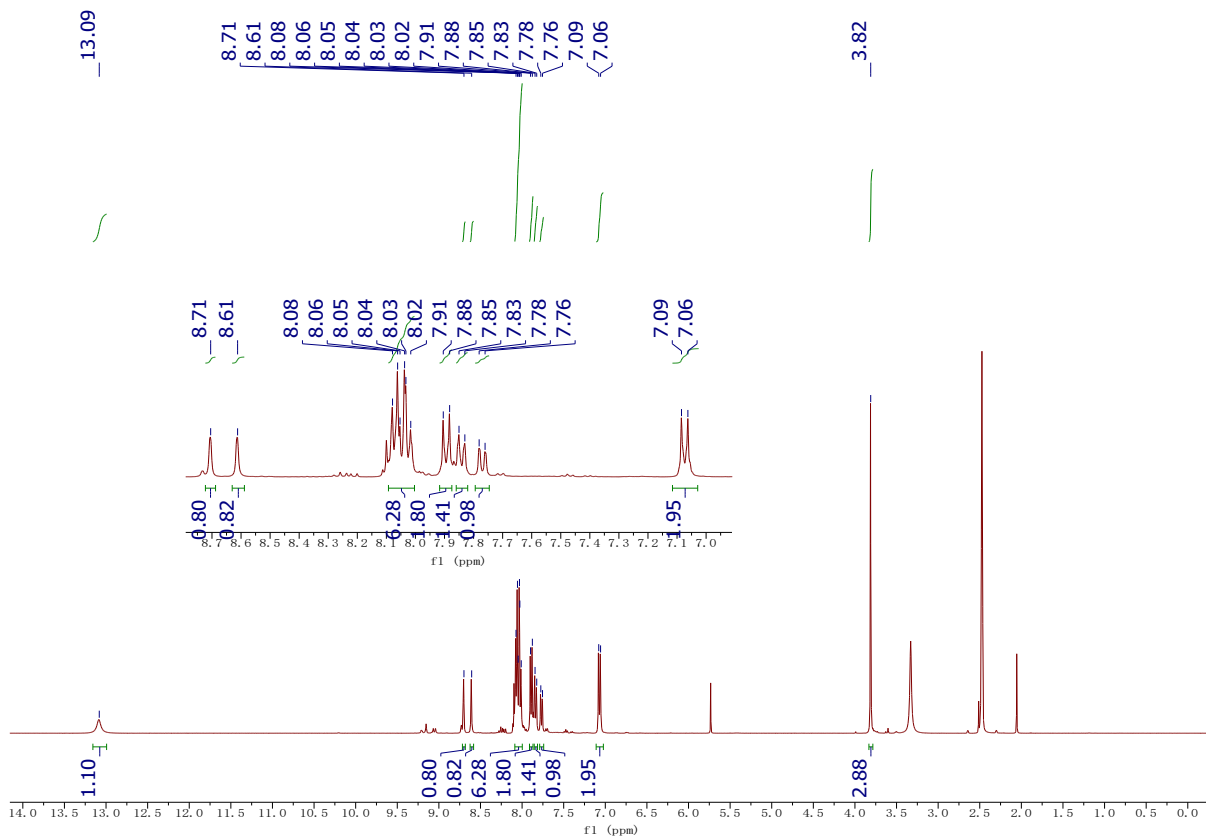


Fig. S60. ^1H NMR of Compound **PQ-Ph-OCH₃-Ph-COOH** in $\text{DMSO}-d_6$.

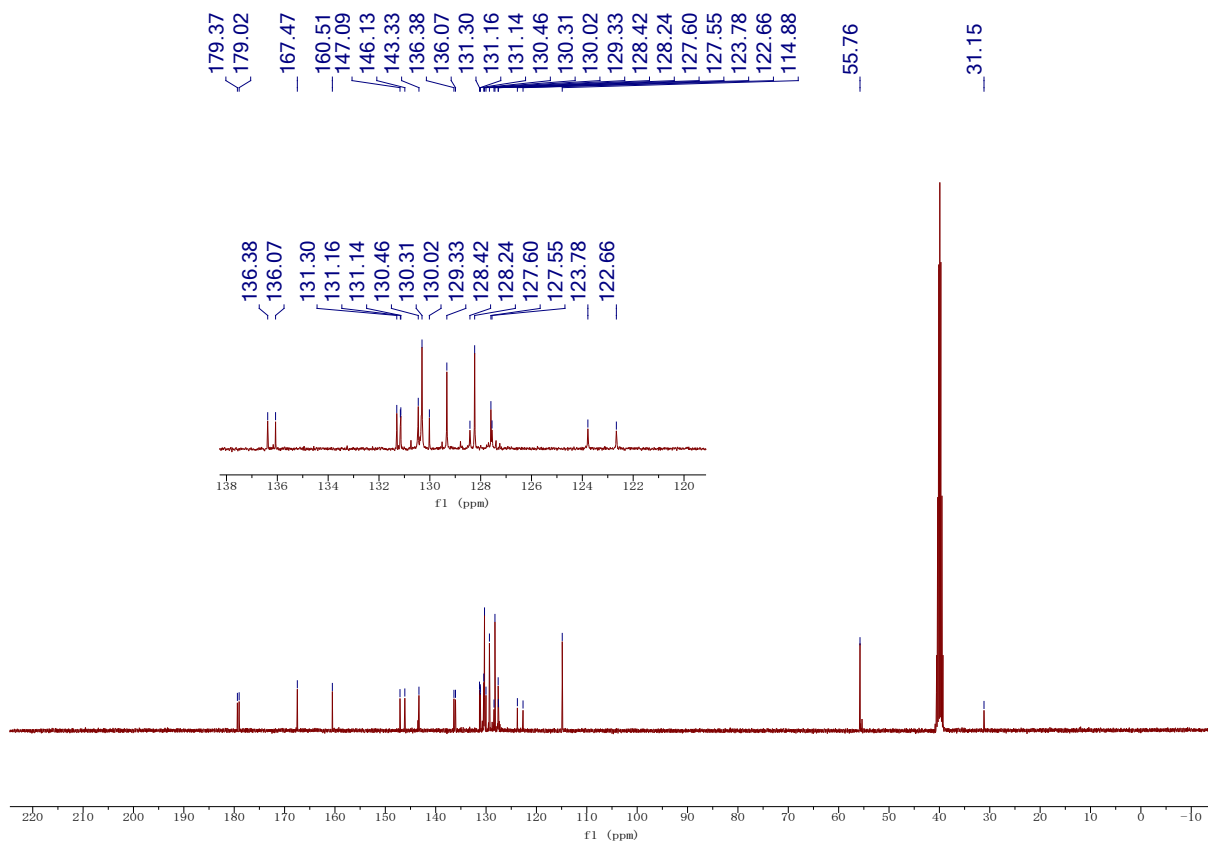


Fig. S61. ^{13}C NMR of Compound **PQ-Ph-OCH₃-Ph-COOH** in $\text{DMSO-}d_6$.

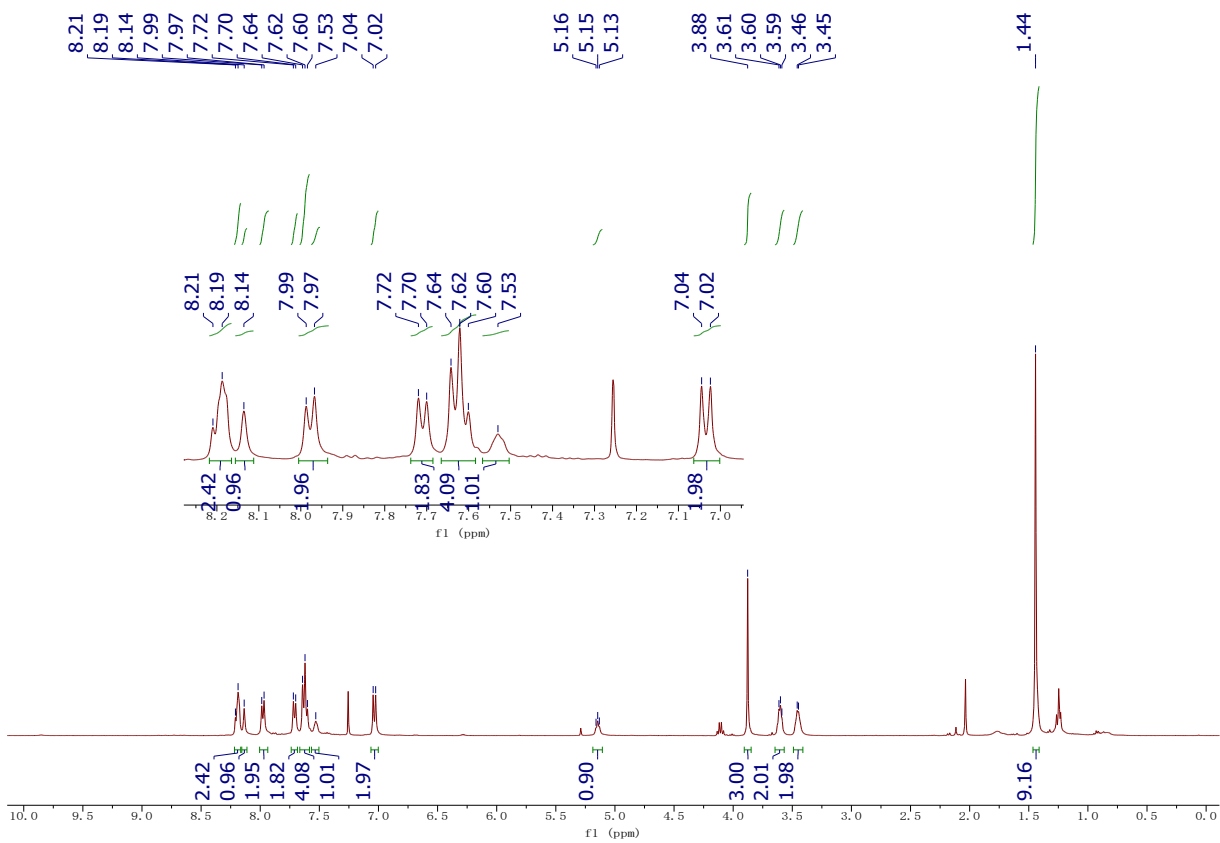


Fig. S62. ^1H NMR of Compound **PQ-Ph-OCH₃-Ph-Amide** in CDCl_3 .

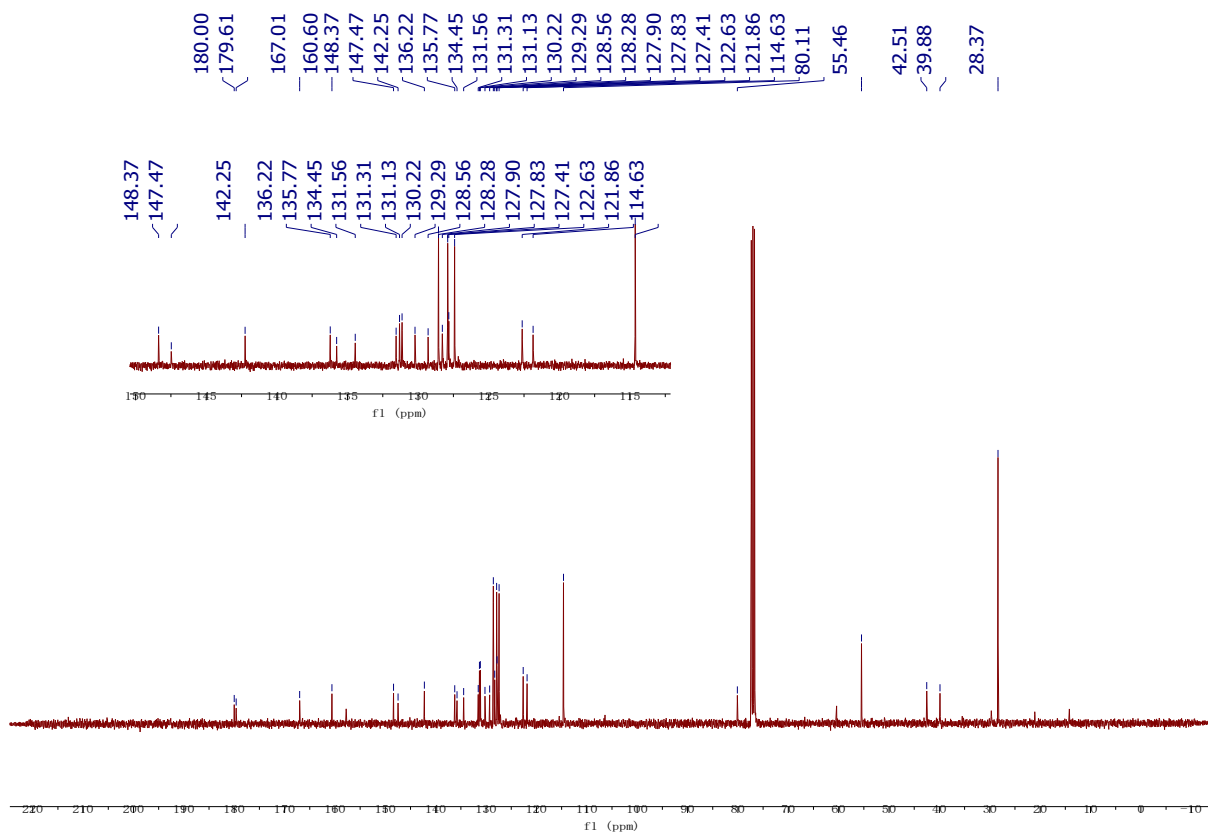


Fig. S63. ^{13}C NMR of Compound PQ-Ph-OCH₃-Ph-Amide in CDCl₃.

4. Photophysical and Photochemical Studies by UV-Vis, Fluorescence, IR Spectroscopy, HPLC, and UPLC-MS

4.1. UV-Vis and Fluorescence Spectra

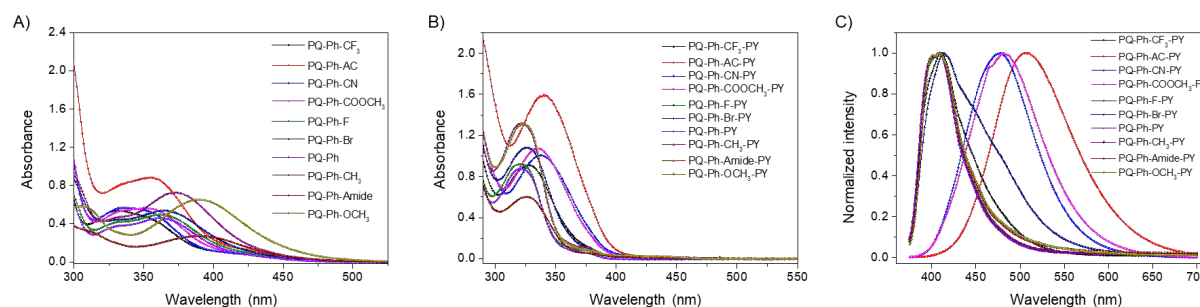


Fig. S64. UV-Vis absorption spectra of A) **PQ-Ph-R** (50 μM in MeCN), B) **PQ-Ph-R-PY** (50 μM in MeCN), and C) emission spectra of **PQ-Ph-R-PY** (5 μM in MeCN, λ_{exc}=330 nm). All measurements were performed at 20 °C.

The photocyclization reaction was followed in MeCN using both UV-Vis and fluorescence spectroscopies. Representative spectra are shown for the reaction of **PQ-Ph-OCH₃** with **PY** (Figure S65B and C). Upon irradiation (LED, 390 nm), the main absorption band (λ_{max} around 390 nm depending on R), that tails into the visible region of the spectrum, rapidly bleaches and new maxima around 320 nm are observed (Figure S65B). Simultaneously, a strong increase in fluorescence intensity in the corresponding emission spectrum is observed, *i.e.*, a bright blue fluorescence at λ_{max}=409 nm, indicating the generation of the fluorogenic photocycloadduct **PQ-Ph-OCH₃-PY** (Figure S65C). After only 20 s of irradiation, the fluorescence intensity stays constant, pointing to the completion of the reaction.

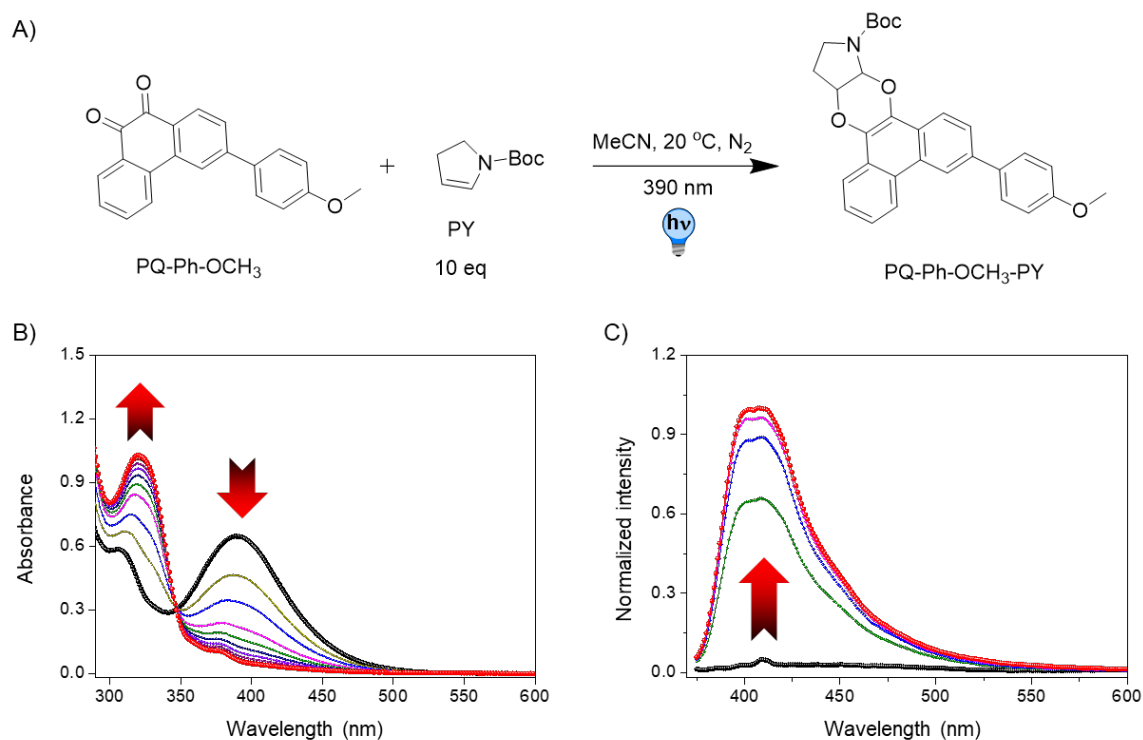


Fig. S65. Photoclick reaction of **PQ-Ph-OCH₃** and **PY** (reaction scheme in A), upon 390 nm LED irradiation under N₂ atmosphere at 20 °C, followed by UV-Vis absorption spectroscopy, shown in B), and emission spectroscopy, displayed in C). (Sampling interval 5 s. Concentration: 50 μM (**PQ-Ph-OCH₃**), 500 μM (**PY**), for emission spectra, $\lambda_{\text{ex}}=330$ nm)

4.2. Analysis of reactions rates

To assess the different reaction rates of the photo-induced [4+2] cycloaddition of the various phenanthrenequinone (**PQs**) substrates with **DF**, **PY**, and other potential reaction partners (**ERAs**), we adapted procedures previously published for the evaluation of the kinetics of chemical [6] and photochemical click reactions.[7] Photochemical transformations are strongly dependent on the used light source and setup, *etc.*, as shown *e.g.* for photocatalytic transformations [8] and photoclick reactions.[9] Therefore, we determined the respective rate constants *via* UV-Vis absorption spectroscopy using the fixed LED setup described above to ensure reliable comparability of the individual substrates. All reactions were performed at the same concentration (**PQs**: 50 μM, **ERAs**: 500 μM) and under irradiation with the same light

source and intensity, independently from the molar attenuation coefficient of the respective **PQs** at this wavelength. Both the wavelength of irradiation ($\lambda_{\text{exc}}=390$ nm) and λ_{obs} were chosen in the spectral regions where only the starting materials, **PQ**, and the photoclick product, absorb. Rate constants k_{obs} for the different **PQs** (50 μM) were measured under *pseudo*-first-order conditions with a 10-fold excess of **DF**, **PY**, or other **ERAs** in MeCN (N_2 atmosphere) by time-dependent analysis. The appropriate volume of the prepared stock solutions were mixed to achieve the desired final concentration in sample vials, and the mixtures were transferred into a 1 cm optical path quartz optical cuvettes, degassed by N_2 . Signals were read out by monitoring the absorption signal of the **PQs**. The kinetic traces were recorded using the following instrumental parameters: 1 data point per second over the recorded time range. The data was analyzed using single-exponential fits. All data processing was performed using Origin-pro software.

While this treatment does not lead to the best performance of all systems at the applied irradiation wavelength (due to different molar attenuation coefficient at that wavelength), it does (i) facilitate rapid screening of different **ERAs** and (ii) give a good impression of the relative reaction rates between individual **PQ-alkene** systems. To compare the observed rates with previously published ones, we performed the reported reactions.^[9]

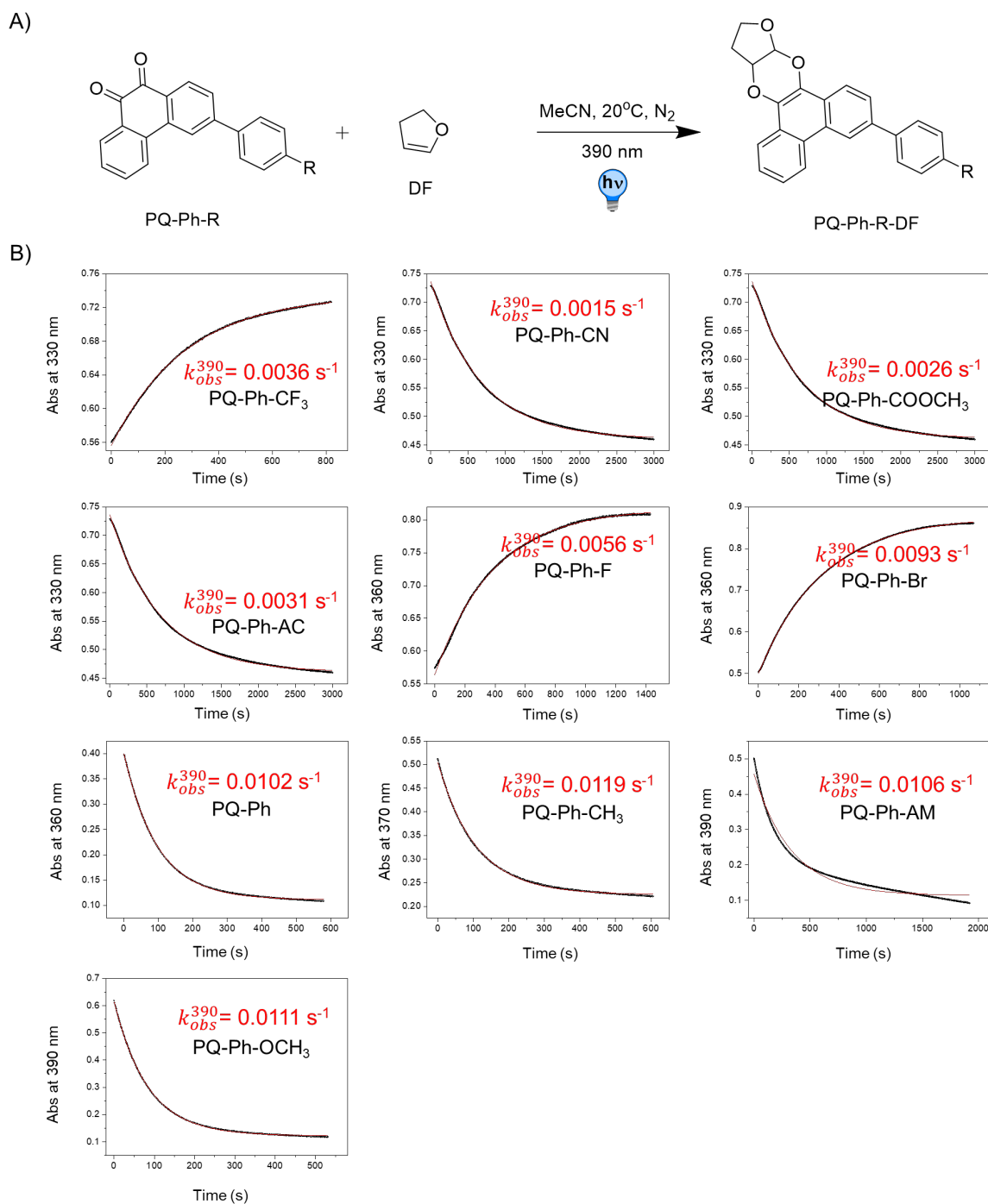


Fig. S66. Photo-induced [4+2] cycloaddition of **PQ-Ph-R** with **DF**. A) reaction scheme, B) kinetic traces of the photocycloaddition between **PQ-Ph-R** (50 μM) with **DF** (500 μM) in 2.5 mL MeCN (N_2 atmosphere); the reaction mixture was irradiated with 390 nm LED at 20 $^\circ\text{C}$. The reaction was monitored by UV-Vis absorption spectroscopy (1 cm cuvette, sample interval 1 s). **PQ-Ph-R-DF** formation was fitted to an exponential rise to the maximum equation, $y = (y_0 - a) e^{-k_{obs}^{390} t} + a$, to give k_{obs}^{390} .

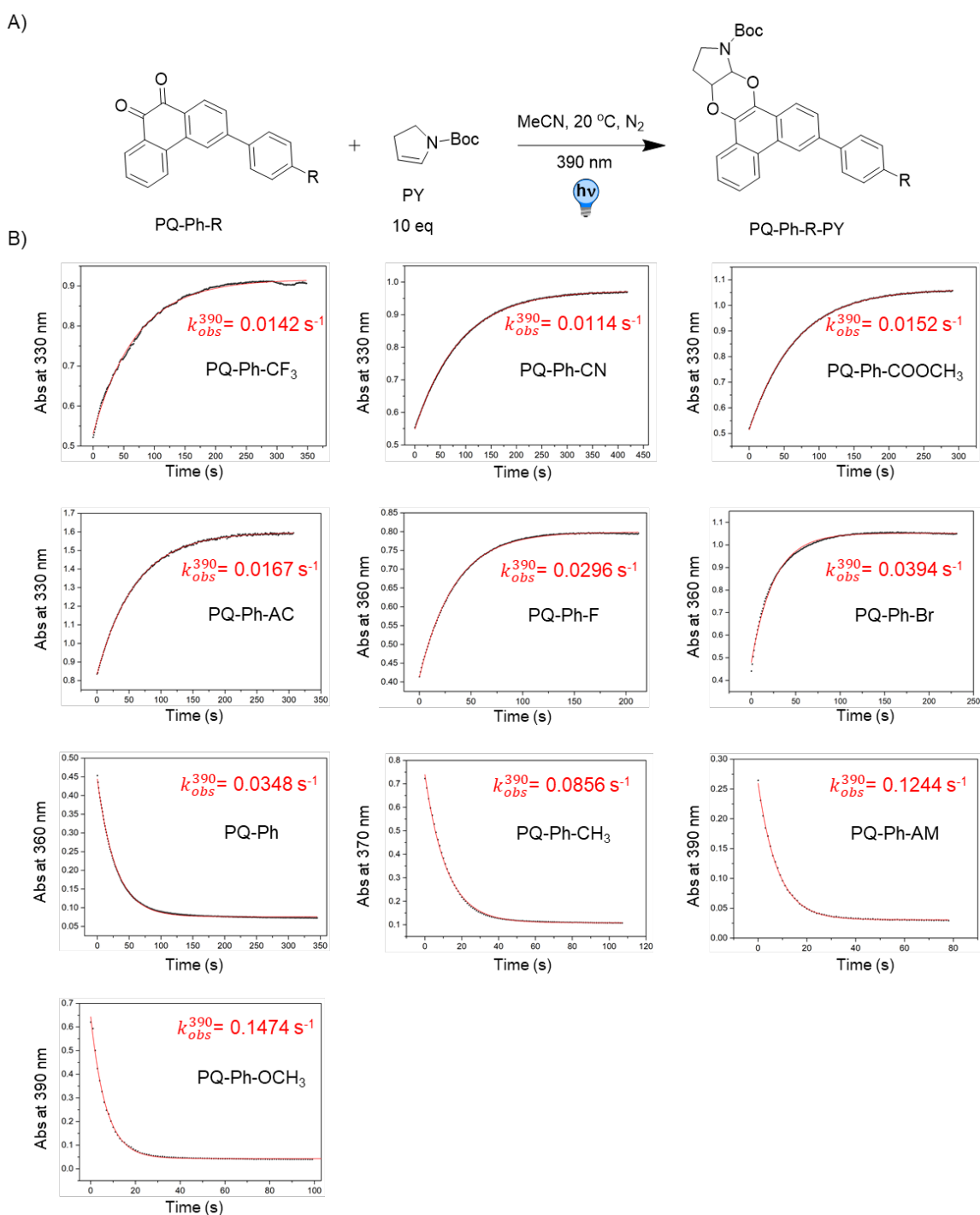


Fig. S67. Kinetic study of photo-induced [4+2] cycloaddition of **PQ-Ph-R** with **PY**. A) reaction scheme, B) kinetic traces of the photocycloaddition between **PQ-Ph-R** (50 μ M) toward **PY** (500 μ M) in 2.5 mL MeCN (N_2 atmosphere); the reaction mixture was irradiated with 390 nm LED at 20 $^{\circ}C$. The reaction was monitored by UV-Vis absorption spectroscopy (1 cm cuvette, sample interval 1 s). **PQ-Ph-R-PY** formation was fitted to an exponential rise to the maximum equation, $y = (y_0 - a) e^{-k_{obs}^{390} t} + a$, to give k_{obs}^{390} .

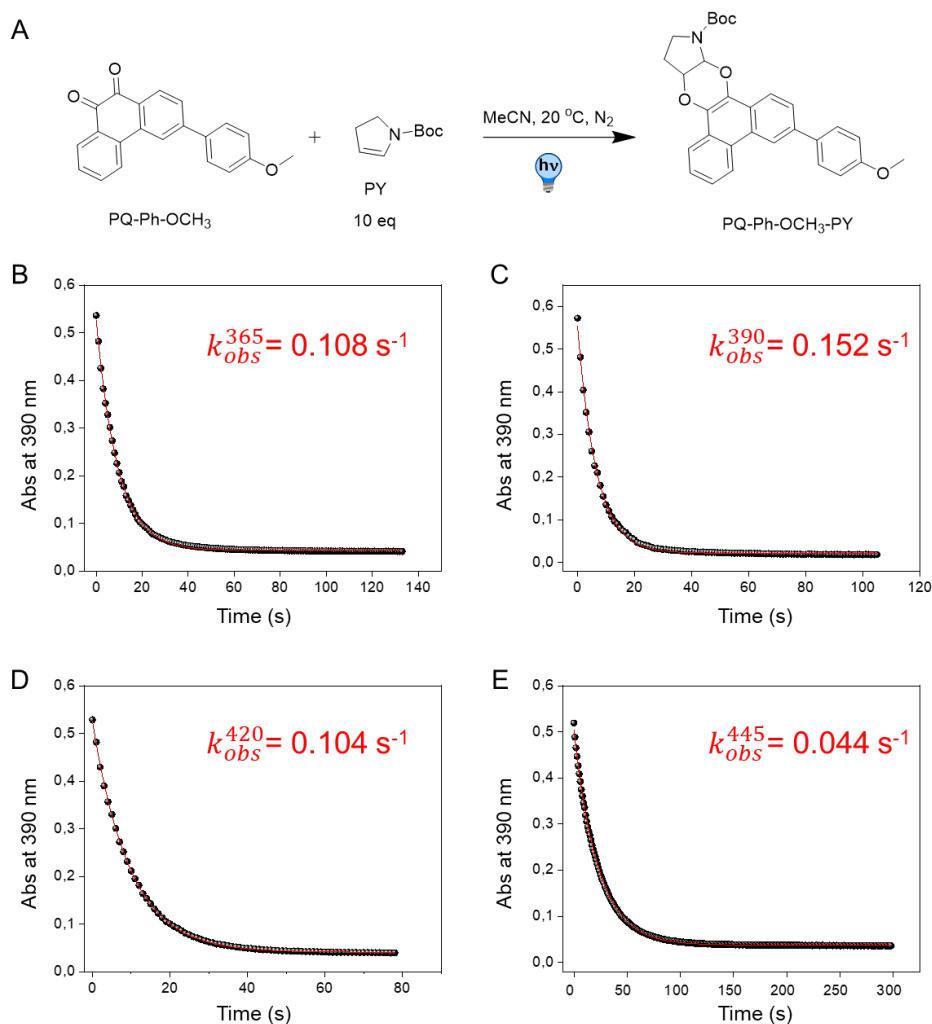


Fig. S68. Photo-induced [4+2] cycloaddition of **PQ-Ph-OCH₃** with **PY** upon different light irradiation. A) reaction scheme, kinetic traces of the photocycloaddition between **PQ-Ph-OCH₃** (50 μ M) with **PY** (500 μ M) in 2.5 mL MeCN (N_2 atmosphere) upon irradiation with B) a 365 nm, C) a 390 nm, D) a 420 nm, and E) a 445 nm LED at 20 °C. The reaction was monitored by UV-Vis absorption spectroscopy (1 cm cuvette, sample interval 1 s). **PQ-Ph-OCH₃ -PY** formation was fitted to an exponential rise to the maximum equation, $y = (y_0 - a) e^{-k_{obs} \cdot t} + a$, to give k_{obs} .

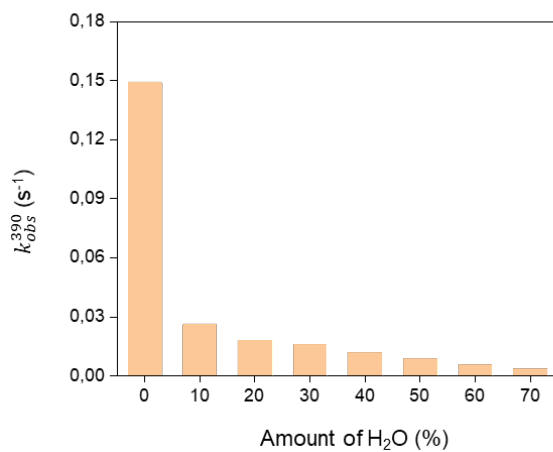
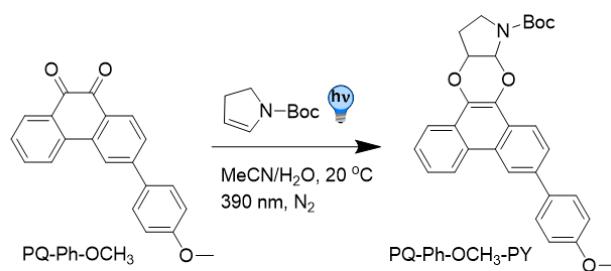


Fig. S69. Kinetic analysis of the photocycloaddition between **PQ-Ph-OCH₃** and **PY** in a water/MeCN solvent mixture (from 0 vol% to 70 vol% water addition).

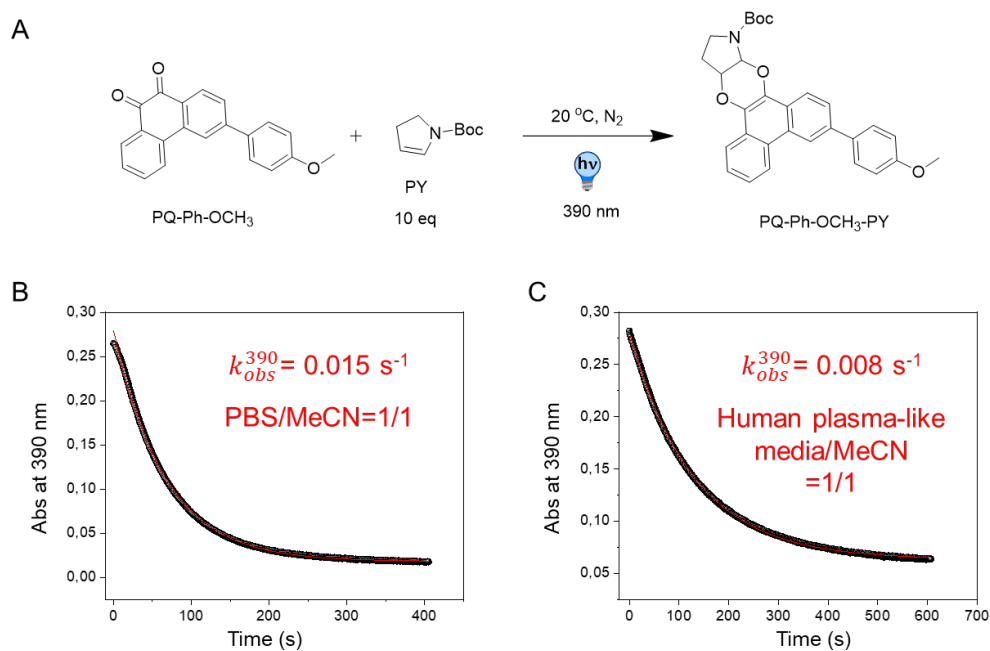


Fig. S70. Kinetic traces of the photocycloaddition between **PQ-Ph-OCH₃** and **PY**. A) Reaction scheme. B) and C) Kinetic traces of the photoclick reaction between **PQ-Ph-OCH₃** (50 μ M) and 10 eq **PY** in 2.5 mL PBS buffer/MeCN (1/1, v/v, B) or human plasma-like media/MeCN (1/1, v/v, C), N₂ atmosphere; the reaction mixture was irradiated with a 390 nm LED at 20 °C. The formation of the [4+2] cycloaddition product **PQ-Ph-OCH₃-PY** was monitored by UV-Vis absorption spectroscopy ($\lambda_{\text{obs}}=390$ nm, 1 cm cuvette, sample interval 1 s) and the trace was fitted exponentially using the equation, $y = (y_0 - a) e^{-k_{\text{obs}} t} + a$, to give k_{obs}^{390} .

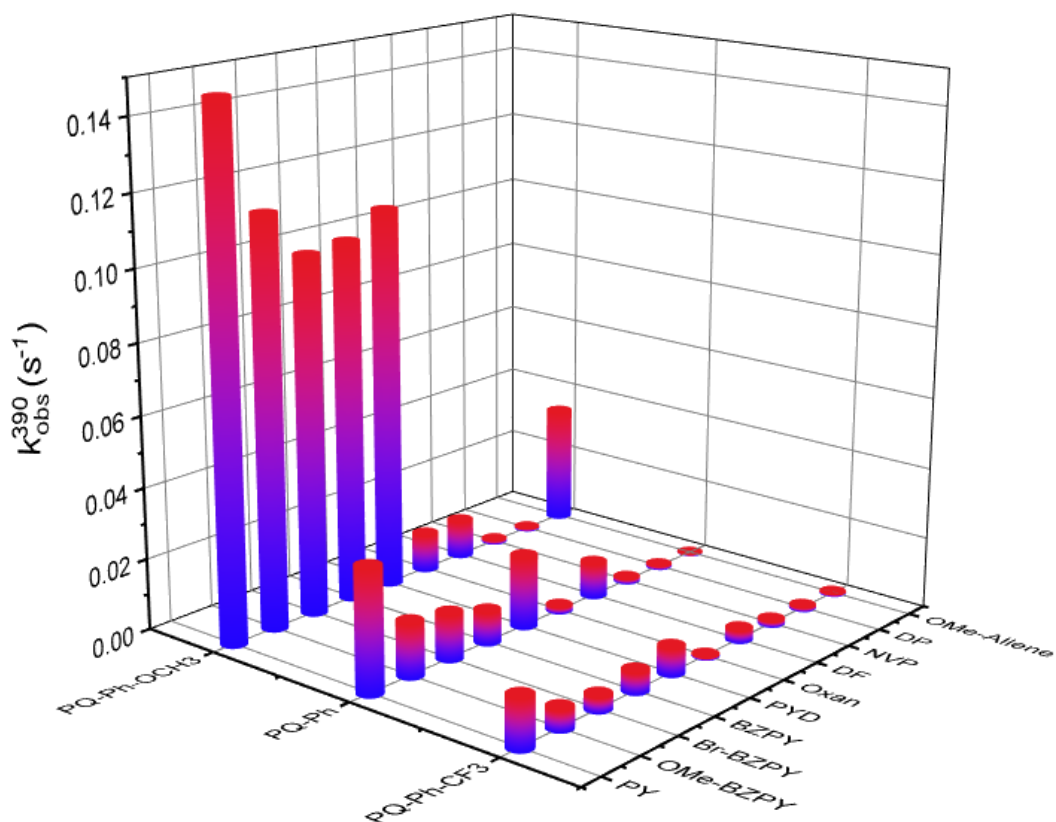


Fig. S71. Reaction rate constants k_{obs}^{390} (s^{-1}) for the [4+2] cycloaddition of **PQ-Ph-OCH₃**, **PQ-Ph**, and **PQ-Ph-CF₃** with different ERAs. The mixture of 50 μ M **PQ-Ph-R** and 500 μ M ERAs in MeCN was irradiated with 390 nm LED, all of the reactions were followed over time by UV-Vis absorption spectroscopy (1 cm cuvette, 2.5 mL sample volume, N₂ atmosphere, 20 °C, sample interval 1 s) and the data was fitted by equation: $y = (y_0 - a) e^{-k_{obs}^{390} t} + a$, to give k_{obs}^{390} .

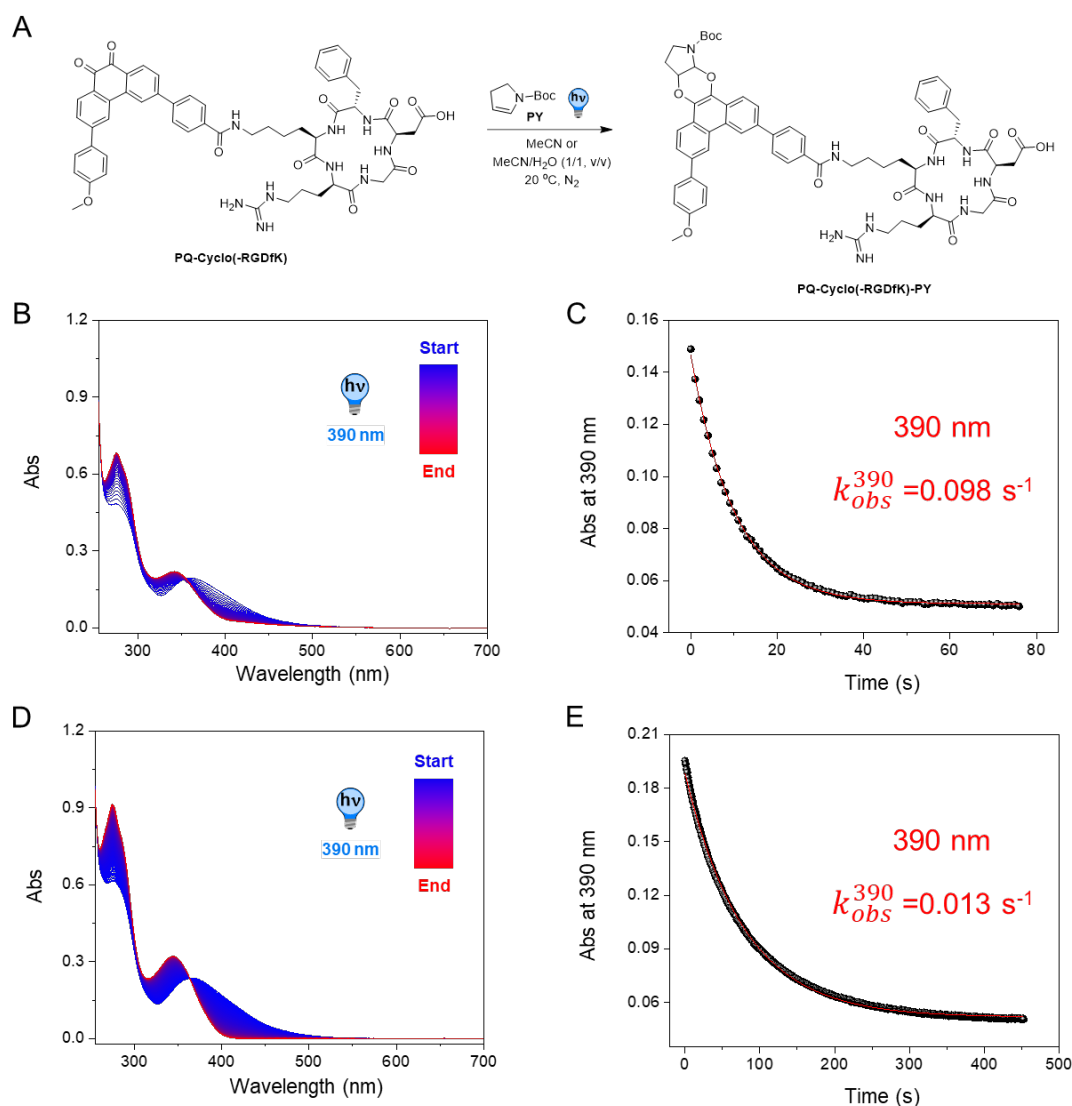


Fig. S72. Photocycloaddition between **PQ-Cyclo(RGDfK)** and **PY**. A) Reaction scheme. B–E) Time-resolved UV-Vis absorption spectra and kinetic traces of the photocycloaddition between **PQ-Cyclo(RGDfK)** and **PY**. 20 μM **PQ-Cyclo(RGDfK)** with 10 eq **PY** in 2 mL MeCN (B, C) or H₂O/MeCN (1/1, v/v, D, E), respectively, under N₂ atmosphere; the reaction mixture was irradiated with 390 nm LED at 20 °C. The formation of the [4+2] cycloaddition product **PQ-Cyclo(RGDfK)-PY** was monitored by UV-Vis absorption spectroscopy ($\lambda_{\text{obs}}=390$ nm, 1 cm cuvette, sample interval 1 s) and the trace was fitted exponentially using the equation, $y = (y_0 - a) e^{-k_{\text{obs}}^{\text{390}} t} + a$, to give $k_{\text{obs}}^{\text{390}}$.

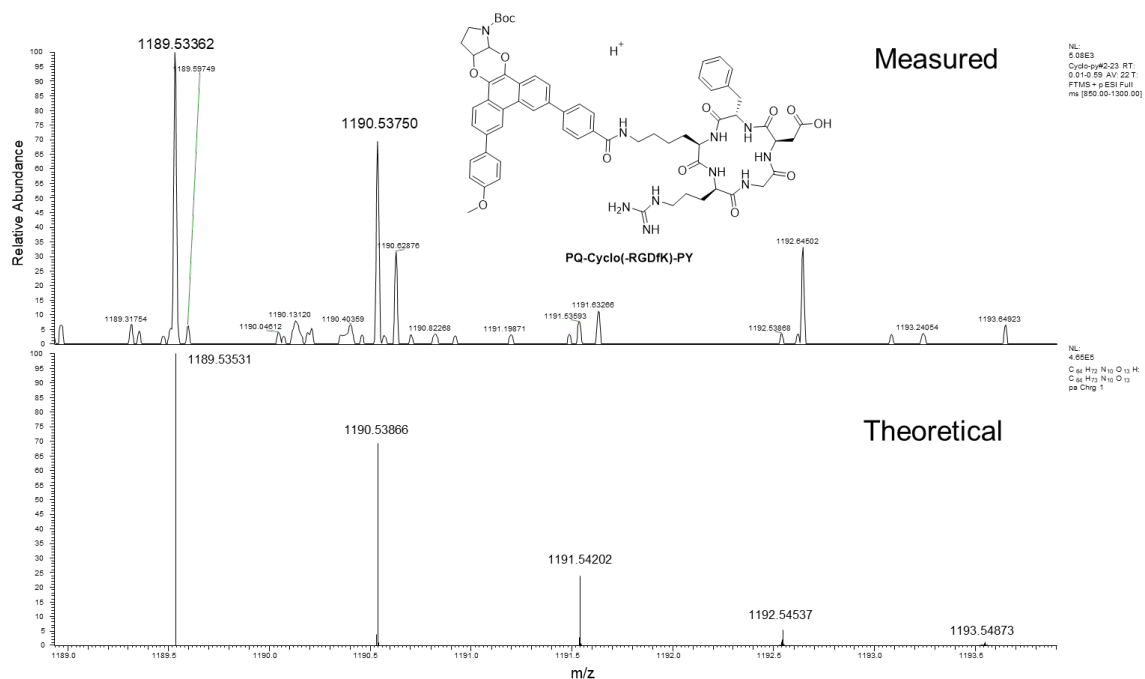


Fig. S73. HR-MS of **PQ-Cyclo(RGDfK)-PY** (top: measured; bottom: simulated).

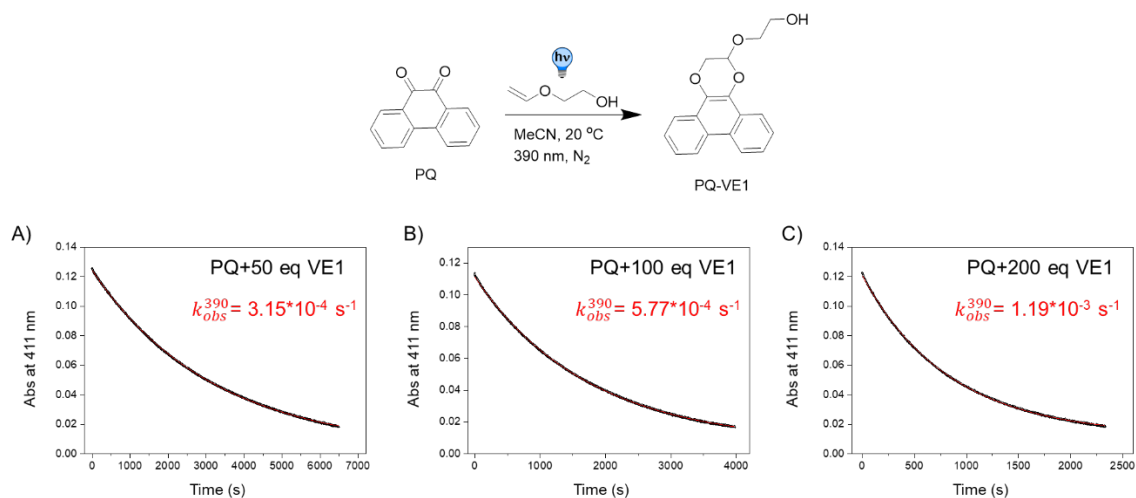


Fig. S74. Kinetics traces of the photocycloaddition between **PQ** and **VE1**. 50 μM **PQ** with different concentrations of **VE1** ((A)2.5 mM, (B) 5 mM, and (C)10 mM respectively) in 2.5 mL MeCN (N₂ atmosphere); the reaction mixture was irradiated with 390 nm LED at 20 °C. The formation of the [4+2] cycloaddition product **PQ-VE1** was monitored by UV-Vis absorption spectroscopy (λ_{obs} =411 nm, 1 cm cuvette, sample interval 1 s) and the trace was fitted exponentially using the equation, $y = (y_0 - a) e^{-k_{obs} t} + a$, to give k_{obs}^{390} .

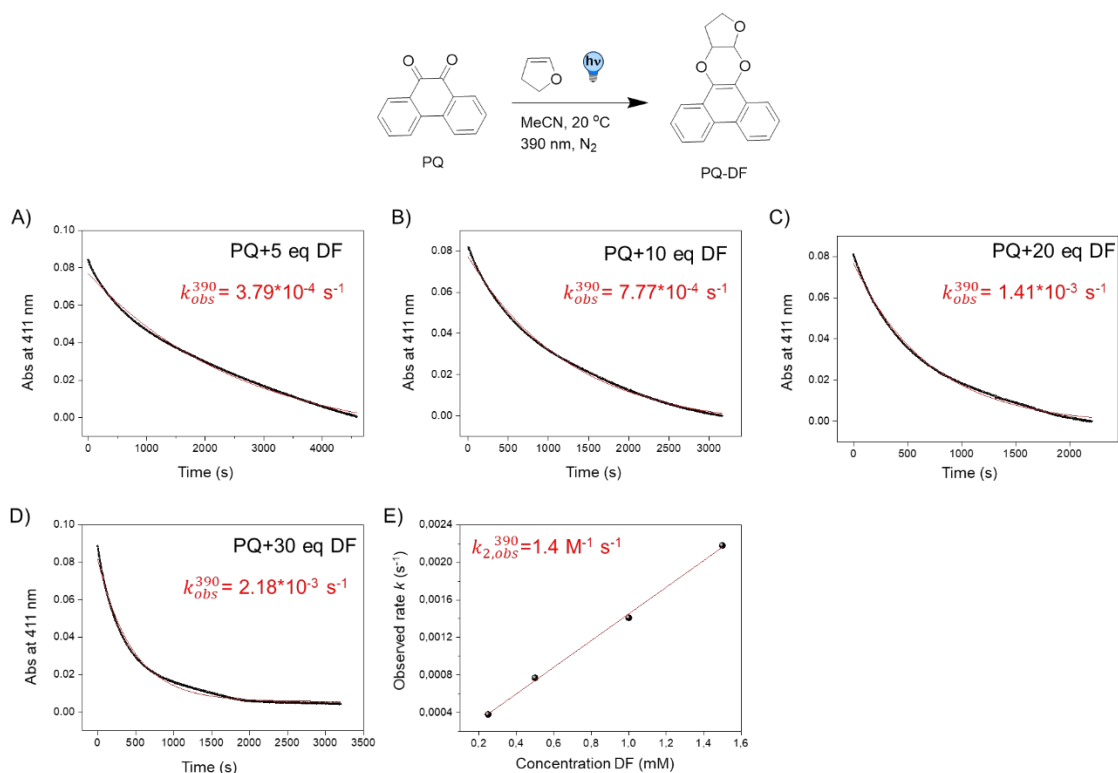


Fig. S75. Kinetics traces of the photocycloaddition between **PQ** and **DF**. 50 μM **PQ** with different concentrations of **DF** ((A) 0.25 mM, (B) 0.5 mM, (C) 1 mM, and (D) 1.5 mM, respectively) in 2.5 mL MeCN (N₂ atmosphere); the reaction mixture was irradiated with 390 nm LED at 20 °C. The formation of the [4+2] cycloaddition product **PQ-DF** was monitored by UV-Vis absorption spectroscopy ($\lambda_{\text{obs}}=411$ nm, 1 cm cuvette, sample interval 1 s) and the trace was fitted exponentially using the equation, $y = (y_0 - a) e^{-k_{obs}^{390} \cdot t} + a$, to give k_{obs}^{390} . E) Plot of k_{obs}^{390} vs **DF** concentration. The second-order rate constant $k_{2,obs}^{390}$ was determined to be 1.4 $\text{M}^{-1} \text{s}^{-1}$ based on the slope of the fitted line.

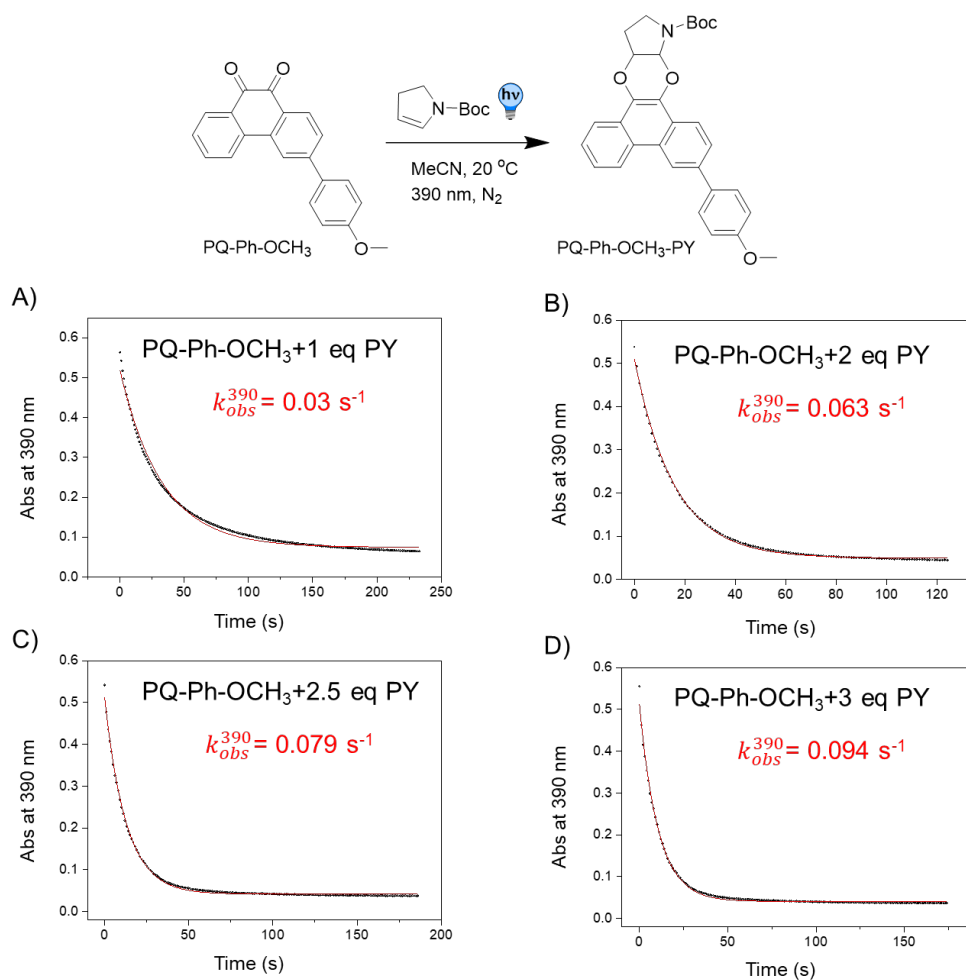


Fig. S76. Kinetics traces of the photocycloaddition between **PQ-Ph-OCH₃** and **PY**. 50 μM **PQ-Ph-OCH₃** with different concentrations of **PY** ((A) 0.05 mM, (B) 0.1 mM, (C) 0.125 mM, and (D) 0.15 mM respectively) in 2.5 mL MeCN (N₂ atmosphere); the reaction mixture was irradiated with 390 nm LED at 20 °C. The formation of the [4+2] cycloaddition product **PQ-Ph-OCH₃-PY** was monitored by UV-Vis absorption spectroscopy ($\lambda_{obs}=390 \text{ nm}$, 1 cm cuvette, sample interval 1 s) and the trace was fitted exponentially using the equation, $y = (y_0 - a) e^{-k_{obs} \cdot t} + a$, to give k_{obs}^{390} .

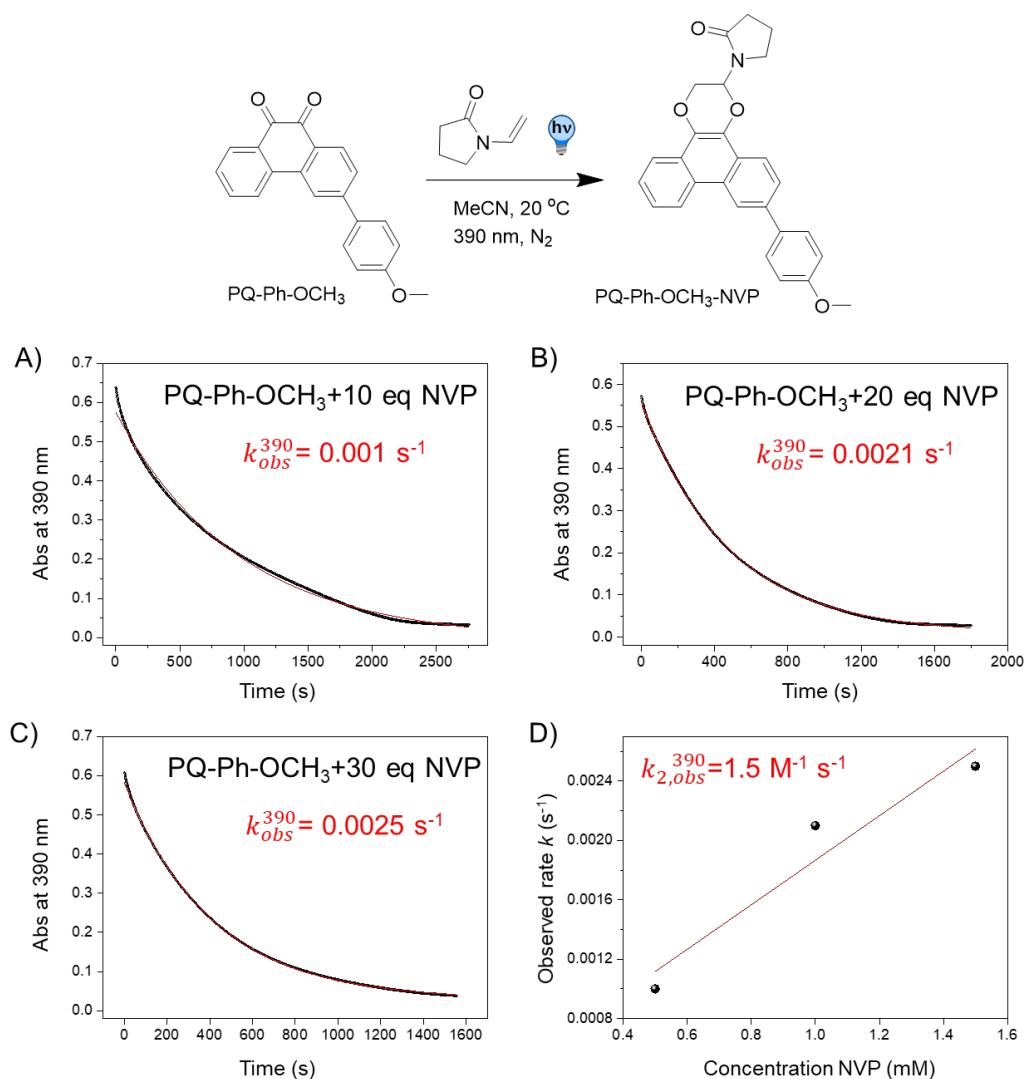


Fig. S77. Kinetics measurement of the photocycloaddition between **PQ-Ph-OCH₃** and **NVP**. 50 μM **PQ-Ph-OCH₃** with different concentrations of **NVP** ((A)0.5 mM, (B) 1 mM, and (C)1.5 mM, respectively) in 2.5 mL MeCN (N₂ atmosphere); the reaction mixture was irradiated with 390 nm LED at 20 °C. The [4+2] cycloaddition product **PQ-Ph-OCH₃-NVP** was monitored by UV-Vis absorption spectroscopy (at 390 nm, 1 cm cuvette, sample interval 1 s). **PQ-Ph-OCH₃-NVP** formation was fitted to an exponential rise to the maximum equation, $y = (y_0 - a) e^{k_{obs} \cdot t} + a$, to give k_{obs}^{390} . E) Plot of k_{obs}^{390} vs **NVP** concentration. The second-order rate constant $k_{2,obs}^{390}$ was determined to be $1.5 \text{ M}^{-1} \text{ s}^{-1}$ based on the slope of the fitted line.

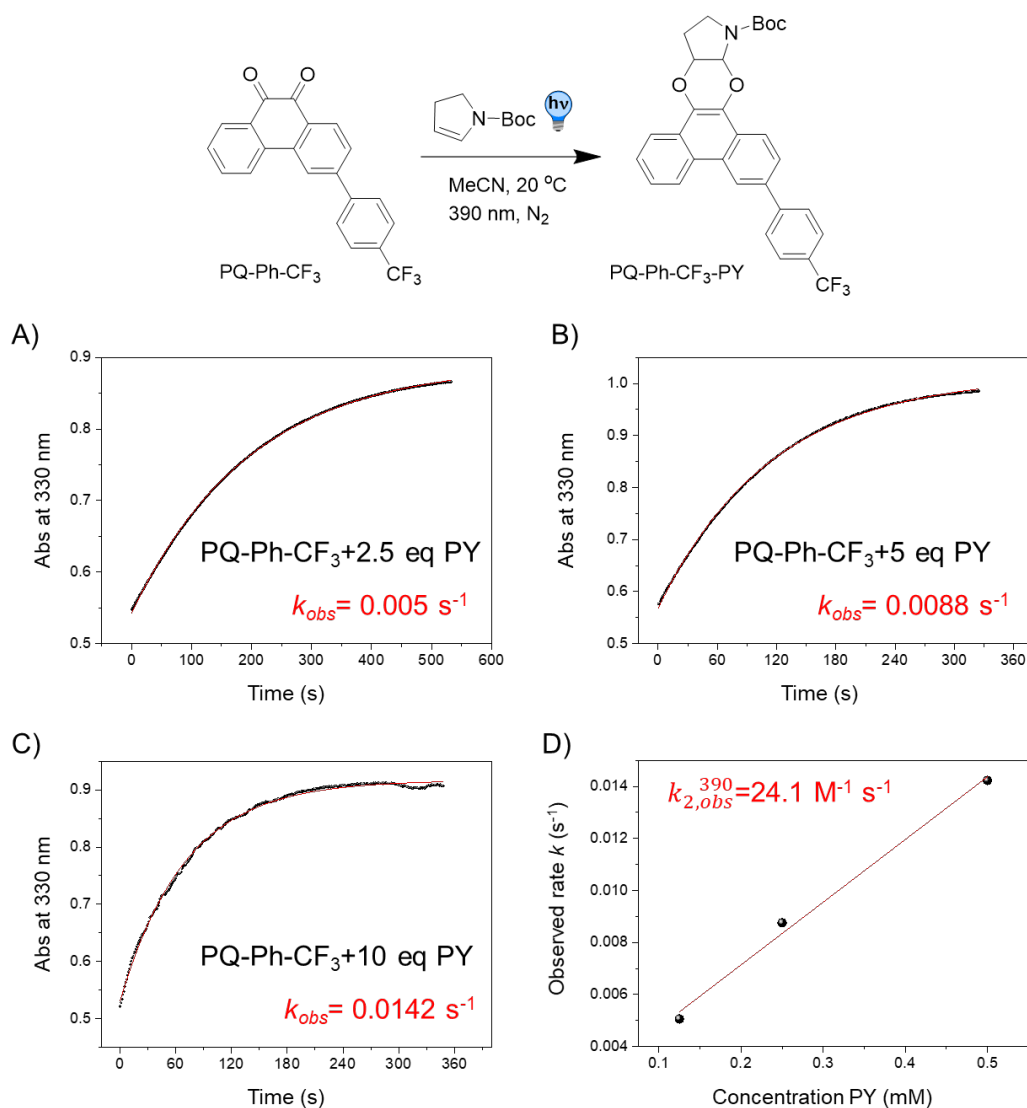


Fig. S78. Kinetics measurement of the photocycloaddition between **PQ-Ph-CF₃** and **PY**, 50 μM **PQ-Ph-CF₃** with different concentrations of **PY** ((A)0.125 mM, (B) 0.25 mM, and (C)0.5 mM, respectively) in 2.5 mL MeCN (N₂ atmosphere); the reaction mixture was irradiated with 390 nm LED at 20 °C. The [4+2] cycloaddition product **PQ-Ph-CF₃-PY** was monitored by UV-Vis absorption spectroscopy (at 390 nm, 1 cm cuvette, sample interval 1 s). **PQ-Ph-CF₃-PY** formation was fitted to an exponential rise to the maximum equation, $y = (y_0 - a) e^{k_{obs} \cdot t} + a$, to give k_{obs}^{390} . E) Plot of k_{obs}^{390} vs **PY** concentration. The second-order rate constant $k_{2,obs}^{390}$ was determined to be $24.1 \text{ M}^{-1} \text{ s}^{-1}$ based on the slope of the fitted line.

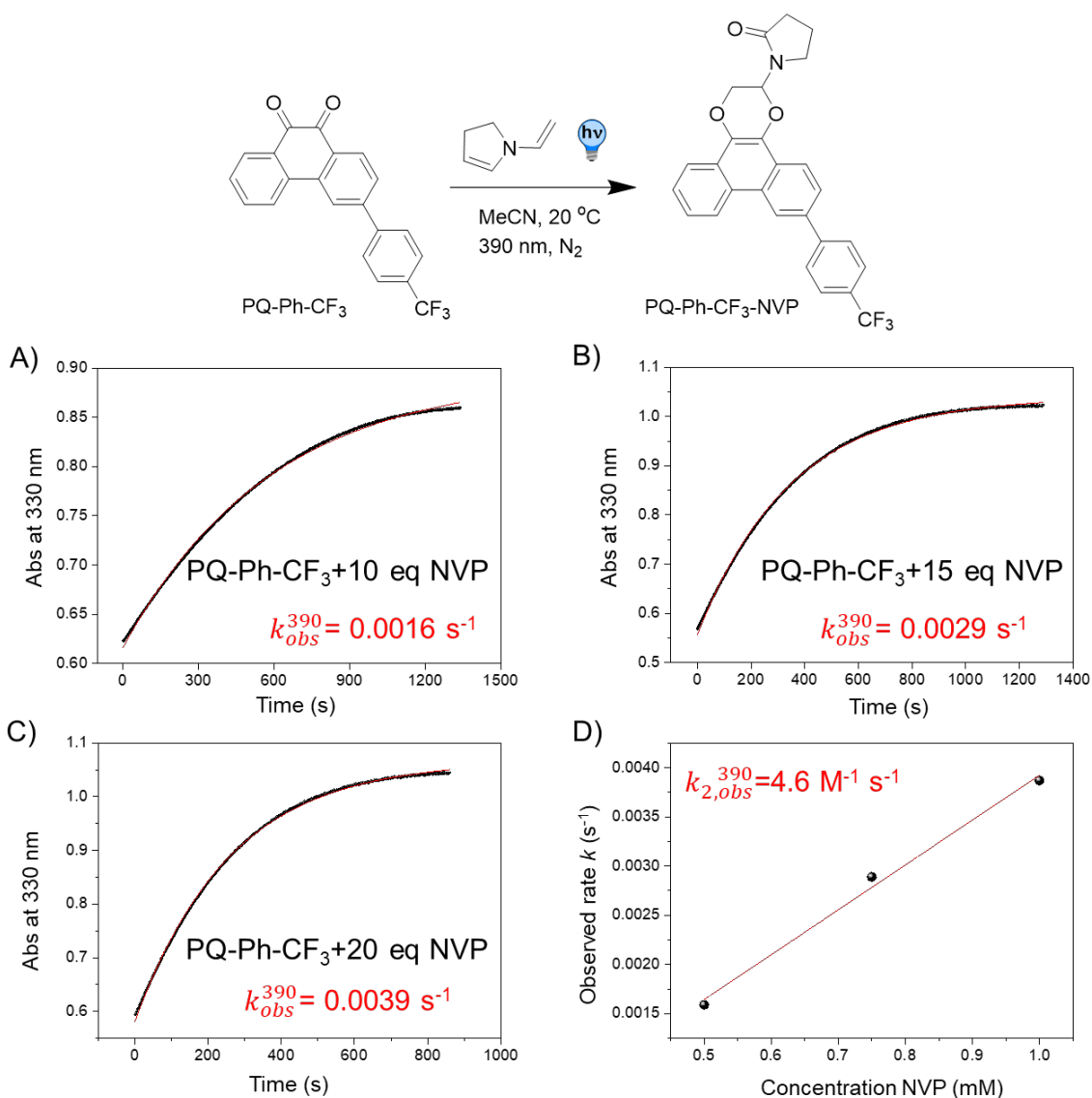


Fig. S79. Kinetics measurement of the photocycloaddition between **PQ-Ph-CF₃** and **NVP**. 50 μM **PQ-Ph-CF₃** with different concentrations of **NVP** ((A)0.5 mM, (B) 0.625 mM, and (C)1 mM, respectively) in 2.5 mL MeCN (N₂ atmosphere); the reaction mixture was irradiated with 390 nm LED at 20 °C. Time-course of the reaction between **PQ-Ph-CF₃** and **NVP**. The [4+2] cycloaddition product **PQ-Ph-CF₃-NVP** was monitored by UV-Vis absorption spectroscopy (at 390 nm, 1 cm cuvette, sample interval 1 s). **PQ-Ph-CF₃-NVP** formation was fitted to an exponential rise to the maximum equation, $y = (y_0 - a) e^{-k_{obs} t} + a$, to give k_{obs}^{390} . E) Plot of k_{obs}^{390} vs. **NVP** concentration. The second-order rate constant, $k_{2,obs}^{390}$, was determined to be $4.6 \text{ M}^{-1} \text{ s}^{-1}$ based on the slope of the fitted curve.

4.3. Photoclick reaction quantum yields

UV/Vis evolution spectra were recorded using the setup described above with the 390B LED (for detailed information see SI section 4.2). The photon flux was determined using standard ferrioxalate actinometry, which provided a value of 3.94052×10^{-5} mol photons s^{-1} for the 390B LED.^[10] Spectra were collected over 10000 seconds, exported, and processed in SpectraGryph and OriginPro. Baseline corrections were carried out to correct for baseline drifting, after which the data was processed in QYMain (<https://www.nature.com/articles/srep41145#Sec14>) developed by Stranius & Börjesson.^[11]

$$\text{Eq.: } (d[A]/dt = I \cdot QY(A \rightarrow B) \cdot \beta_A / (N_A \cdot V) + I \cdot QY(B \rightarrow A) \cdot \beta_B / (N_A \cdot V) + [A] \cdot k(B \rightarrow A))$$

was used to fit the data collected in the first 10% reaction process using the following molar extinction coefficients and absorbance data at the irradiation wavelength (390 nm). Normalized absorbance ($\lambda=460$ nm) fitting plot and Φ_P are shown below:

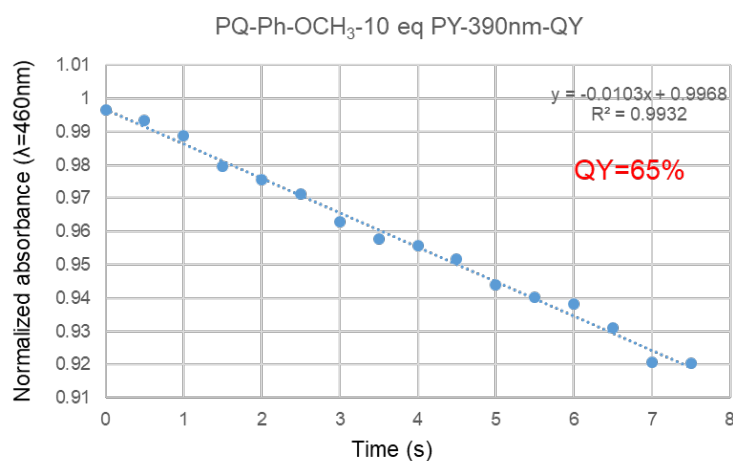


Fig. S80. Photoclick reaction of **PQ-Ph-OCH₃** (1 mM) with 10 eq **PY** (10 mM). The measurement was done in a 1 cm quartz cuvette with a 390 nm LED irradiation in N₂ atmosphere at 20 °C, followed by UV-Vis absorption spectra.

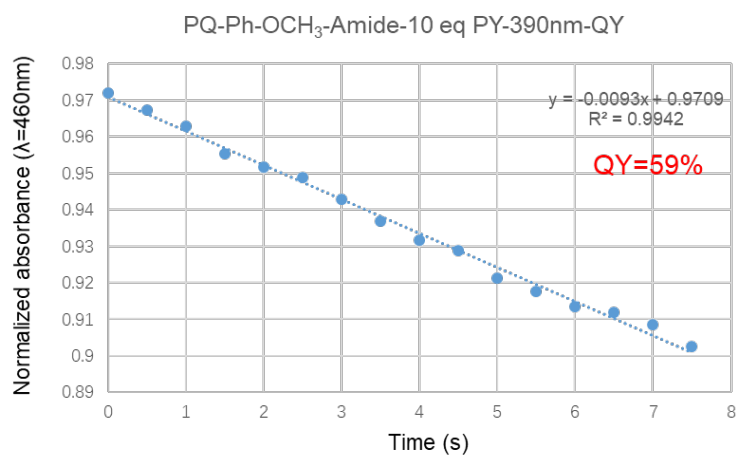


Fig. S81. Photoclick reaction Quantum Yield calculation of **PQ-Ph-OCH₃-Amide** (1 mM) toward 10 eq **PY** (10 mM). The measurement was done in a 1 cm quartz cuvette with a 390 nm LED irradiation in N₂ atmosphere at 20 °C, followed by UV-Vis absorption spectra.

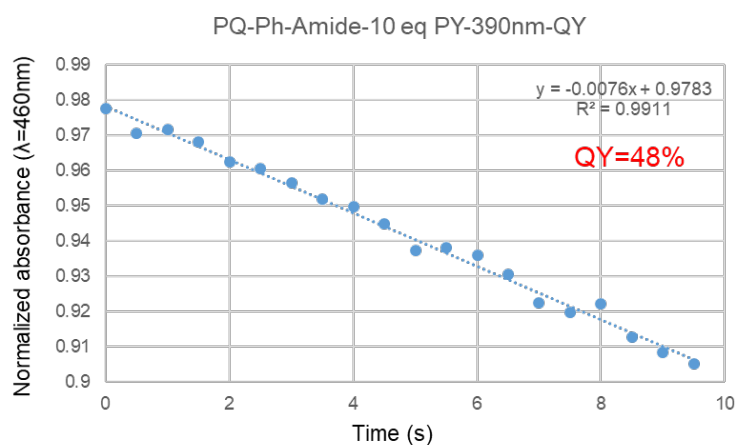


Fig. S82. Photoclick reaction Quantum Yield calculation of **PQ-Ph-Amide** (1 mM) toward 10 eq **PY** (10 mM). The measurement was done in a 1 cm quartz cuvette with a 390 nm LED irradiation in N₂ atmosphere at 20 °C, followed by UV-Vis absorption spectra.

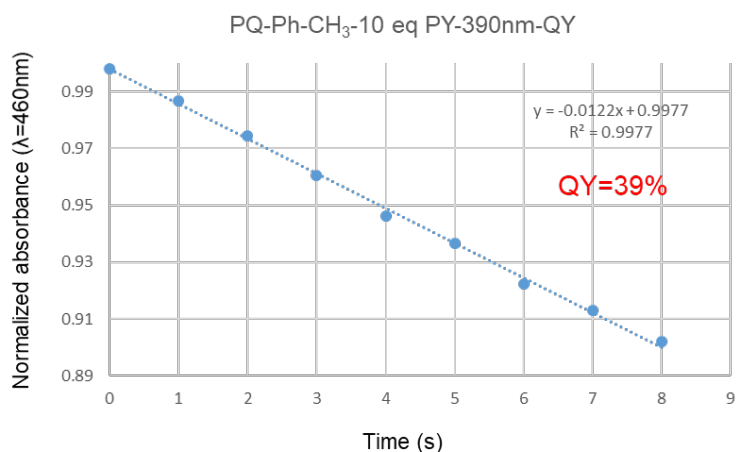


Fig. S83. Photoclick reaction Quantum Yield calculation of **PQ-Ph-CH₃** (0.5 mM) toward 10 eq **PY** (5 mM). The measurement was done in a 1 cm quartz cuvette with a 390 nm LED irradiation in N₂ atmosphere at 20 °C, followed by UV-Vis absorption spectra.

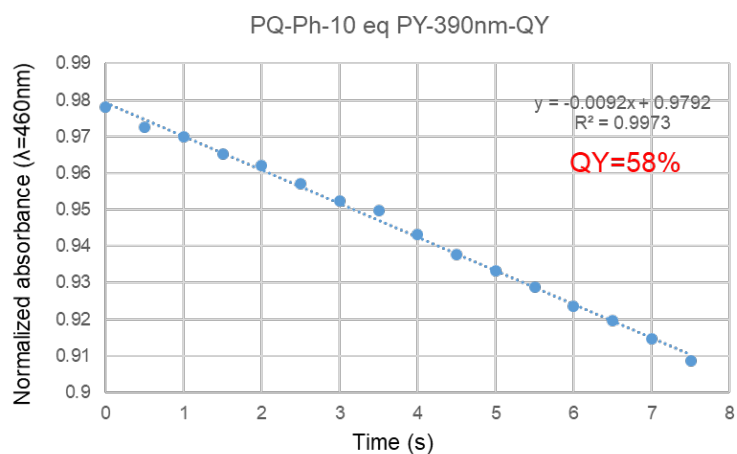


Fig. S84. Photoclick reaction Quantum Yield calculation of **PQ-Ph** (1 mM) toward 10 eq **PY** (10 mM). The measurement was done in a 1 cm quartz cuvette with a 390 nm LED irradiation in N₂ atmosphere at 20 °C, followed by UV-Vis absorption spectra.

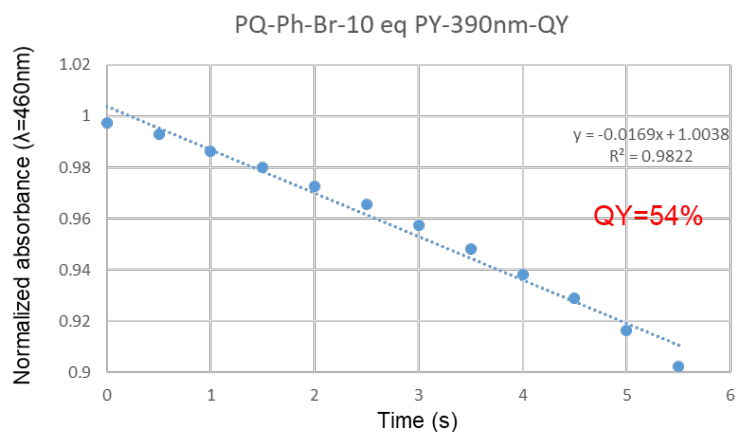


Fig. S85. Photoclick reaction Quantum Yield calculation of **PQ-Ph-Br** (0.5 mM) toward 10 eq **PY** (5 mM). The measurement was done in a 1 cm quartz cuvette with a 390 nm LED irradiation in N₂ atmosphere at 20 °C, followed by UV-Vis absorption spectra.

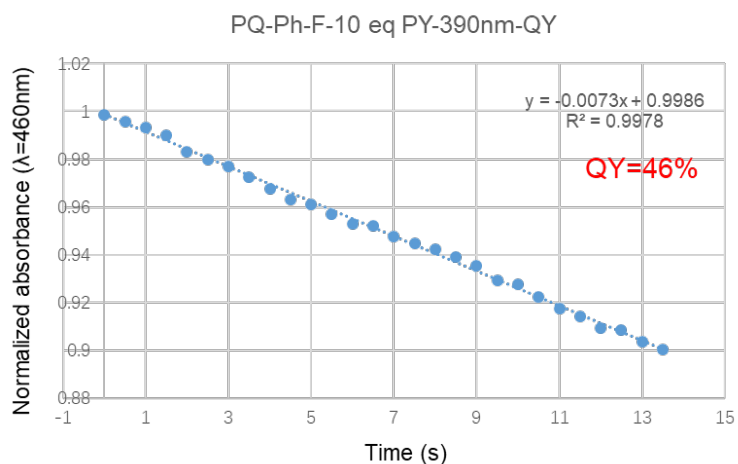


Fig. S86. Photoclick reaction Quantum Yield calculation of **PQ-Ph-F** (1 mM) toward 10 eq **PY** (10 mM). The measurement was done in a 1 cm quartz cuvette with a 390 nm LED irradiation in N₂ atmosphere at 20 °C, followed by UV-Vis absorption spectra.

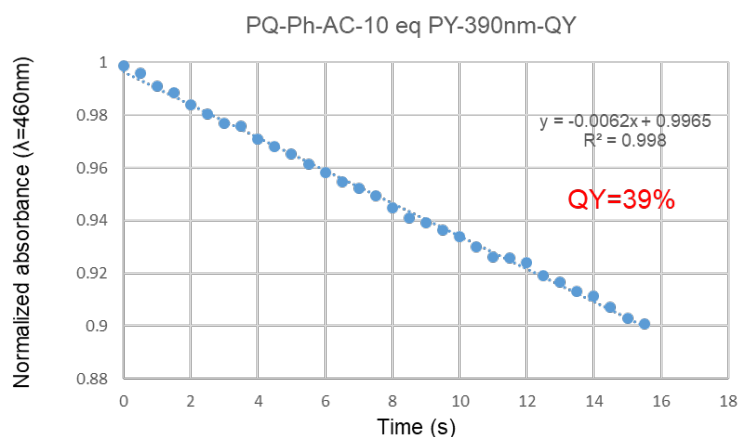


Fig. S87. Photoclick reaction Quantum Yield calculation of **PQ-Ph-AC** (1 mM) toward 10 eq **PY** (10 mM). The measurement was done in a 1 cm quartz cuvette with a 390 nm LED irradiation in N₂ atmosphere at 20 °C, followed by UV-Vis absorption spectra.

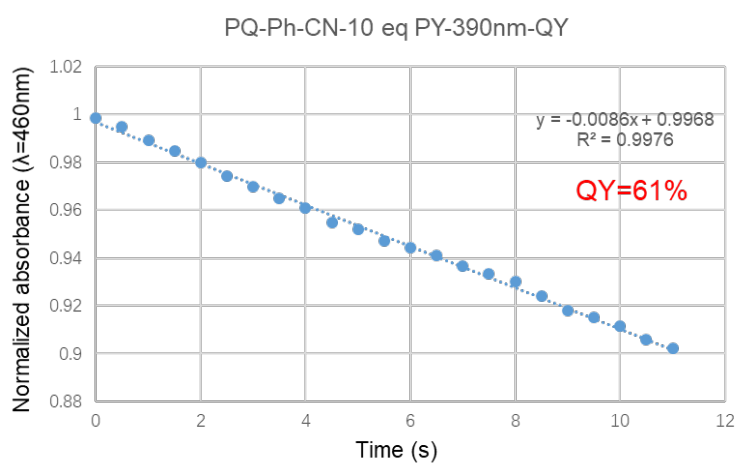


Fig. S88. Photoclick reaction Quantum Yield calculation of **PQ-Ph-CN** (1.125 mM) toward 10 eq **PY** (11.25 mM). The measurement was done in a 1 cm quartz cuvette with a 390 nm LED irradiation in N₂ atmosphere at 20 °C, followed by UV-Vis absorption spectra.

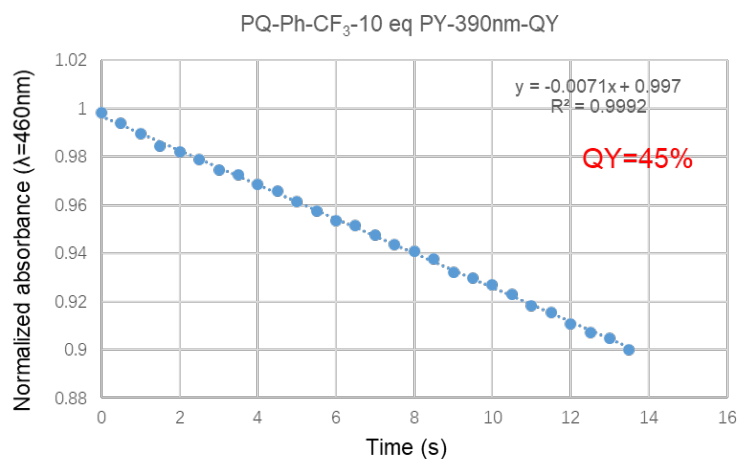


Fig. S89. Photoclick reaction Quantum Yield calculation of **PQ-Ph-CF₃** (1 mM) toward 10 eq **PY** (10 mM). The measurement was done in a 1 cm quartz cuvette with a 390 nm LED irradiation in N₂ atmosphere at 20 °C, followed by UV-Vis absorption spectra.

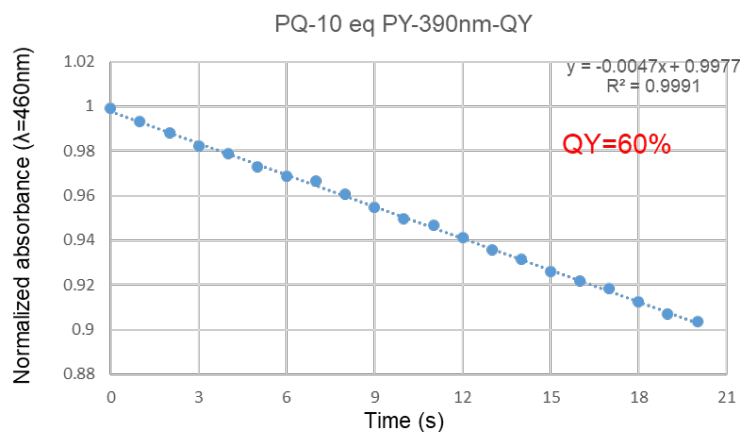


Fig. S90. Photoclick reaction Quantum Yield calculation of **PQ** (2 mM) toward 10 eq **PY** (20 mM). The measurement was done in a 1 cm quartz cuvette with a 390 nm LED irradiation in N₂ atmosphere at 20 °C, followed by UV-Vis absorption spectra.

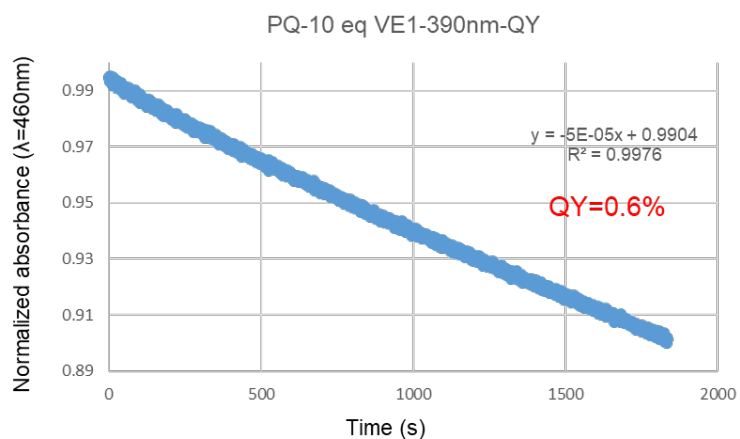


Fig. S91. Photoclick reaction Quantum Yield calculation of **PQ** (2 mM) toward 10 eq **VE1** (20 mM). The measurement was done in a 1 cm quartz cuvette with a 390 nm LED irradiation in N_2 atmosphere at 20 °C, followed by UV-Vis absorption spectra.

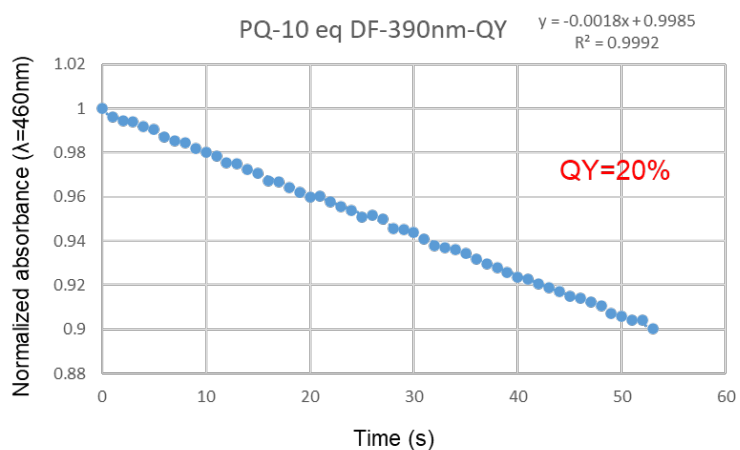


Fig. S92. Photoclick reaction Quantum Yield calculation of **PQ** (1.5 mM) toward 10 eq **DF** (15 mM). The measurement was done in a 1 cm quartz cuvette with a 390 nm LED irradiation in N_2 atmosphere at 20 °C, followed by UV-Vis absorption spectra.

4.4. HPLC Traces for the following of the orthogonal photoclick reaction in solution

HPLC analysis of the orthogonal photoclick reaction system with 1:1:1:1 ratio: **PQ-Ph-OCH₃** (50 μM, 1 eq), **PQ-Ph-CF₃** (50 μM, 1 eq), **PY** (50 μM, 1 eq), and **NVP** (50 μM, 1 eq) were added into a Schlenk tube (MeCN) and deoxygenated by N₂. A hand-held LED lamp (395 nm, 88 mW/cm²) was used as a light source and positioned at a fixed distance. The Schlenk tube was exposed to irradiation with this hand-held 395 nm LED lamp for different time points (0 s, 30 s, 60 s, 120 s, 240 s, 480 s, and 720 s) and the samples were analyzed by HPLC. The corresponding HPLC traces are shown below:

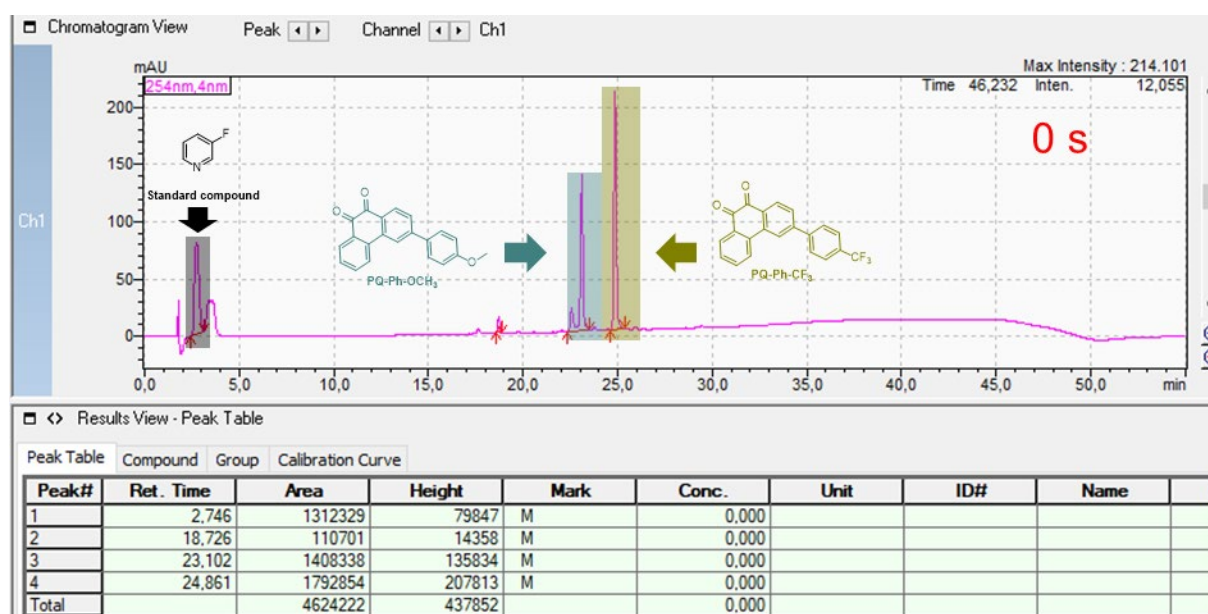


Fig. S93. HPLC trace of the reaction mixture after 0 s irradiation with 395 nm LED lamp

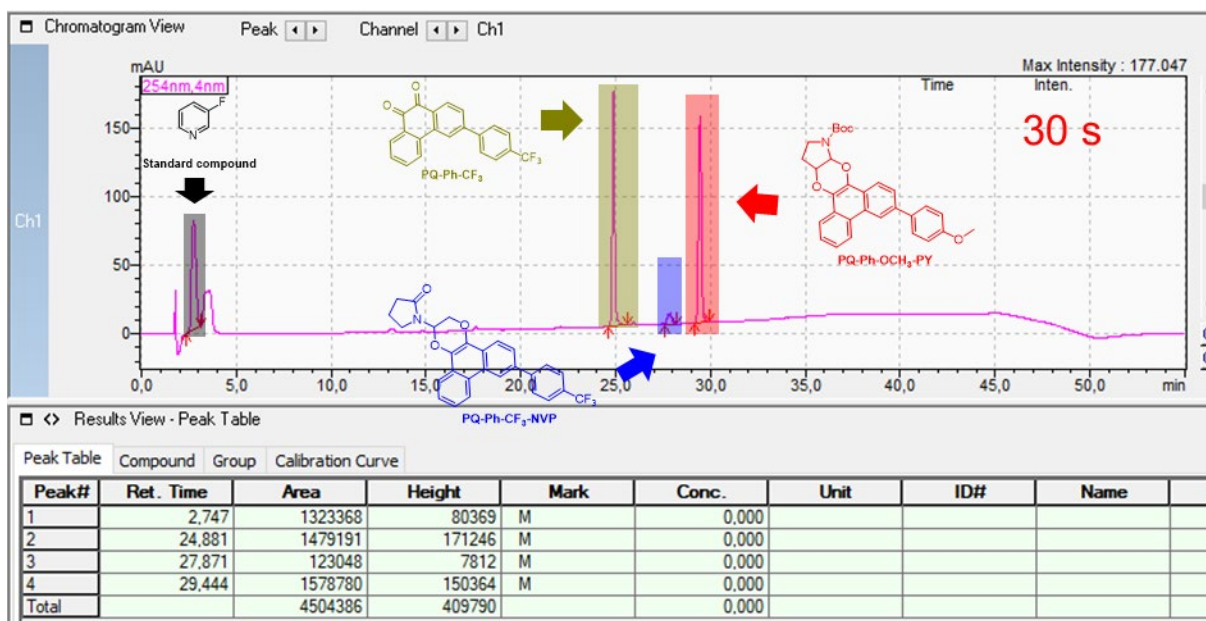


Fig. S94. HPLC trace of the reaction mixture after 30 s irradiation with 395 nm LED lamp

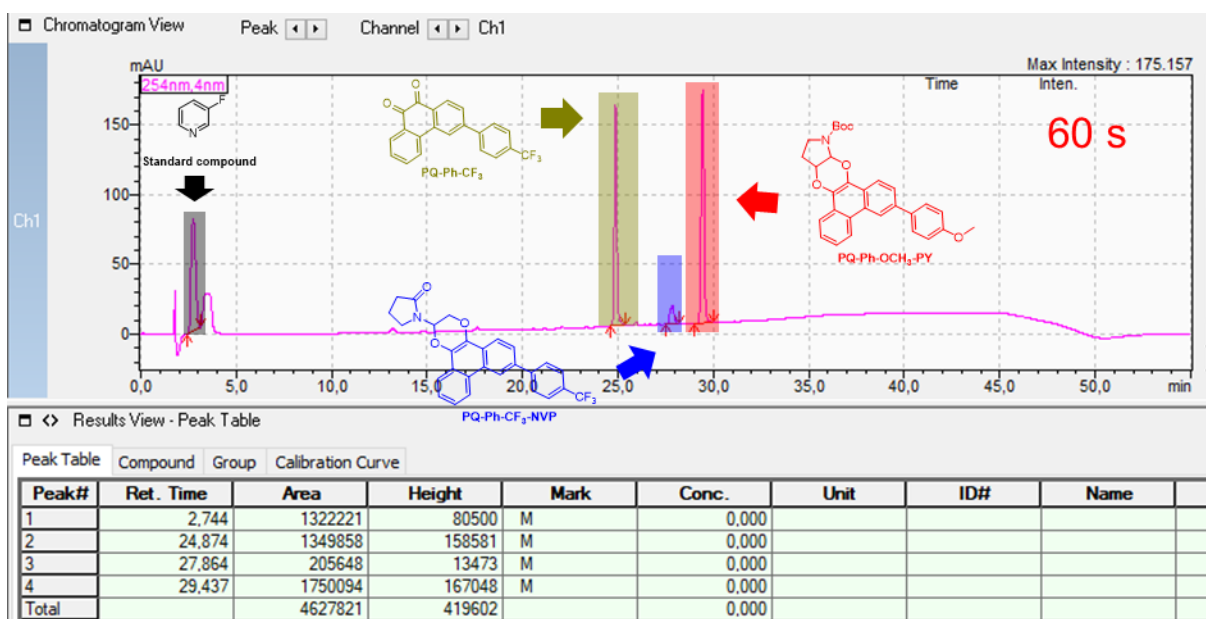


Fig. S95. HPLC trace of the reaction mixture after 60 s irradiation with 395 nm LED lamp

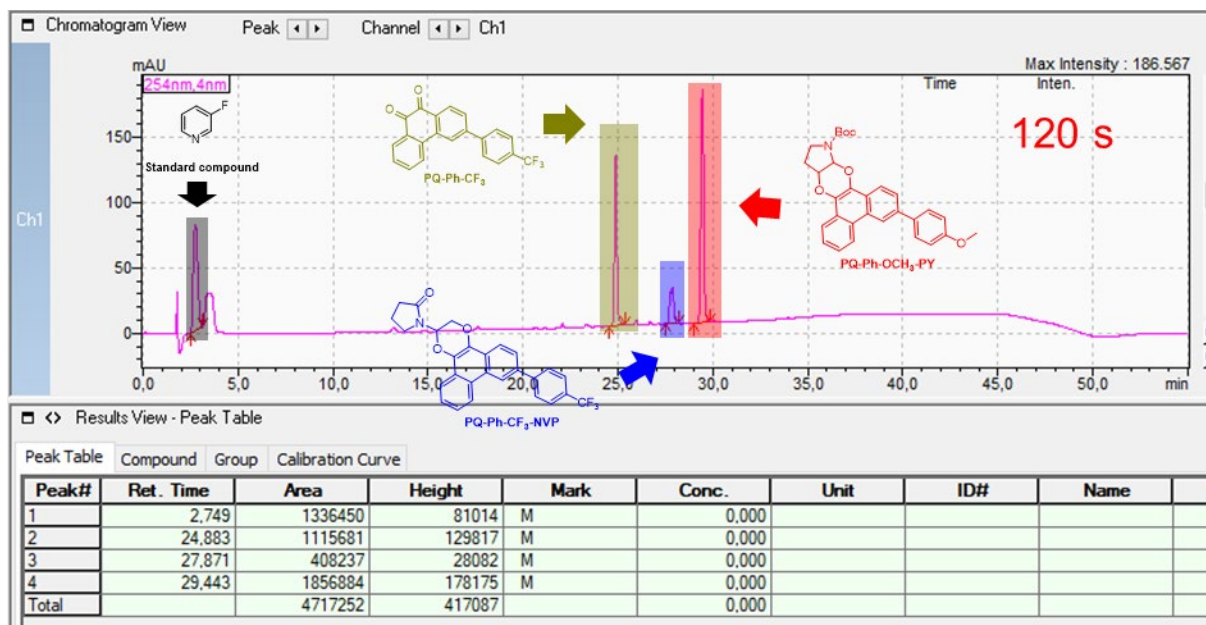


Fig. S96. HPLC trace of the reaction mixture after 120 s irradiation with 395 nm LED lamp

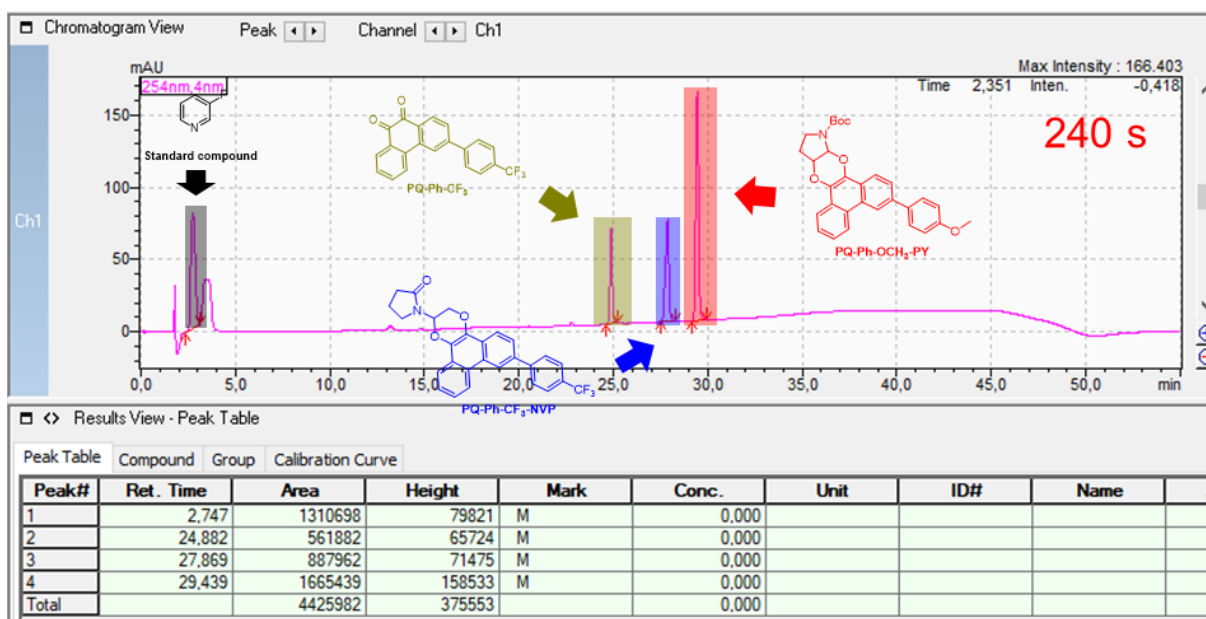


Fig. S97. HPLC trace of the reaction mixture after 240 s irradiation with 395 nm LED lamp

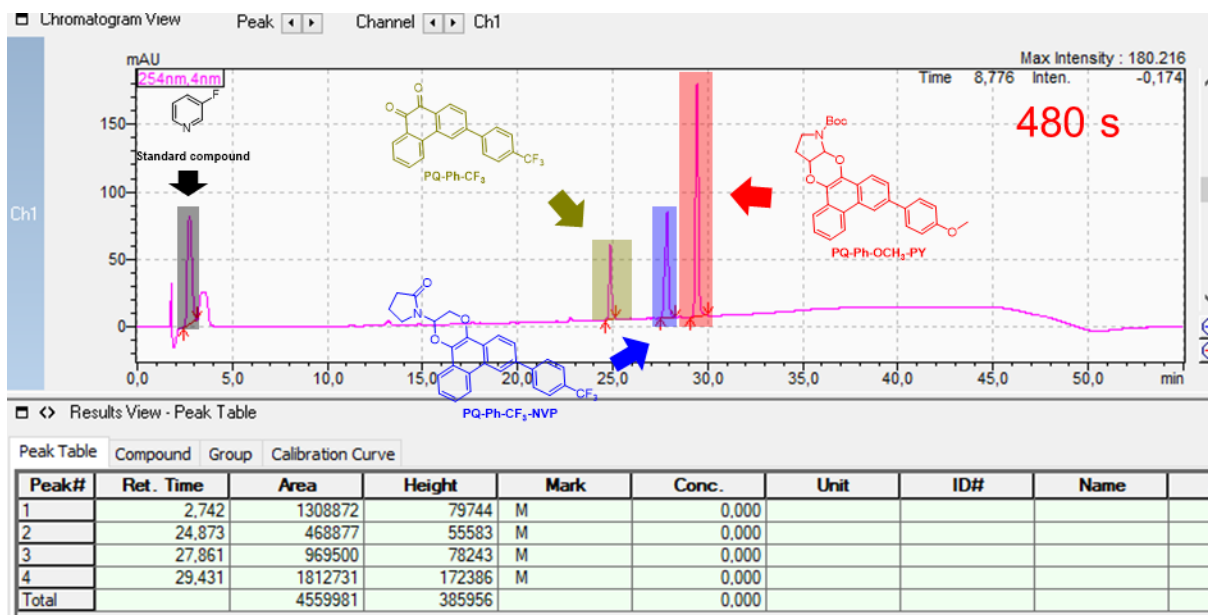


Fig. S98. HPLC trace of the reaction mixture after 480 s irradiation with 395 nm LED lamp

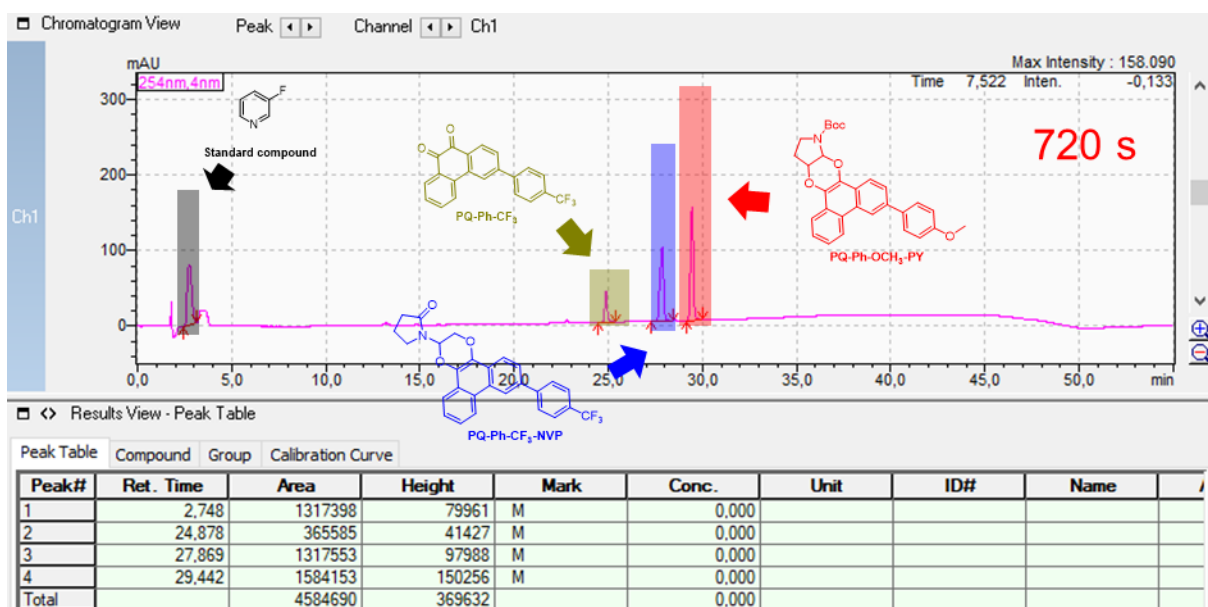


Fig. S99. HPLC trace of the reaction mixture after 720 s irradiation with 395 nm LED lamp

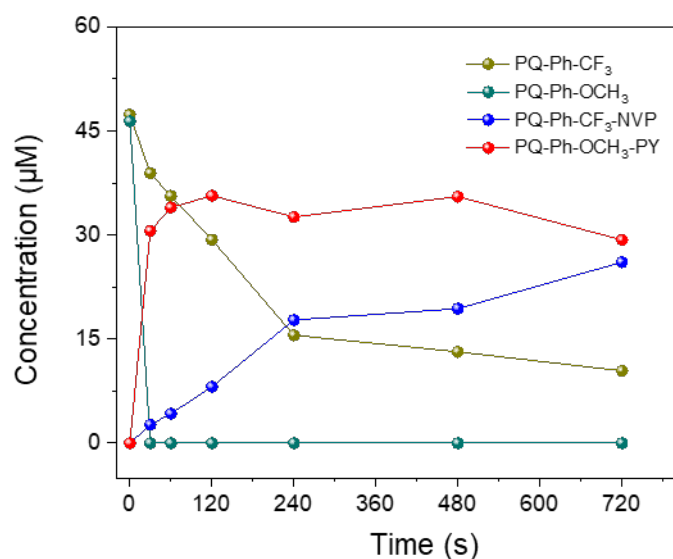


Fig. S100. Quantitative HPLC analysis of **PQ-Ph-OCH₃**, **PQ-Ph-CF₃**, **PY**, and **NVP** orthogonal photoclick reaction.

HPLC analysis of the orthogonal photoclick reaction system with 1:1.75:1:50 ratio: **PQ-Ph-OCH₃** (100 µM, 1 eq), **PQ-Ph-CF₃** (100 µM, 1 eq), **PY** (175 µM, 1.75 eq), and **NVP** (5.00 mM, 50 eq) were added into a Schlenk tube (MeCN) and deoxygenated by N₂. A hand-held LED lamp (395 nm, 88 mW/cm²) was used as a light source and positioned at a fixed distance. The Schlenk tube was exposed to irradiation with this hand-held 395 nm LED lamp for different time points (0 s, 30 s, 60 s, and 90 s) and the samples were analyzed by HPLC. The corresponding HPLC traces are shown below:

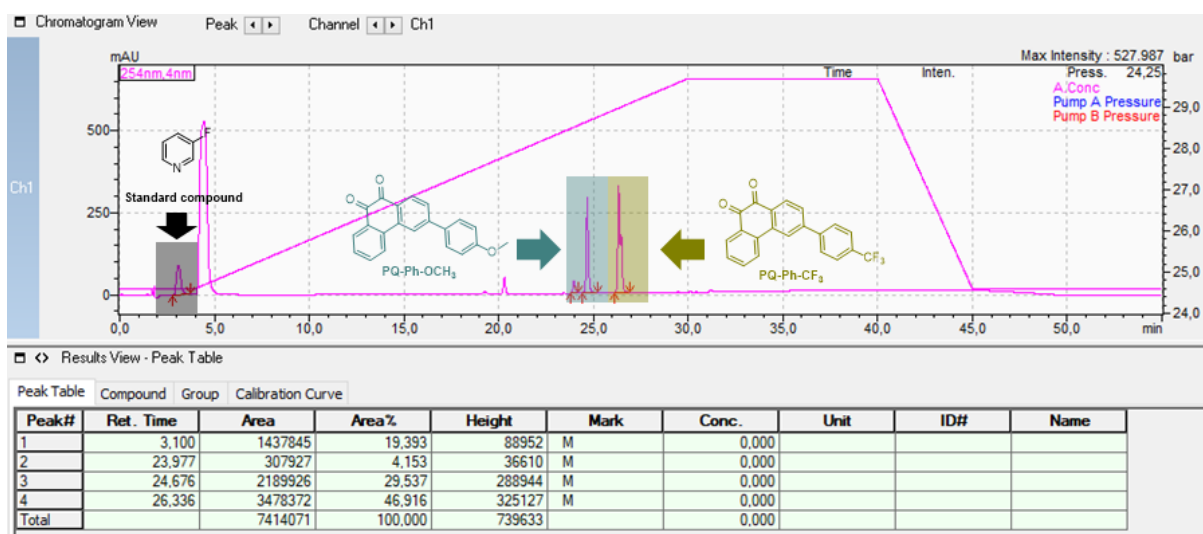


Fig. S101. HPLC trace of the reaction mixture after 0 s irradiation with 395 nm LED lamp.

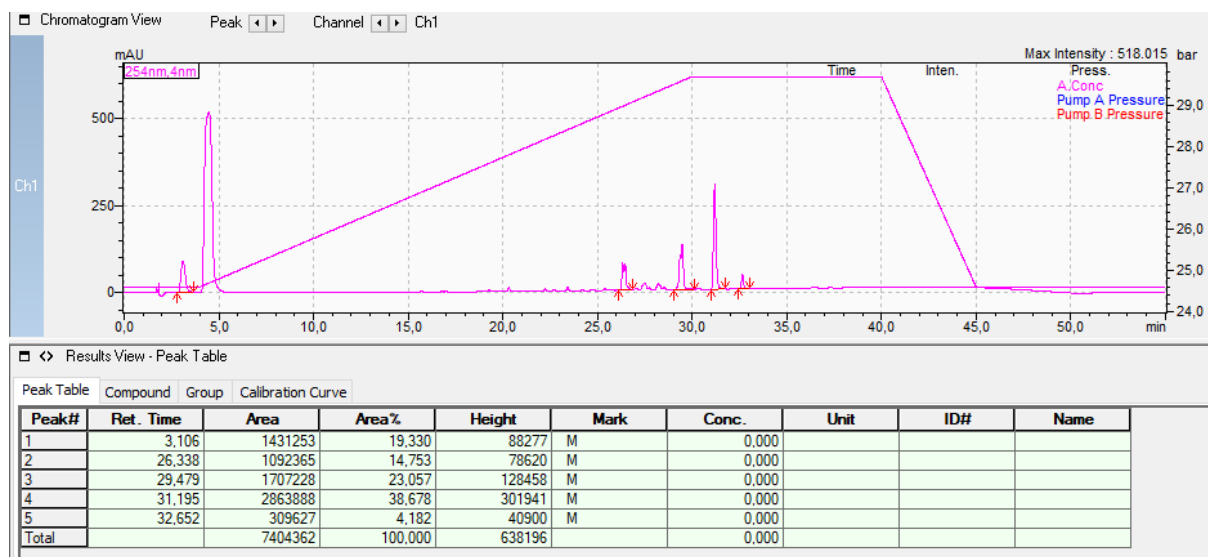


Fig. S102. HPLC trace of the reaction mixture after 30 s irradiation with 395 nm LED lamp.

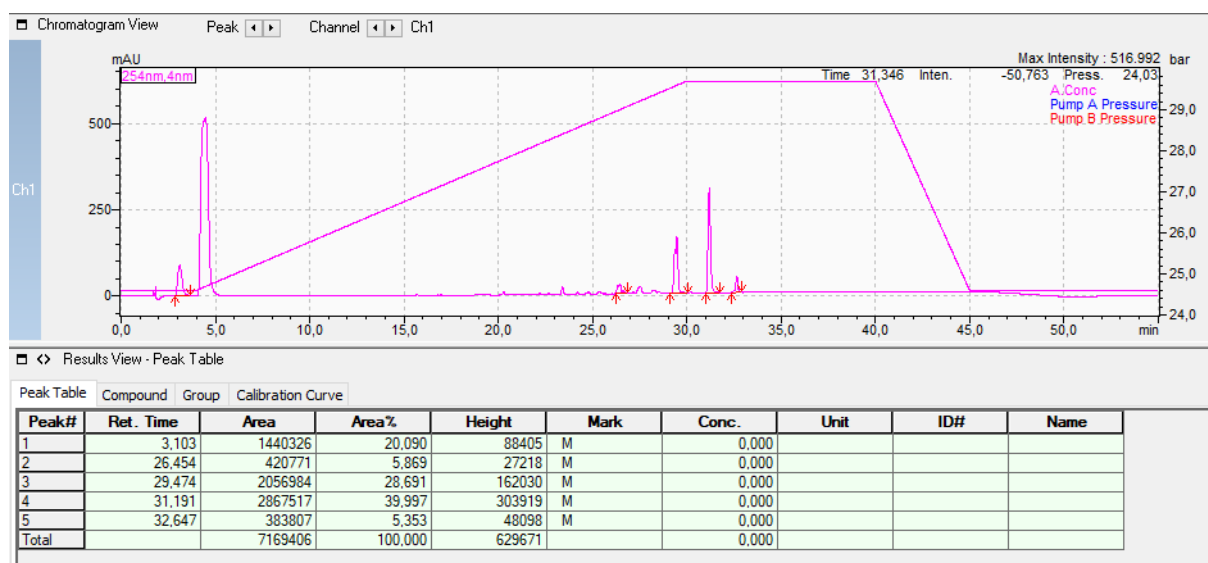


Fig. S103. HPLC trace of the reaction mixture after 60 s irradiation with 395 nm LED lamp.

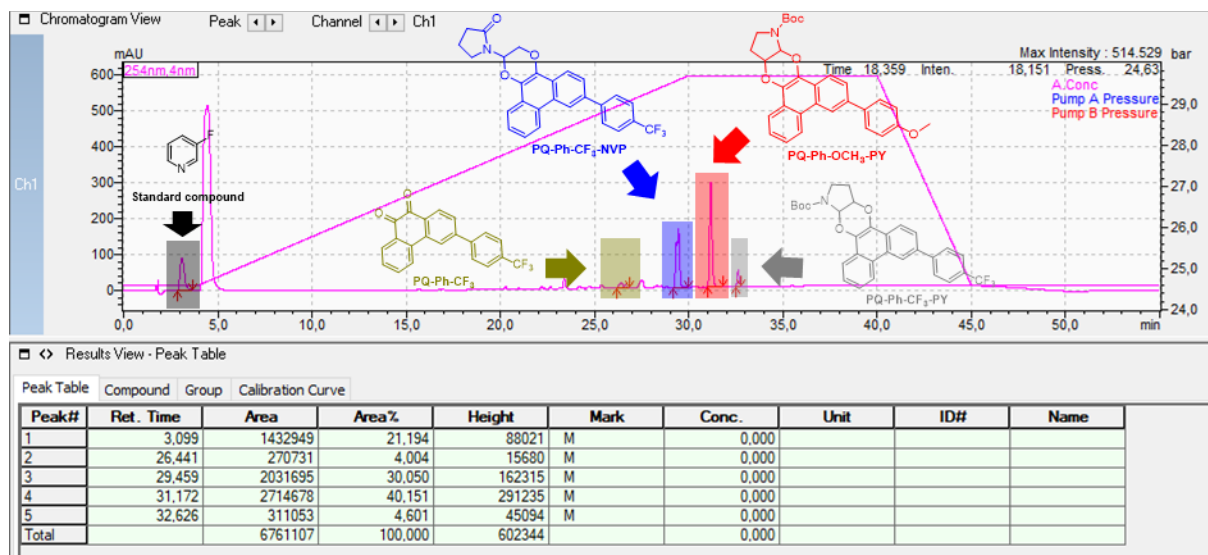


Fig. S104. HPLC trace of the reaction mixture after 90 s irradiation with 395 nm LED lamp.

4.5. Fluorescence Quantum Yields and Solvatofluorochromism

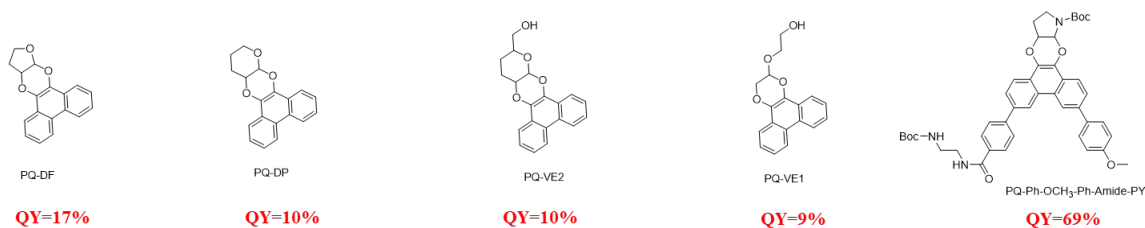


Fig. S105. Fluorescence quantum yield (Φ_F) of PQ-DF, PQ-DP, PQ-VE2, PQ-VE1, and PQ-Ph-OCH₃-Ph-Amide-PY. Concentration of photoclick product was 10 μ M. All measurements were done in MeCN, with a 1 cm quartz cuvette, 20 $^{\circ}$ C, λ_{ex} =330 nm.

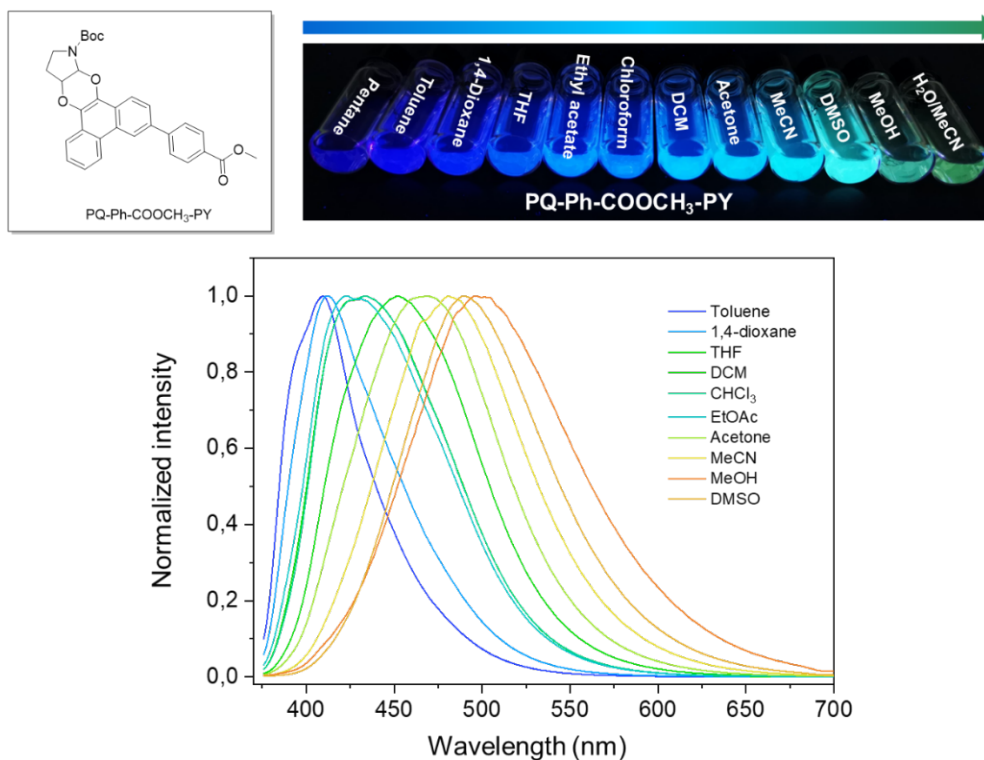


Fig. S106. Normalized fluorescence spectra of **PQ-Ph-COOCH₃-PY** in solvents with different polarities. **PQ-Ph-COOCH₃-PY** (5 μ M) in a 1 cm quartz cuvette, 20 °C, λ_{ex} =330 nm.

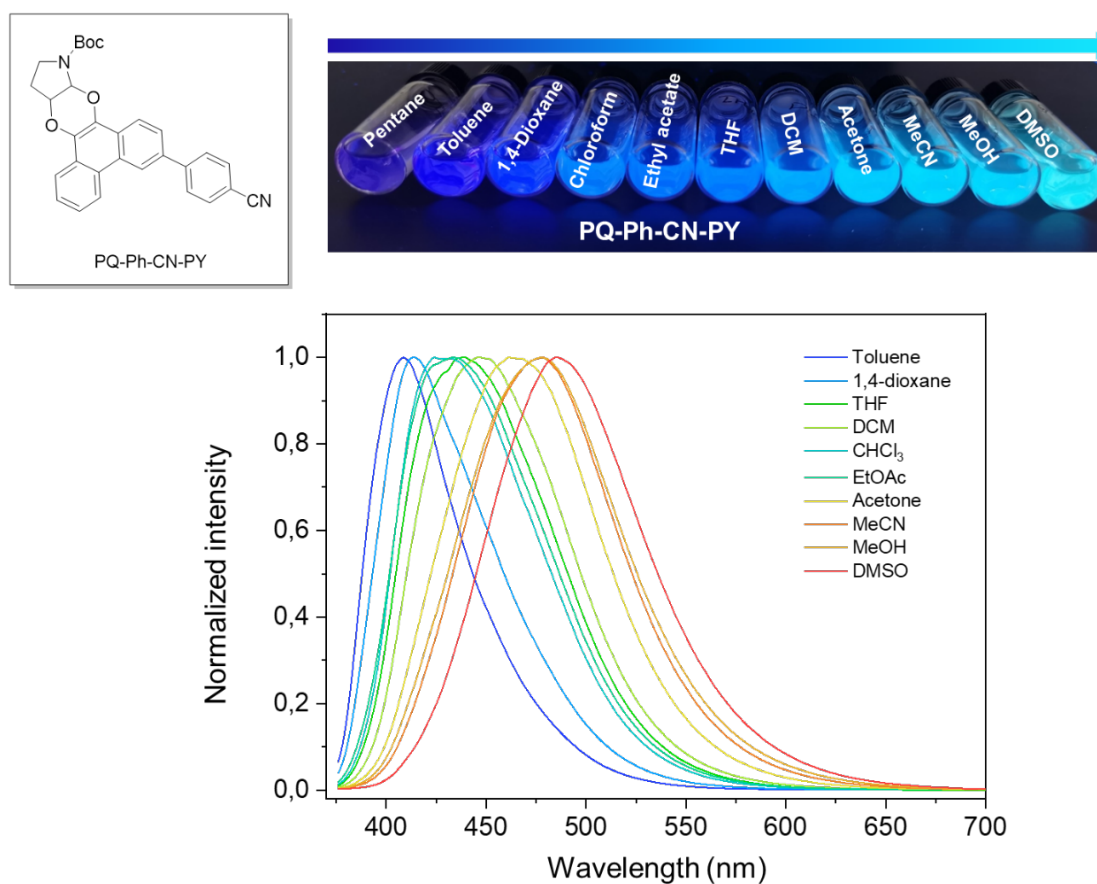


Fig. S107. Normalized fluorescence spectra of **PQ-Ph-CN-PY** in solvents with different polarities. **PQ-Ph-CN-PY** (5 μM) in a 1 cm quartz cuvette, 20 $^{\circ}\text{C}$, $\lambda_{\text{ex}}=330$ nm.

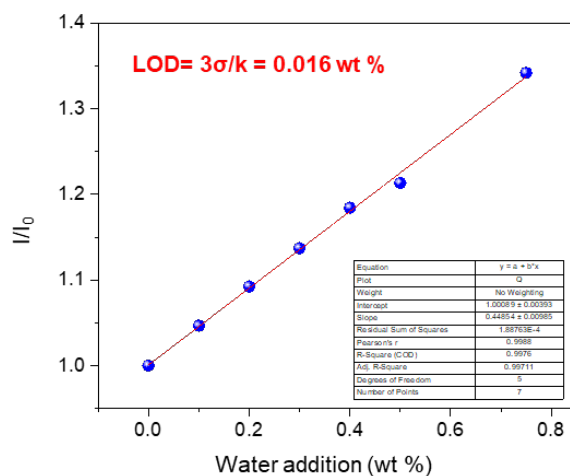


Fig. S108. The plot of I/I_0 versus water content (wt %), where I_0 and I represent the maximum emission intensity in the absence and presence of water (0-0.75 wt %) respectively. Concentration of **PQ-Ph-Ac-PY** was 50 μM . All measurements were done in dioxane, with a 1 cm quartz cuvette, 20 $^{\circ}\text{C}$, $\lambda_{\text{ex}}=330$ nm.

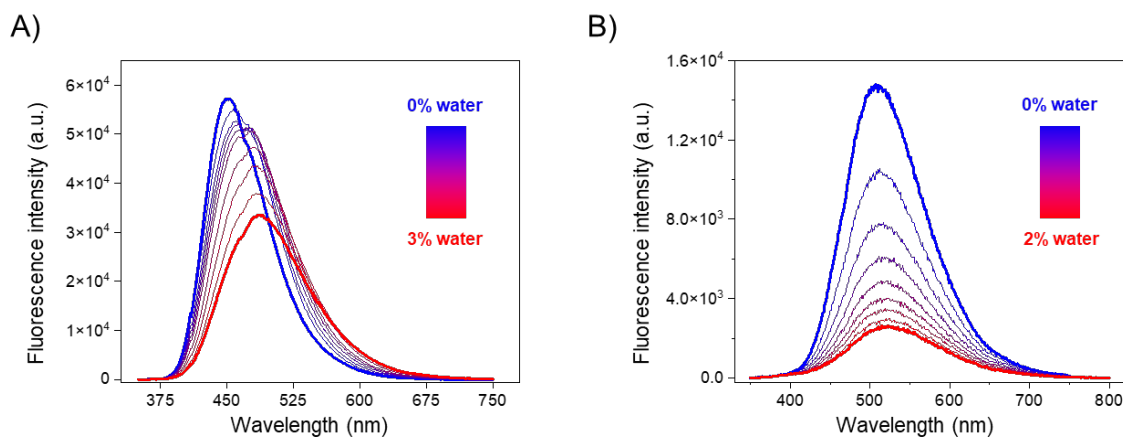


Fig. S109. Emission spectra changes of **PQ-Ph-AC-PY** (5 μM) in A) THF and B) MeCN with different water content (0-3 wt % and 0-2 wt % respectively, $\lambda_{\text{ex}} = 330$ nm).

4.6. HPLC traces and additional measurements of photoclick reaction on surface

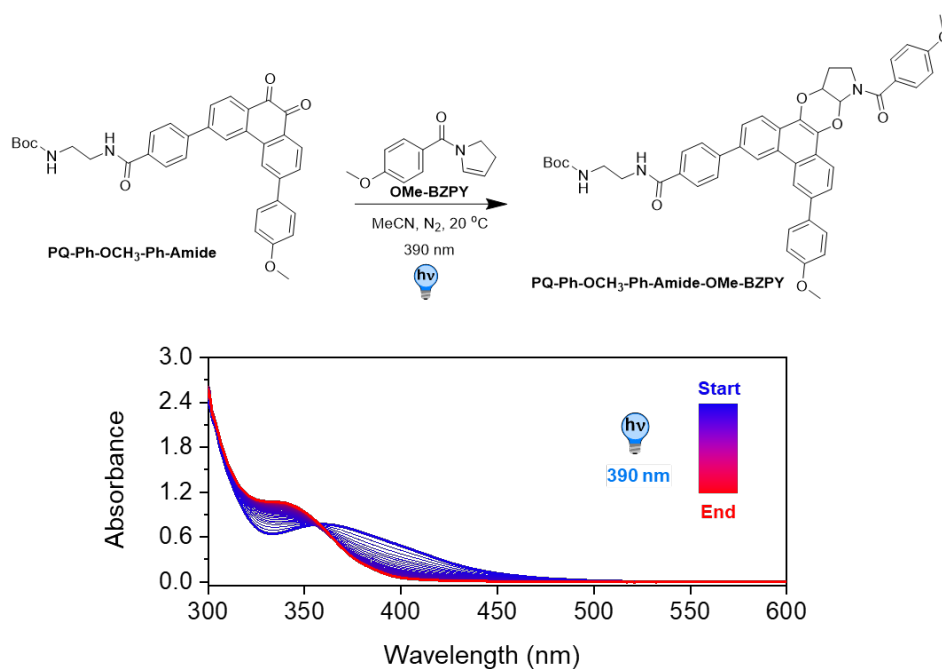


Fig. S110. Time-resolved UV-Vis absorption spectra of the photocycloaddition between **PQ-Ph-OCH₃-Ph-Amide** (50 μ M) towards **OMe-BZPY** (500 μ M) in MeCN (2.5 mL, N₂ atmosphere); the reaction mixture was irradiated with 390 nm LED at 20 °C. The reaction was monitored by UV-Vis absorption spectroscopy (1 cm cuvette, sample interval 1 s).

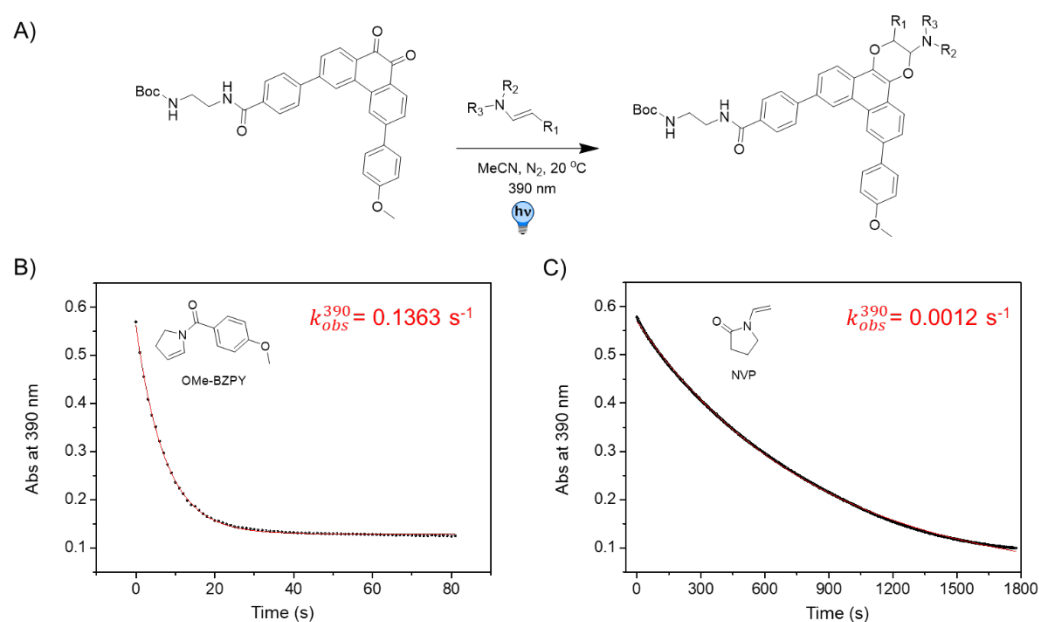


Fig. S111. Reaction rate constants k_{obs}^{390} (s^{-1}) for the **PQ-Ph-OCH₃-Ph-Amide** (50 μ M) with A) **OMe-BZPY** (500 μ M), and B) **NVP** (500 μ M). All measurements were performed in MeCN (N_2 atmosphere) at 20 °C and using the same setup as described in section 4.2.

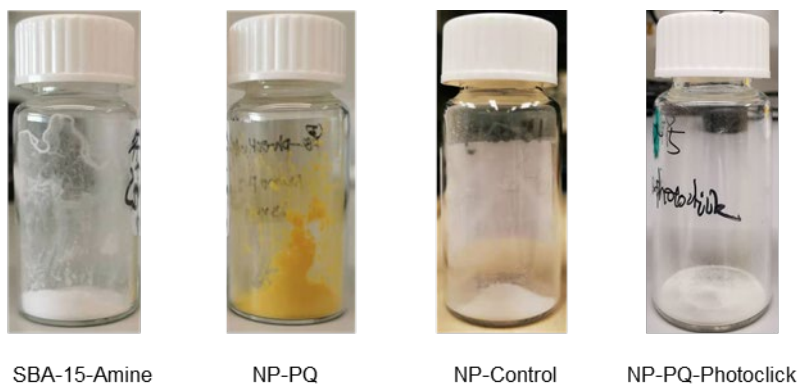


Fig. S112. Photograph of nanoparticles, from left to right is **SBA-15-Amine**, **NP-PQ**, **NP-Control**, and **NP-PQ-Photoclick** respectively.

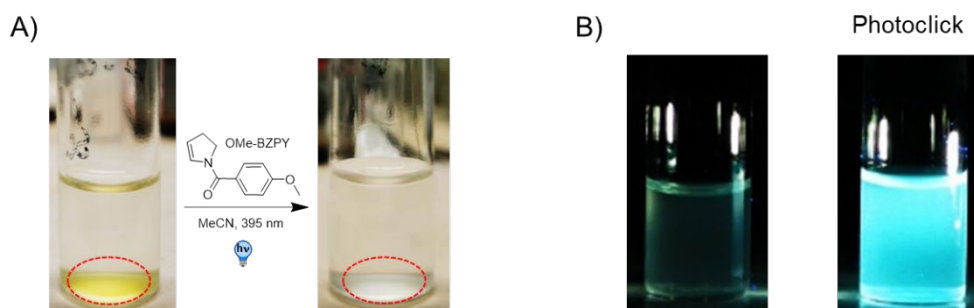


Fig. S113. Photograph of photoclick reaction on nanoparticles in MeCN solution.

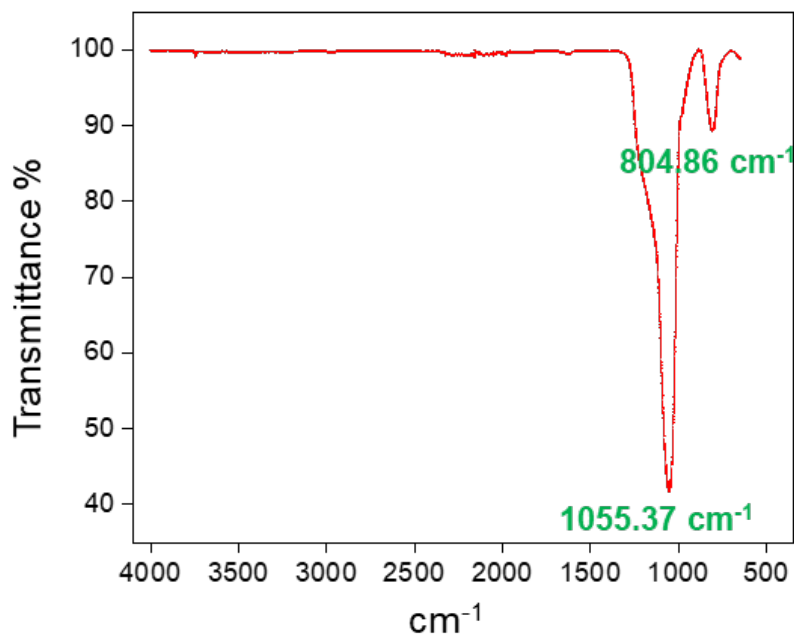


Fig. S114. IR spectra analysis of SBA-15-Amine nanoparticle.

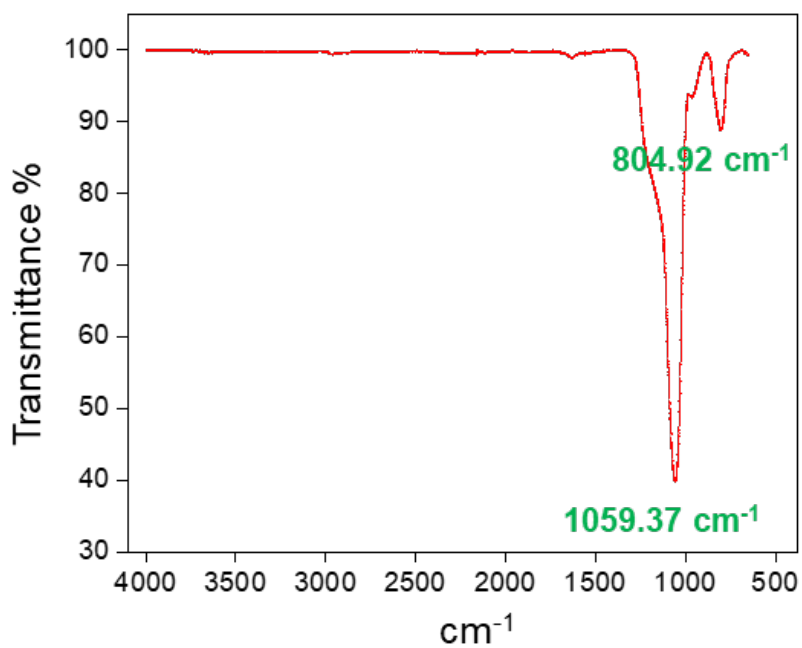


Fig. S115. IR spectra analysis of NP-Control nanoparticle.

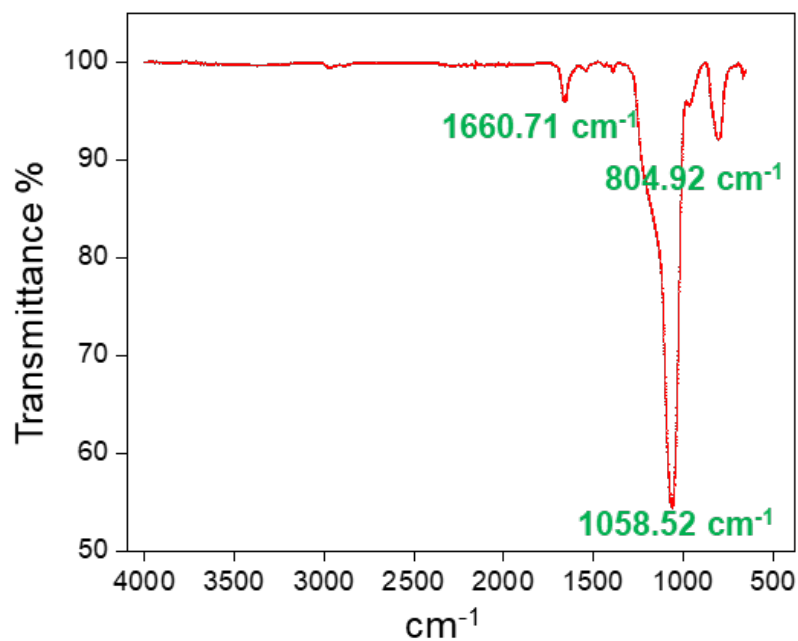


Fig. S116. IR spectra analysis of NP-PQ nanoparticle.

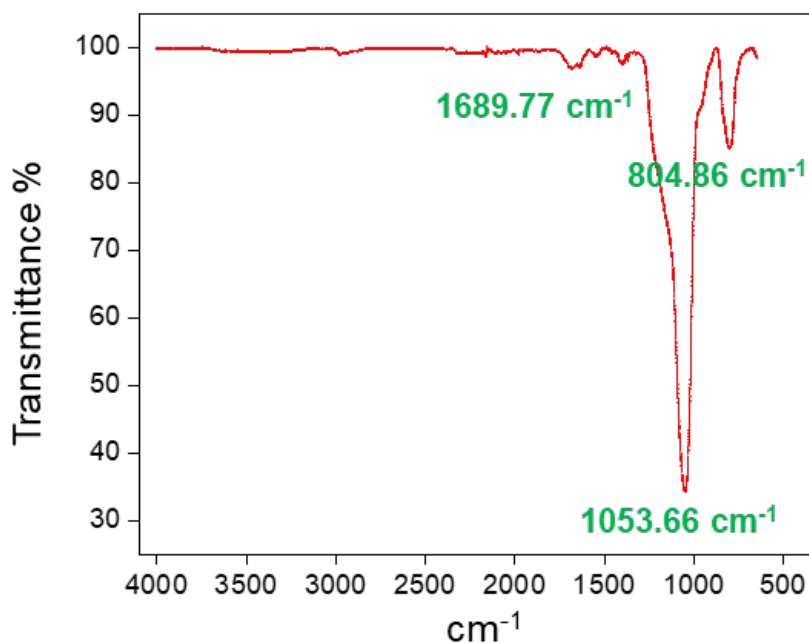


Fig. S117. IR spectra analysis of NP-PQ-Photoclick nanoparticle.

HPLC analysis of competition experiment on SBA-15 nanoparticles: NP-PQ (1.5 mg), OMe-BZPY (100 μ M), and NVP (100 μ M) were added into a Schlenk tube (7 mL MeCN) deoxygenated by N₂. A hand-held LED lamp (395nm, 88 mW/cm²) was used as a light source

and positioned in a fixed distance. The Schlenk tube was exposed to irradiation with this hand-held 395 nm LED lamp for different time points (0 s, 15 s, 30 s, 60 s, 90 s, and 120 s) and the samples were analyzed by HPLC. The corresponding HPLC traces shown below:

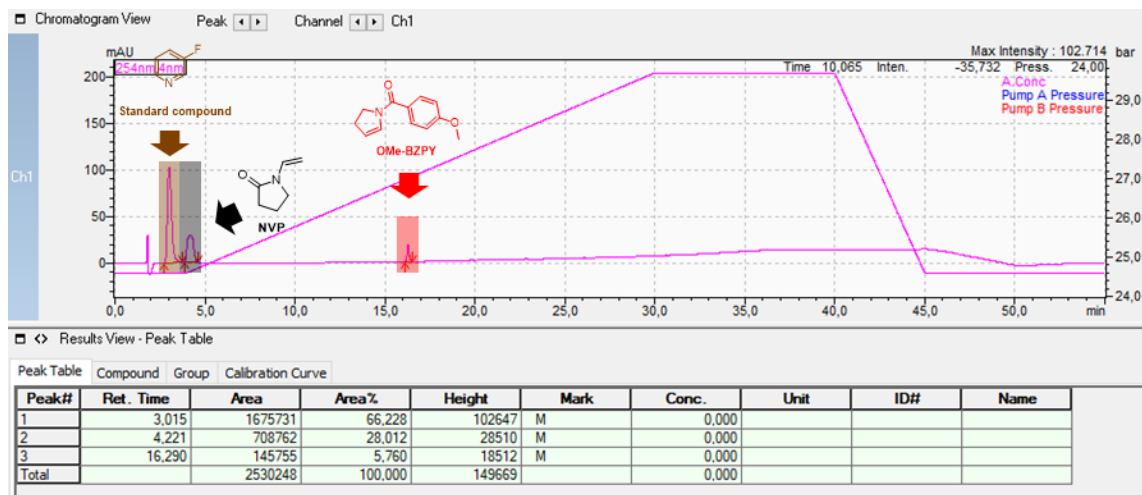


Fig. S118. HPLC trace of the reaction mixture after 0 s irradiation with 395 nm LED lamp.

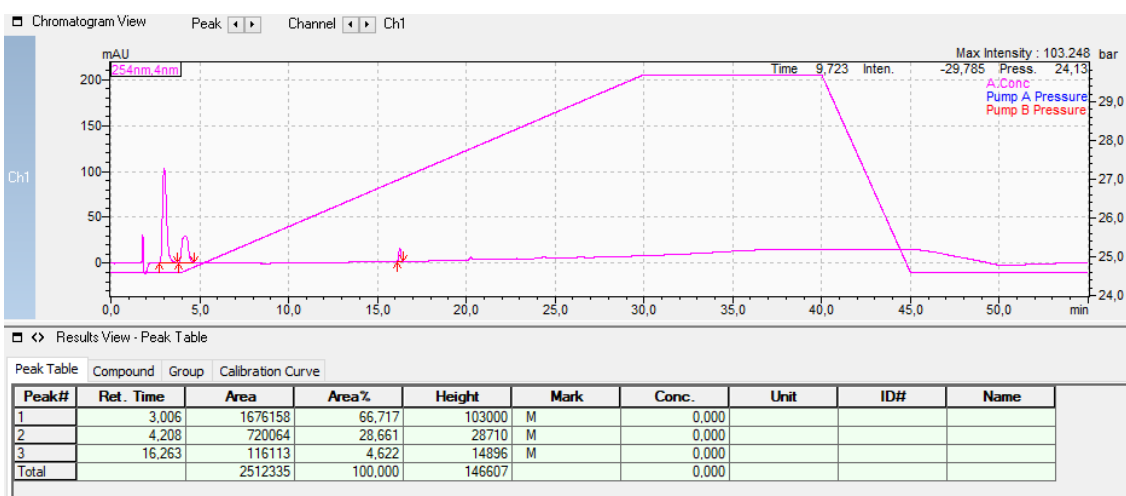


Fig. S119. HPLC trace of the reaction mixture after 15 s irradiation with 395 nm LED lamp.

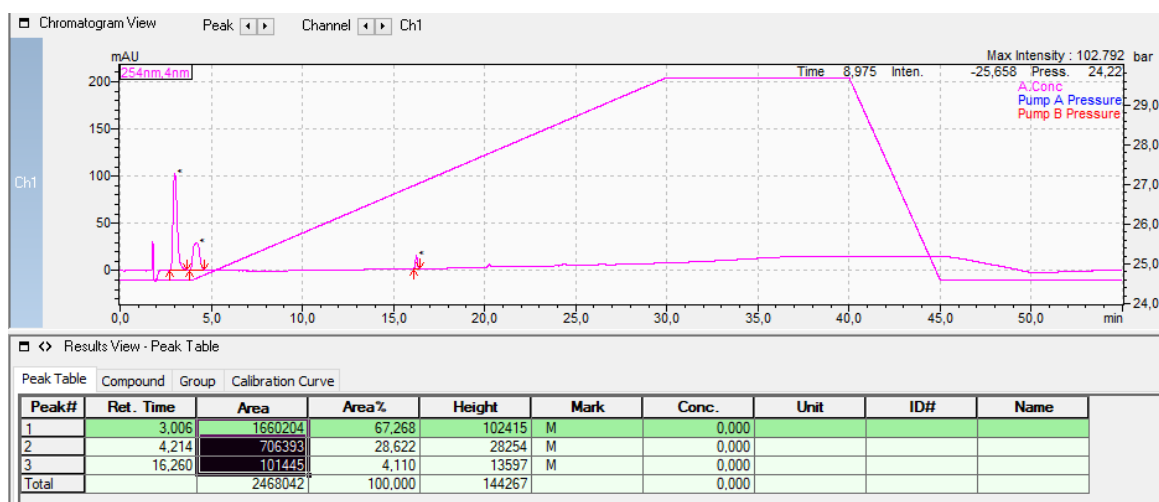


Fig. S120. HPLC trace of the reaction mixture after 30 s irradiation with 395 nm LED lamp.

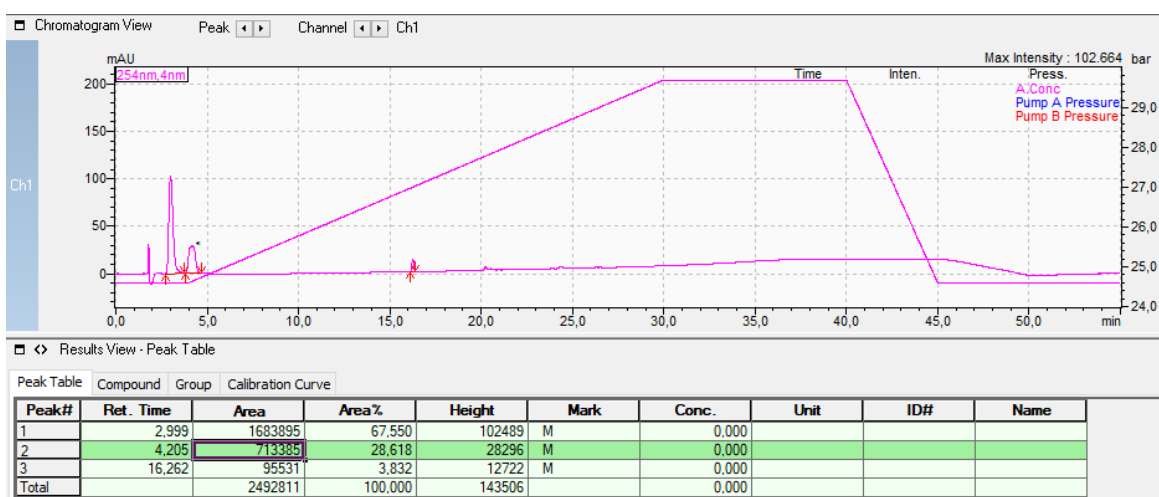


Fig. S121. HPLC trace of the reaction mixture after 60 s irradiation with 395 nm LED lamp.

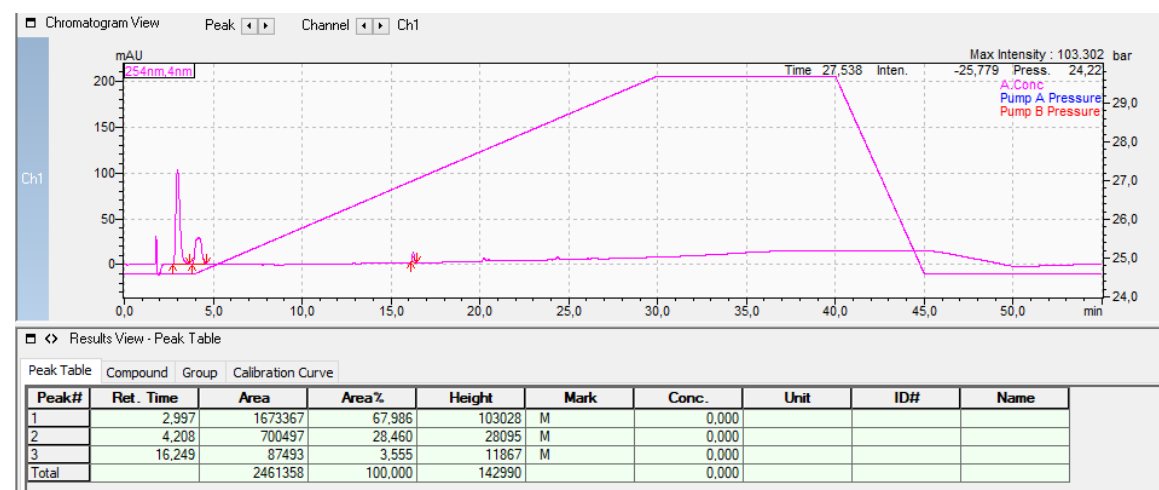


Fig. S122. HPLC trace of the reaction mixture after 90 s irradiation with 395 nm LED lamp.

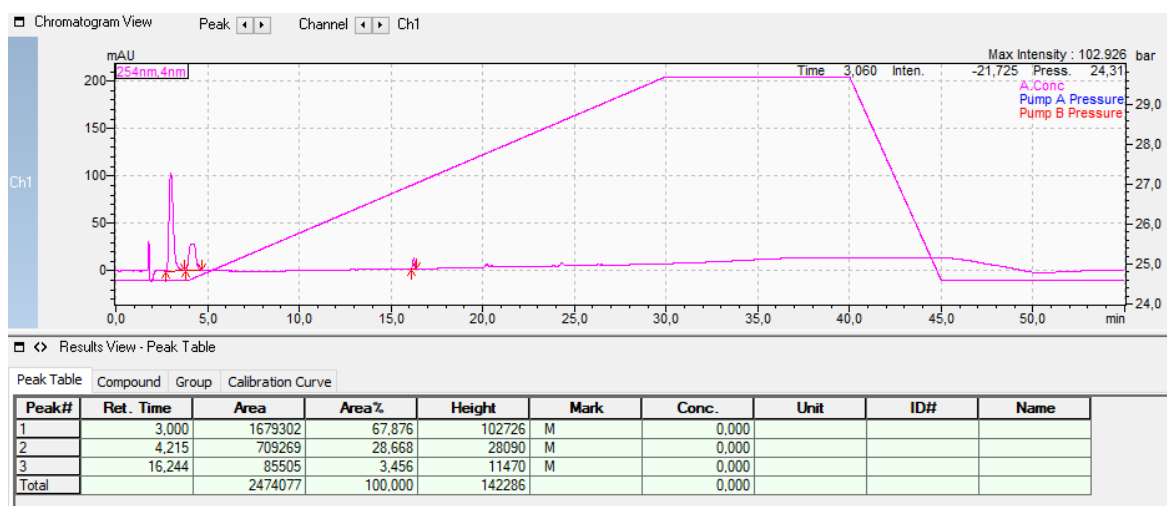


Fig. S123. HPLC trace of the reaction mixture after 120 s irradiation with 395 nm LED lamp.

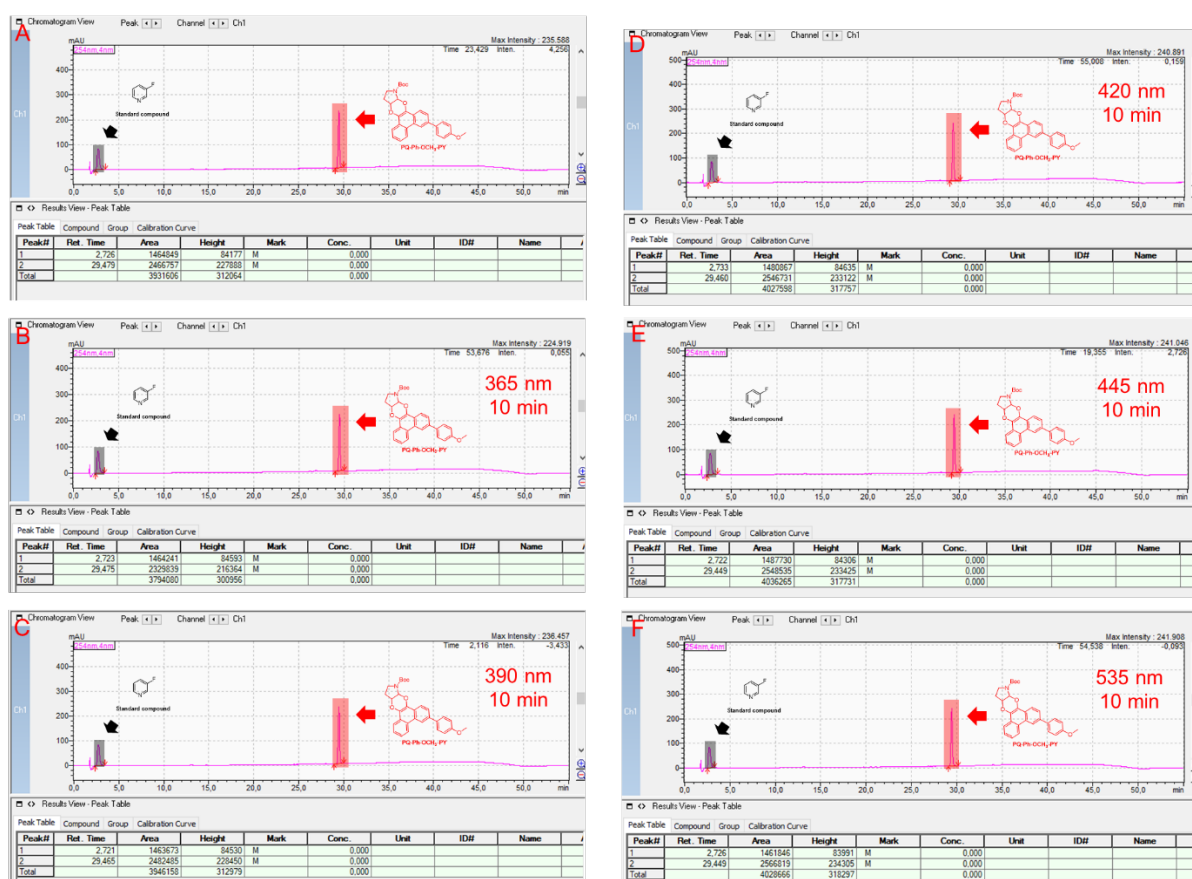


Fig. S124. Photostability analysis of PQ-Ph-OCH₃-PY by HPLC. 50 μ M PQ-Ph-OCH₃-PY in MeCN was irradiated by various of light (365 nm, 390 nm, 420 nm, 445 nm, and 535 nm respectively) for 10 min at 20 $^{\circ}$ C.

5. Author Contributions

Y.F., N.A.S., W.S., and B.L.F. conceived the project and designed phenanthrenequinone derivatives and enamine compounds. B.L.F., W.S., and N.A.S. guided the research. Y.F. synthesized of the phenanthrenequinone derivatives and together with R.T. synthesized enamines. Y.F. performed UV-Vis experiments. Y.F., N.A.S, performed and analyzed HPLC experiments. Emission spectroscopy and fluorescence quantum yield calculation were performed by Y.F. and R.T. Photoclick reaction on functionalize silica nanoparticles were performed by Y.F. and, R.B. Y.F., N.A.S., W.S., and B.L.F. wrote the manuscript with support and contributions from all authors.

6. References

- [1] L. N. Lameijer, S. Budzak, N. A. Simeth, M. J. Hansen, B. L. Feringa, D. Jacquemin, W. Szymanski, *Angew. Chem. Int. Ed.* **2020**, *59*, 21663–21670.
- [2] P. Spieß, M. Berger, D. Kaiser, N. Maulide, *J. Am. Chem. Soc.* **2021**, *143*, 10524–10529.
- [3] R. Mi, X. Zhang, J. Wang, H. Chen, Y. Lan, F. Wang, X. Li, *ACS Catal.* **2021**, *11*, 6692–6697.
- [4] L. He, L. Zhao, D.-X. Wang, M.-X. Wang, *Org. Lett.* **2014**, *16*, 5972–5975.
- [5] R. Brilmayer, S. Kübelbeck, A. Khalil, M. Brodrecht, U. Kunz, H. Kleebe, G. Buntkowsky, G. Baier, A. Andrieu-Brunsen, *Adv. Mater. Interfaces* **2020**, *7*, 1901914.
- [6] K. Lang, L. Davis, S. Wallace, M. Mahesh, D. J. Cox, M. L. Blackman, J. M. Fox, J. W. Chin, *J. Am. Chem. Soc.* **2012**, *134*, 10317–10320.
- [7] J. Li, H. Kong, L. Huang, B. Cheng, K. Qin, M. Zheng, Z. Yan, Y. Zhang, *J. Am. Chem. Soc.* **2018**, *140*, 14542–14546.
- [8] T. D. Svejstrup, A. Chatterjee, D. Schekin, T. Wagner, J. Zach, M. J. Johansson, G. Bergonzini, B. König, *ChemPhotoChem* **2021**, *5*, 808–814.
- [9] Y. Fu, H. Helbert, N. A. Simeth, S. Crespi, G. B. Spoelstra, J. M. van Dijn, M. van Oosten, L. R. Nazario, D. van der Born, G. Luurtsema, W. Szymanski, P. H. Elsinga, B. L. Feringa, *J. Am. Chem. Soc.* **2021**, *143*, 10041–10047.
- [10] N. A. Simeth, S. Kobayashi, P. Kobauri, S. Crespi, W. Szymanski, K. Nakatani, C. Dohno, B. L. Feringa, *Chem. Sci.* **2021**, *12*, 9207–9220.

[11] K. Stranius, K. Börjesson, *Sci. Rep.* **2017**, 7, 1–9.